NASA CONTRACTOR REPORT

NASA CR-1679

NASA CR-1679

AN INVESTIGATION OF THE HIGH SPEED TURBULENT BOUNDARY LAYER WITH HEAT TRANSFER AND ARBITRARY PRESSURE GRADIENT

Part I – Summary Report

by Constantino Economos and John Boccio

Prepared by
GENERAL APPLIED SCIENCE LABORATORIES, INC.
Westbury, L. I., N. Y. 11590
for Langley Research Center

NATIONAL AERONAUTICS AND SPACE ADMINISTRATION • WASHINGTON, D. C. • DECEMBER 1970

1. Report No.	2. Government Accession No.	3. Recipient's Catalog No.
NASA CR-1679		

4. Title and Subtitle	5. Report Date
AN INVESTIGATION OF THE HIGH SPEED TURBULENT BOUNDARY LAYER WITH HEAT TRANSFER AND ARBITRARY PRESSURE GRADIENT. PART I - SUMMARY REPORT	December 1970
	6. Performing Organization Code
7. Author(s)	8. Performing Organization Report No.
Constantino Economos, and John Boccio	GASL TR-719 Part I
	10. Work Unit No.
	126-13-10-13-23
9. Performing Organization Name and Address	11. Contract or Grant No.
Generai Applied Science Laboratories, Inc. Westbury, L. I., New York 11590	NAS 1-8424
	13. Type of Report and Period Covered
12. Sponsoring Agency Name and Address	Contractor Report
National Aeronautics and Space Administration Washington, D.C. 20546	14. Sponsoring Agency Code

15. Supplementary Notes

16. Abstract

This report describes the analysis developed for investigating the behavior of high-speed turbulent boundary layers under conditions involving both heat transfer and arbitrary streamwise pressure gradient. The approach utilizes a compressibility transformation in conjunction with an integral technique to describe the fluid-dynamic behavior. The corresponding thermodynamic behavior is described by implicit-finite-difference solution of the energy conservation equation written in terms of total enthalpy.

One feature of the analyses involves the use of certain correlative procedures developed in Part II of this report. In this latter document the properties of the transformation theory were reexamined from a fundamental level with the aim of overcoming some of its shortcomings and enlarging its applicability to include the more general problem treated herein.

The details of the numerical and computational procedures utilized to implement the analysis are presented in Part III of this report. A variety of numerical results are presented in this document. These include comparisons with other predictive methods and with experimental data. Additional results showing eddy viscosity, shear stress and mixing length distribution in high-speed flows are also presented.

17. Key Words (Suggested by Author(s))	18. Distribution Statement
Turbulent boundary layer Heat transfer Pressure gradient Transformation (Mathematics)	Unclassified - Unlimited

19. Security Classif. (of this report)	20. Security Classif. (of this page)	21. No. of Pages	22. Price*
Unclassified	Unclassified	119	$3.00

*For sale by the National Technical Information Service, Springfield, Virginia 22151

FOREWORD

The present report is one of a series of three reports which describe analyses and computational procedures developed for describing the behavior of high speed-turbulent boundary layers under conditions involving both heat transfer and arbitrary pressure gradient. Part I, serves as a summary report and describes the analysis which is utilized in the numerical calculation scheme. In Part II, the fundamental properties of of the compressibility transformation used in the analysis are examined in detail. Part III, describes the numerical and computational procedures involved and serves as a computer program manual.

The titles in the series are:

Part I Summary Report - "An Investigation of the High Speed Turbulent Boundary Layer with Heat Transfer and Arbitrary Pressure Gradient," by C. Economos and J. Boccio.

Part II- "The Compressibility Transformation - General Considerations," by C. Economos.

Part III- "Computer Program Manual," by J. Schneider and J. Boccio.

This investigation was conducted for the Langley Research Center, National Aeronautics and Space Administration under Contract No. NAS1-8424 with Mr. Kazimierz R. Czarnecki as the NASA Technical Monitor.

The contractors' report number is GASL TR-719.

SUMMARY

This report describes the analysis developed for investigating the behavior of high-speed turbulent boundary layers under conditions involving both heat transfer and arbitrary streamwise pressure gradient. The approach utilizes a compressibility transformation in conjunction with an integral technique to describe the fluid-dynamic behavior. The corresponding thermodynamic behavior is described by implicit-finite-difference solution of the energy conservation equation written in terms of total enthalpy.

Within this framework the turbulent Prandtl number is included as a parameter and provision for its spatial variation by means of a special subroutine package, which allows the incorporation of a variety of arbitrarily selected models. Other options include the use of either equilibrium air chemistry or the perfect gas assumption.

One feature of the analysis involves the use of certain correlative procedures developed in Part II of this report. In this latter document the properties of the transformation theory were reexamined from a fundamental level with the aim of overcoming some of its shortcomings and enlarging its applicability to include the more general problem treated herein. The details of the numerical and computational procedures utilized to implement the analysis are presented in Part III of this report. A variety of numerical results are presented in this document. These include comparisons with other predictive methods and with experimental data. Additional results showing eddy viscosity, shear stress and mixing length distribution in high-speed flows are also presented.

TABLE OF CONTENTS

AN INVESTIGATION OF THE HIGH SPEED TURBULENT BOUNDARY LAYER WITH HEAT TRANSFER AND ARBITRARY PRESSURE GRADIENT

By C. Economos and J. Boccio
General Applied Science Laboratories, Inc.

I. INTRODUCTION

The overall objective of the investigation described in this report was the development, within the framework of a compressibility transformation, a computer program capable of describing the behavior of high-speed turbulent boundary layers under conditions involving both heat transfer and arbitrary streamwise pressure gradient. The desirability of such an approach rests on the fact that no empirical assumptions regarding the mechanism of turbulent momentum transport need to be introduced insofar as the variable property (VP) flow field is concerned. Instead, it suffices to specify this behavior in the transformed constant-property (CP) plane where a reliable description is currently available, at least from a phenomenological point of view.

The idea of relating a VP boundary layer to a CP counterpart is not new. In the case where the product of viscosity and density is constant and the pressure gradient zero or of some special form, the transformations of References 1 through 4 relate laminar two-dimensional compressible boundary layers to corresponding incompressible ones. Investigations have also been conducted to extend the concept of such transformations to turbulent flows. Some of the investigators were Laufer, Reference 5, Mager, Reference 6, Culick and Hill, Reference 7, Burggraf, Reference 8, Coles, Reference 9, and Crocco, Reference 10. Apart from the concept of a transformation, the hypotheses of an effective temperature, a laminar film and a constant sublayer Reynolds number have been used to represent the compressible turbulent boundary layer by an incompressible counterpart. The reader is referred to Coles for an excellent review.

The essential difference in treatment of laminar and turbulent boundary layers is that laminar-boundary-layer theory rests on firm physical grounds, whereas its turbulent counterpart inevitably contains a certain element of arbitrariness due to incomplete understanding of the turbulent shear process. Nevertheless, for the CP case, a quite accurate semi-empirical

formulation has been developed due mainly to the existence of a substantial body of low speed experimental data. Unfortunately, similar data for VP flows is virtually non-existent so that extrapolation of CP concepts for use in high speed flows, is at best, a questionable procedure.

The successful application of a transformation technique requires, of course, the utilization of an adequate CP formulation. This aspect will be discussed in some detail in a subsequent section. However, the particular choice of compressibility transformation is of paramount importance and its selection demands careful scrutiny of the various approaches which have been proposed.

The essential feature of the earliest approach (e.g., Mager and Burggraf) was the assumption that both the Reynolds' stress and the stream function were invariant under the transformation. It was Coles who later suggested that these assumptions were neither warranted nor appropriate. Indeed, by eliminating these arbitrary restraints, he was able to develop a more realistic correspondence in the sense that the thermodynamic state of the companion CP flow was entirely arbitrary.

Despite this significant advance, it was soon found that the Coles transformation exhibited several important weaknesses. Thus, for example, it was shown in Reference 11 that the detailed mapping of velocity profiles obtained in high speed constant pressure flows was incorrect; i.e., the CP "law of the wake" or "defect law" was not recovered. In addition, the values of skin friction coefficient inferred from the transformed profiles were in considerable disagreement with the experimental data. This latter deficiency was apparently eliminated, at least for flows with moderate heat transfer, by replacing Coles "substructure" hypothesis by the so-called "sub-layer" hypothesis as outlined in Reference 11.

Additional evidence of the original transformation inability to properly transform the wake region of VP velocity profiles was presented in Reference 12. Here, extension to the case of mass transfer at constant pressure was developed by modifying the Coles stretching for the stream function. Analysis of a series of velocity profiles obtained with helium injection indicated that the wake portion of the profiles was systematically distorted with increasing helium wall concentration. Ultimately, it was shown that this distortion could be correlated by means of a density ratio across the boundary layer. A more detailed discussion of

this aspect may be found in Reference 13 which constitutes Part II of this report.

Of added significance were the findings reported by Bertram, Reference 14. Here, it was shown that for flows with high heat transfer the Baronti-Libby form of the transformation (Reference 11) tended to overestimate the skin-friction coefficient. In Reference 13 this anamolous behavior was examined in detail and it was found that this defect could be eliminated by utilizing a modified form of the transformation which associates a high speed constant pressure flow with heat transfer to a CP counterpart with mass transfer. Basically, the difference between this form of the transformation and that developed in Reference 11 is due to the use of differing "closure" principles to complete the formulation. Thus, in Reference 11 it is assumed, a priori, that zero mass transfer and pressure gradient map to zero mass transfer and pressure gradient whereas in Reference 13 only the identity mapping for zero pressure gradient is imposed. Closure is then obtained by satisfying the first compatability condition on the differential equation for momentum with the mass transfer considered to be an arbitrary parameter. It is interesting to note that the closure rule utilized by Libby and Baronti, Reference 15, is the exact opposite of the aforementioned; i.e., zero mass transfer is assumed to prevail in both planes while the pressure gradients are related by means of the first compatability condition. Lewis, Reference 16, first examined the possibility of treating flows with both mass transfer and pressure gradient and utilized both the first and second compatability relations to obtain closure. However, his development was somewhat restrictive and implied that the condition $\rho\mu$ = constant was a necessary condition for application of the compressibility transformation to this more general case. However, in Reference 13, it is shown that this is not a necessary condition and a more general set of compatability conditions are evolved which permit application of this methodology to flows where the thermodynamic behavior is quite arbitrary.

The main point of the foregoing discussion is to emphasize that, at the present time, the concept of a compressibility transformation is still in a developmental stage. Many questions remain to be answered in this area and several important anamolies still need to be resolved. Nevertheless, the approach which was utilized in this study is believed to be the best which can be formulated at this time. Specifically, there is utilized herein the interpretation of the compressibility transformation proposed

in Reference 15 since a CP formulation with simultaneous pressure gradient and mass transfer is not currently available. Accordingly, it is recognized, at the outset, that the resulting analysis will not be strictly applicable for the high heat transfer case; i.e., $W \lesssim 0.4$. The analysis also incorporates the empirical correlation developed in Reference 13 which eliminates the distortion of the defect region of the velocity profiles. Since this correlation was developed by examination of zero pressure gradient profiles it is not known whether it is strictly applicable to flows with pressure gradient. Nevertheless, it was included herein in order that the general analysis, when applied to zero pressure gradient flows, yield the improved representation which this correlation provides.

This transformation was used in conjunction with a suitable CP formulation and integral techniques to provide a description of the fluid mechanical behavior. The thermodynamics is described by means of a finite-difference solution of the conservation equation for total enthalpy. The details of this development are given in the next section while the resulting computer program is described in Part III of this report. Finally numerical results are compared with other prediction techniques as well as with experimental results.

SYMBOLS

A	constant, taken here to be 2.43
A_{ij}	elements of ordinary differential equations, c.f., Appendix A and Eq. (57)
A_m^n, B_m^n, C_m^n	tri-diagonalized elements of the finite-difference form of the energy equations, c.f., Eq. (62)
a_m, b_m c_m	functions of variable-grid-system and initial step size, c.f., definitions following Eq. (62).
b	constant, taken here to be 7.5
c_f	skin friction coefficient
C_i	column vector relating to right-hand-side of the system of ordinary differential equations, c.f., Appendix A and Eq. 57)
F_m^n	column vector relating to right-hand-side of the finite-difference form of the energy equation, c.f., Eq. (62)
$f_1, f_2,$ f_3	functional forms, c.f., Eq. (60)
G_j	coefficients of power series relating $g=g(\tilde{\psi})$, c.f., Appendix B
G_{ij}	functional form, c.f., Appendix B, Eq. (B5)
$\bar{G}_{ij}$	functional form, c.f., Appendix B, Eq. (B6)
$\tilde{G}_{ij}$	functional form, c.f., Appendix B, Eq. (B7)
$\tilde{\bar{G}}_{ij}$	functional form, c.f., Appendix B, Eq. (B8)
g	total enthalpy ratio, H/H_e
H	form factor or total enthalpy, ft^2/sec^2
$\tilde{H}_e$	H_e/h_e
h	static enthalpy, ft^2/sec^2

$I_1(\bar{\eta})$	integral of velocity distribution, $\int_o^{\bar{\eta}} \tilde{u} d\bar{\eta}$
$I_2(\bar{\eta})$	integral of velocity distribution, $\int_o^{\bar{\eta}} \tilde{u}^2 d\bar{\eta}$
$I_3(\bar{\eta})$	integral of density distribution, $\int_o^{\bar{\eta}} (1/\tilde{\rho}-1) d\bar{\eta}$
K	conducitivity, lb/sec ^oR
L	reference length, ft.
ℓ	mixing length
M_e	external Mach number
p; P	pressure, lb/ft^2; correlation parameter
P_e	"effective" Prandtl number, c.f., Eq. (4)
P_L	laminar Prandtl number
P_T	turbulent Prandtl number
P_t	turbulent Prandtl number based upon static temperature, c.f., Eq. (6)
$q_1, q_2, q_3 \cdots q_6$	functional forms, c.f., Appendix A
R_θ	Reynolds number based on momentum thickness
R_e/L	unit Reynolds number, 1/ft.
R_y	Reynolds number based on local external conditions and normal coordinate
$\bar{R}$	Reynolds number based upon boundary layer height; $(\bar{\rho}\ \bar{u}_{e,o}\bar{\delta}/\bar{\mu})$
R_j	coefficients of the power series expansion relating $\tilde{\rho}\tilde{\mu}$ to $\tilde{\psi}$, c.f., Eq. (66)
R_{ij}	functional form, c.f., Eq. (68)
r	radius of body of revolution, ft.
T	temperature, ^oR
$\bar{U}_e$	$\bar{u}_e/\bar{u}_{e,0}$
u,v	velocities respectively along and normal to body, ft/sec
$\bar{u}_\tau$	shearing velocity, $(\bar{\tau}_w/\bar{\rho})^{\frac{1}{2}}$, ft/sec
W	T_w/T_{t_e}
x,y	space coordinates respectively along and normal to body, ft/sec

$\overline{y}^+$	local Reynolds number based on shear velocity, $(\overline{\rho} u_\tau \overline{y}/\overline{\mu})$
$\overline{\alpha}$	variable-grid-system parameter, c.f., Fig. 4
β	parameters in the description of the incompressible eddy viscosity, c.f., Eq. (42a) and (42b)
Γ	functional form, $(1/\overline{y}^+)_s \int_o^{\overline{y}^+} (1/\tilde{\rho}) d\overline{y}^+$
γ	adiabatic exponent or intermittancy, c.f., Eq. (73)
δ	boundary layer height, ft.
δ^*	displacement thickness, ft.
ϵ	kinematic eddy viscosity, ft^2/sec
$\overline{\eta}$	$\overline{y}/\overline{\delta}$
$\overline{\eta}^*$	0.5
$\tilde{\eta}$	$\eta \rho_e/\overline{\rho}$
Θ	$(\tilde{\rho}/\tilde{\mu})_s$
θ	momentum thickness, ft
μ	molecular viscosity, lb sec/ft^2
ν	kinematic viscosity, ft^2/sec
ξ, η, σ	Coles scaling parameters
π	Coles wake parameter
$(\pi)_{corr}$	wake parameter obtained from correlation, Eq. (71)
ρ	density, lb sec^2/ft^4
Σ	incompressible momentum thickness normalized with respect to boundary layer height
$\tilde{\sigma}$	$\sigma \mu_e/\overline{\mu}$
τ	shear stress, lb/ft^2
Φ_1, Φ_2	functional forms, c.f., Eq. (60)
$\overline{\omega}$	skin friction parameter, $(\overline{u}_e/\overline{u}_\tau)$
$\chi, \overline{\chi}$	Reynolds numbers based upon an initial unit Reynolds number; $(\rho_e u_e/\mu_e)_o (x-x_o)$; $(\overline{\rho} u_e/\overline{\mu})_o (\overline{x}-\overline{x}_o)$

ψ	stream function
$\bar{\psi}$	$\psi/\bar{\mu}$, $ft^2/lb\text{-}sec$
$\bar{\Omega}$	incompressible displacement thickness normalized with respect to boundary layer height

Subscripts

a	pertains to axisymmetric problem
e	pertains to conditions external to boundary layer
F.P.	flat plate
L	pertains to laminar flow
T	pertains to turbulent flow
t	pertains to total conditions
s	pertains to laminar sublayer edge
o	initial starting point
w	pertains to wall conditions
I	region from wall to edge of laminar sublayer
II	region from edge of laminar sublayer to edge of boundary layer
2-D	used to differentiate between two-dimensional problems and axisymmetric problem
$( )_{max}$	maximum value within boundary layer
$( )_{min}$	minimum value within boundary layer
∞	free-stream conditions

Superscripts

$( )'$	$d/d\bar{x}$
$(\tilde{})$	normalization with respect to corresponding external value unless otherwise noted, i.e., $\tilde{u} = u/u_e$
$(\bar{})$	pertains to properties in incompressible plane unless otherwise noted

II. GENERAL FORMULATION

A. Fundamental Describing Equations for the VP Flow

The conservation equations describing the mean properties of a two-dimensional turbulent compressible boundary layer flow are taken to be the same as for laminar flow with the molecular transport coefficients replaced by their turbulent counterparts. It is further assumed that the requisite transport parameters can be related to each other. That is, the concept of an effective Prandtl number is introduced to relate eddy conductivity to eddy viscosity. Accordingly, the conservation equations in coordinates normal and parallel to the body are taken to be*

Mass

$$\frac{\partial}{\partial x}(\rho u) + \frac{\partial}{\partial y}(\rho v) = 0 \tag{1}$$

Momentum

$$\rho u \frac{\partial u}{\partial x} + \rho v \frac{\partial u}{\partial y} = -\frac{dp_e}{dx} + \frac{\partial}{\partial y}\left[(\rho\epsilon+\mu)\frac{\partial u}{\partial y}\right] \tag{2}$$

Energy

$$\rho u \frac{\partial g}{\partial x} + \rho v \frac{\partial g}{\partial y} = \frac{\partial}{\partial y}\left[\frac{(\rho\epsilon+\mu)}{P_e}\frac{\partial g}{\partial y} + (u_e^2/2H_e)(\rho\epsilon+\mu)(1-1/P_e) \cdot \frac{\partial (u/u_e)^2}{\partial y}\right] \tag{3}$$

---

* For simplicity, the equations for planar flow are set down here. The required modifications for axisymmetric flow are discussed in Appendix C .

where

$g \equiv H/H_e$ = stagnation enthalpy ratio

$\rho\epsilon \equiv$ turbulent eddy viscosity

$\mu \equiv$ molecular viscosity

The effective Prandtl number, P_e, is defined as

$$P_e = \{[P_L(1+ \rho\epsilon/\mu)]^{-1} + [P_T(1 + \mu/\rho\epsilon)]^{-1}\}^{-1} \tag{4}$$

where subscripts L and T refer to laminar and turbulent properties, respectively. It should be noted that as

$$(\rho\epsilon + \mu) \rightarrow \mu \; ; \; P_e \rightarrow P_L$$

while for

$$(\rho\epsilon+\mu) \rightarrow \rho\epsilon \; ; \; P_e \rightarrow P_T$$

To generate Equation (4) it is tacitly assumed that the conductivity K, is the sum of the laminar and turbulent counterparts and that

$$K = K_L + K_T = [(\rho\epsilon+\mu)/P_e] \tag{5}$$

The turbulent Prandtl number P_T as used in Equation (4) can be referred to as the "total" Prandtl number since it is associated with total enthalpy gradients. Recently, Bushnell and Beckwith, Ref. 17, reviewed the relation between this Prandtl number and that which is associated with static enthalpy gradients; namely, P_t. Neglecting third order correlations, they concluded that the relation between P_T and P_t is given by

$$P_T = P_t \left\{ 1 + \frac{u_e^2}{2H_e} (P_t - 1) \frac{\partial \tilde{u}^2/\partial y}{\partial g/\partial y} \right\}^{-1} \tag{6}$$

By considering a power-law dependence between $(g-g_w)/(1-g_w)$ and $\tilde{u}$ ranging from approximately 1 for flat plate flows to 2 for nozzle flows and examining available data for P_t at various Mach numbers and wall enthalpy ratios, they imply and later demonstrate, that P_T must depend on the upstream history of the flow. In particular, it is shown that the quadratic variation between enthalpy ratio and velocity ratio, which has been observed for tunnel wall boundary layers could be accounted for by choosing values of P_T greater than unity.

In the general formulation which is discussed in Section II.F.5 spatial variation of P_T can be introduced by means of subroutines which allow the use of various models. Thus, as done in Ref. 17, Equation (6) could be introduced if deemed appropriate.

Stream Function

In the ensuing development it will prove convenient to introduce the stream function $\psi(x,y)$ which satisfies Equation (1) identically and is related to the velocity components by

$$\rho v = \frac{\partial \psi}{\partial y} \qquad \rho u = - \frac{\partial \psi}{\partial x} \tag{7}$$

Boundary Conditions

The external boundary conditions are taken to be

$$u \to u_e(x) \; ; \; g \to 1 \; @ \; y \to \infty \tag{8}$$

so that, in particular, Equation (2) yields

$$\rho_e u_e \frac{du_e}{dx} = - \frac{dp_e}{dx} \tag{9}$$

while at the wall the "no slip" condition and the existence of a laminar sublayer requires

$$v,u \to 0 \; ; \; \rho\epsilon \to \mu_w \; ; \; g \to g_w ; \; P_e \to P_{L_w} \; @ \; y \to 0 \tag{10}$$

In this case Equation (2) yields

$$\rho_e u_e \frac{du_e}{dx} + \left(\frac{\partial \tau}{\partial y} \right)_w = 0 \qquad (11)$$

where we have used (9) with $\tau \equiv \mu \partial u/\partial y$. The remaining variables, ρ, g, and/or their derivatives can formally be considered to take on their respective wall values. In practice, of course, the latter would be evaluated by specification of one of several heat exchange configurations at the surface (e.g., adiabatic wall, specified wall temperature, etc.) together with appropriate thermodynamic relations.

B. The Transformation Relations and Their Immediate Implications

After Coles, Ref. 9, there are now introduced three scaling quantities which relate the spatial coordinates and fluid dynamic variables of the VP flow with those of a companion CP flow described by

$$\frac{\partial \bar{u}}{\partial \bar{x}} + \frac{\partial \bar{v}}{\partial \bar{y}} = 0 \qquad (12)$$

$$\overline{\rho u} \frac{\partial \bar{u}}{\partial \bar{x}} + \overline{\rho v} \frac{\partial \bar{u}}{\partial \bar{y}} = - \frac{d\bar{p}_e}{d\bar{x}} + \frac{\partial}{\partial \bar{y}} \left[(\overline{\rho \epsilon} + \bar{\mu}) \frac{\partial \bar{u}}{\partial \bar{y}} \right] \qquad (13)$$

$$\overline{\rho u} = \frac{\partial \bar{\psi}}{\partial \bar{y}} \qquad \overline{\rho v} = - \frac{\partial \bar{\psi}}{\partial \bar{x}} \qquad (14)$$

where $\bar{\rho}$ and $\bar{\mu}$ are constants. In the further development the scaling parameters will be modified somewhat in order to insure that the physical properties of the CP flow, $\bar{\rho}$, $\bar{\mu}$ do not appear explicitly in the analysis. Specifically, the two flows are assumed related according to*

$$\bar{\psi}(\bar{x}, \bar{y}) = \sigma(x) \psi(x, y) \qquad (15)$$

* As indicated in Section I, closure of the transformation in the present formulation is obtained by mapping zero wall mass transfer to zero wall mass transfer. For a more generalized formulation it would be necessary to replace Eq. (15) with a modified stream function stretching of the form $\bar{\psi} - \bar{\psi}_w = \sigma(\psi - \psi_w)$ where $\bar{\psi}_w, \psi_w$ represent the wall values of stream function. This aspect is discussed in more detail in Reference 13.

$$\partial\bar{y} = (\rho/\bar{\rho})\ \eta(x)\ \partial y \tag{16}$$

$$d\bar{x} = \xi(x)\ dx \tag{17}$$

In terms of these transformation functions the partial derivatives are related by

$$\frac{\partial}{\partial x} = \xi \frac{\partial}{d\bar{x}} + \frac{\partial \bar{y}}{\partial x} \frac{\partial}{\partial \bar{y}} \tag{18}$$

$$\frac{\partial}{\partial y} = \eta \frac{\rho}{\bar{\rho}} \frac{\partial}{\partial \bar{y}}$$

Application of these rules to the definition of the stream functions, Eq. (7) and (14) yields

$$u/\bar{u} = \eta/\sigma \tag{19}$$

$$\rho v = (\xi/\sigma)(\overline{\rho v}) + \psi\ (d\ln\sigma/dx) - (\overline{\rho u}/\sigma)(\partial\bar{y}/\partial x) \tag{20}$$

Thus, an immediate implication of Eq. (19) is

$$u_e/\bar{u}_e = \eta/\sigma \tag{21}$$

so that

$$u/u_e = \bar{u}/\bar{u}_e$$

Furthermore, as a consequence of Eq. (21) the following correspondence between external conditions, initial conditions and the mapping function is obtained:

$$(\ln \tilde{\sigma})' - (\ln \tilde{\eta})' - (\ln \bar{U}_e)' + [d\ \ln(u_e/\nu_e)/dx](\chi)' = 0 \tag{22}$$

where

$$\tilde{\sigma} \equiv \sigma\mu_e/\bar{\mu} \tag{23a}$$

$$\tilde{\eta} \equiv \eta\rho_e/\bar{\rho} \tag{23b}$$

$$U_e \equiv \bar{u}_e/\bar{u}_{e,0} \tag{23c}$$

$$\chi \equiv (u_{e,0}/\nu_{e,0})(x-x_o) \tag{23d}$$

$$\bar{\chi} \equiv (\bar{u}_{e,0}/\bar{\nu})(\bar{x}-\bar{x}_o) \tag{23e}$$

$$(\,)' \equiv d/d\bar{\chi}$$

and where the subscript zero refers to an initial streamwise station. In addition to the correspondence between the two external flows afforded by Eq. (22), two other inferences may be developed by applying the transformation to the two flows as $y, \bar{y} \to 0$. Since Newtonian shear is assumed to apply there, then

$$\tau_w = (\mu\ \partial u/\partial y)_w, \quad \bar{\tau}_w = \bar{\mu}(\partial\bar{u}/\partial\bar{y})_w \tag{24}$$

Thus, imposing the mapping rules to Eq. (24) and defining a skin friction coefficient for the two flows in the usual way yields

$$c_f/\bar{c}_f = \tilde{\sigma}(\tilde{\rho}\tilde{\mu})_w \tag{25}$$

where

$$\tilde{\rho} \equiv \rho/\rho_e$$

$$\tilde{\mu} \equiv \mu/\mu_e$$

A similar procedure applied to Equation (11) and the corresponding one for the CP flow yields

$$(\ln U_e)' - (\tilde{\eta}/\tilde{\sigma})_o (1/\tilde{\rho})_w (\tilde{\rho}_w\tilde{\mu}_w)^{-1} (\tilde{\sigma}\tilde{\eta})^{-1} (d\ \ln u_e/d\chi)$$

$$- (\tilde{\eta}/\tilde{\sigma})_o\ (\bar{\varphi})^{-2} (u_e/\nu_e)_o^{-1}\ [\partial/\partial\bar{y}\ \ln\ \tilde{\rho}\tilde{\mu}]_w = 0 \tag{26}$$

where from Eq. (21) and (23) the initial values of $\tilde{\eta}$ and $\tilde{\sigma}$, i.e., $\tilde{\eta}_o$ and $\tilde{\sigma}_o$ are related by

$$[\bar{u}_e/\bar{\nu}]_o/[u_e/\nu_e]_o = (\tilde{\sigma}/\tilde{\eta})_o \tag{27}$$

The quantity $\bar{\varphi}$ is a convenient parameter appearing in the CP formulation to which these correspondence laws are coupled and which is to be described subsequently. It is defined by

$$\bar{\varphi} \equiv (\bar{u}_e/\bar{u}_\tau) \equiv \sqrt{(2/\bar{c}_f)} \tag{28}$$

where $\bar{u}_\tau$ denotes the shearing velocity, i.e.,

$$\bar{u}_\tau \equiv (\bar{\tau}_w/\bar{\rho})^{\frac{1}{2}} \tag{29}$$

Equation (26) which is interpreted as relating the scaling parameters $\tilde{\sigma}$, $\tilde{\eta}$ to the unknown velocity distribution $\bar{U}_e$ and to the known velocity distribution $u_e(x)$, indicates that a zero pressure gradient flow in the physical plane maps into a zero pressure gradient flow in the transformed plane if and only if $\rho\mu$ = constant, this implies that either $\mu \sim T$ or the flow is adiabatic.

C. The Momentum Integral Conditions

In addition to the above compatibility condition, there is now imposed the requirement that the scaling parameters are to be selected so that the integral form of the VP momentum equation maps into the corresponding form for the CP flows.

The momentum integral equation for compressible flow is

$$\frac{d\theta}{dx} + \theta\left\{2\frac{d\ \ln u_e}{dx} + \frac{d\ \ln \rho_e}{dx}\right\} + \delta^* \frac{d\ \ln u_e}{dx} = \frac{\tau_w}{\rho_e u_e^2} = \frac{c_f}{2} \tag{30}$$

where θ and δ^* are respectively the momentum and displacement

thicknesses. The corresponding thicknesses in the CP flow are $\bar{\theta}$ and $\bar{\delta}^*$ and it is quite easy to show that the transformation requires

$$\theta = \bar{\theta}/\tilde{\eta} \tag{31}$$

while for the displacement thicknesses the relationship is

$$\delta^* = (1/\tilde{\eta}) \left[\int_0^{\bar{\delta}} (1/\tilde{\rho}-1)d\bar{y} + \bar{\delta}^* \right] \tag{32}$$

Accordingly, normalizing the CP thicknesses by the boundary layer height and defining

$$\bar{\Sigma} \equiv \bar{\theta}/\bar{\delta}$$

$$\bar{\Omega} \equiv \bar{\delta}^*/\bar{\delta}$$

$$\bar{\eta} \equiv \bar{y}/\bar{\delta}$$

Equations (31) and (32) imply that the VP form factor (δ^*/θ) transforms like

$$\delta^*/\theta = (1/\bar{\Sigma}) \left[\int_0^1 (1/\tilde{\rho}-1)d\bar{\eta} + \bar{\Omega} \right] \tag{33}$$

Consider now the correspondence between θ and $\bar{\theta}$ and define a Reynolds number based on boundary layer height as

$$\bar{R} \equiv (\tilde{u}_{e,0}/\bar{\nu}) \ (\bar{\delta})$$

Then from the definition for $\bar{\Sigma}$ and the fact that $\chi = \chi(\bar{\chi})$, the χ-wise variation of θ is given by

$$\frac{d\ln\theta}{d\chi} = \frac{1}{(\chi)'}\,\{(\ln\bar{\Sigma})' + (\ln\bar{R})' - (\ln\tilde{\eta})'\}$$

However, the momentum integral equation in the CP plane can be shown to be

$$(\ln\bar{R})' + (\ln\bar{\Sigma})' + (\ln\bar{U}_e)'\,[2+\bar{\Omega}/\bar{\Sigma}] = (\bar{\varphi}^2\overline{R\Sigma})^{-1} \qquad (34)$$

which when substituted into the above expression yields

$$\frac{d\ln\theta}{d\chi} = \frac{1}{(\chi)'}\,[(\bar{\varphi}^2\overline{R\Sigma})^{-1} - (\ln\bar{U}_e)'\,(2+\bar{\Omega}/\bar{\Sigma}) - (\ln\tilde{\eta})']$$

or, in view of Equation (22)

$$\frac{d\ln\theta}{d\chi} = \frac{1}{(\chi)'}\,\{(\bar{\varphi}^2\overline{R\Sigma})^{-1} - (2+\bar{\Omega}/\bar{\Sigma})\,[(\ln\tilde{\sigma})' + (\chi)'\,\left(\frac{d\ln u_e/\nu_e}{dx}\right)]$$

$$+ (\ln\tilde{\eta})'\,(1+\bar{\Omega}/\bar{\Sigma})\,\} \qquad (35)$$

Finally, substitution of Equations (35) and (25) in Equation (30) yields after some manipulations the requirement that for the VP momentum integral equation to transform to its CP counterpart it is necessary that

$$-(\ln\tilde{\sigma})'\,(2+\bar{\Omega}/\bar{\Sigma}) + (\ln\tilde{\eta})'\,(1+\bar{\Omega}/\bar{\Sigma}) + (\chi)'\left\{\frac{d\ln u_e}{d\chi}\,\left[\frac{\delta^*}{\theta} - \frac{\bar{\Omega}}{\bar{\Sigma}}\right]\right.$$

$$\left. + \frac{d\ln\mu_e}{d\chi}\,\left[2+\frac{\bar{\Omega}}{\bar{\Sigma}}\right] - \frac{d\ln\rho_e}{d\chi}\,\left[1+\frac{\bar{\Omega}}{\bar{\Sigma}}\right] - (\bar{\varphi}^2\overline{R\Sigma})^{-1}\,(\tilde{\sigma}\tilde{\sigma}_o)\,(\tilde{\eta}/\tilde{\eta}_o)\,(\tilde{\rho}\tilde{\mu})_w\right\}$$

$$= -(\bar{\varphi}^2\overline{R\Sigma})^{-1} \qquad (36)$$

In summary, the previous sections have shown that the system of equations describing the velocity field of interest in the VP plane, namely Equations (1) and (2) can be transformed to their respective CP counterparts by introduction of the transformation relations in Equations (15), (16) and (17) provided that the correspondences between gross boundary-layer-parameters are represented by Equations (21), (22), (25), (26), (31), (33), (34), and (36).

It is significant to note at this junction that these correspondences involve the functions $[\partial/\partial\bar{y} \ln \rho\mu]_w$ and $\int_0^{\bar{\eta}} [(1/\tilde{\rho})-1]d\bar{y}$. Evidently, their evaluation requires a knowledge of the energy field within the viscous layer. One possible approach is the utilization of a Crocco integral for total enthalpy, in which case $\tilde{\rho}$ and $\tilde{\mu}$ would be expressible as a function of $\tilde{u}$. Then these functions could be related directly to the present variables. An alternative approach utilizes an "exact" solution of the energy Equation (3) by finite-difference techniques. Both approaches are described in detail in subsequent sections.

D. The Constant Properties Solution

Since successful exploitation of the transformation approach depends to a considerable extent, upon the availability of a suitable constant property formulation, it is relevant to include in this study a discussion of the present status of available prediction methods for the CP flow.

In this connection, it is noted that in recent years Rotta, Ref. 18, 19 and Thompson, Ref. 20 reviewed the then available procedures and concluded that prior to 1966 reasonable performance could be obtained by application of the following methods:

- the entrainment equation of Head, Ref. 21
- the strip-integral method of Moses, Ref. 22
- the application of a constant eddy-viscosity approach of Libby, Baronti, Napolitano, Ref. 23
- the hypothesis of an effective eddy-viscosity proposed by Mellor and Gibson, Ref. 24.

However, their status report indicated that even the best available procedures at that time left room for improvement. Fortunately, due to the re-emergence of interest in turbulent boundary-layer behavior as a practical aerodynamic problem, there have been numerous re-analyses of the boundary layer problem since the Rotta-Thompson reviews. These newer contributions have been categorized and assessed in the recent AFOSR-IFP Conference at Stanford, Ref. 25. It is evident from the Stanford meeting that many of these procedures can make rapid, accurate predictions of the incompressible two-dimensional turbulent boundary layer. High on the list are the strip-integral method of Moses, Ref. 26 and the finite-difference solution of Cebeci and Smith, Ref. 27.

Evidently the preceding development anticipated the use of an integral technique for the current effort. In view of the appraisal made by the AFOSR-IFP Conference on the method of Moses as one of the more applicable integral approaches, it would appear therefore, that this choice is justified. The particular method actually employed is that of Ref. 28 which is virtually identical to that of Moses (Ref. 22) and in particular includes and anticipates a modification which is later introduced by Moses in Ref. 26.

In accordance with the selected method, the development of the boundary layer is described by a set of three equations containing three functions of the streamwise coordinate, i.e., $\overline{c}_f(\overline{x})$, $\overline{\delta}(\overline{x})$ and the Coles (Ref. 29) wake parameter, $\pi(\overline{x})$. The first two describing equations are Coles' skin friction law and the von Karman momentum-integral-equation; the third equation is Moses' auxiliary equation obtained by satisfying the momentum-integral-equation up to half the boundary-layer height. It has been shown in Ref. 28 that a modified form of the Clauser eddy-viscosity-model (Ref. 30) yields improved predictions for flows with adverse pressure gradients. This modification consists of taking the momentum thickness, rather than the displacement thickness as the length scale of the effective eddy viscosity. A similar conclusion was also arrived at by Moses in Ref. 26 as indicated previously.

Thus taking the work of Coles, Ref. 30, as a starting point, a two layer model for the velocity is assumed, i.e.,*

$$\tilde{u} = \begin{cases} \overline{RU}_e \eta / \overline{\varphi}^2 & 0 < \overline{\eta} \leq \overline{\eta}_s \\ (A/\overline{\varphi})\left[\ln\left(b \frac{\overline{RU}_e}{\overline{\varphi}} \overline{\eta}\right) + 2\pi(3\overline{\eta}^2 - 2\overline{\eta}^3)\right] & \eta_s < \eta \leq 1 \end{cases} \tag{37}$$

where use is made of the polynomial approximation of Moses, Ref. 22, to Coles wake function. A direct consequence of Equation (37) is the skin friction law stating that:

$$(A/\overline{\varphi})\left[\ln(\overline{RU}_e b / \overline{\varphi}) + 2\pi\right] = 1 \tag{38}$$

and the representation of the normalized displacement and momentum thicknesses by

$$\overline{\Omega} = (A/\overline{\varphi})\ (1 + \pi) \tag{39}$$

$$\overline{\Sigma} = (A/\overline{\varphi})\{(1+\pi) - (A/\overline{\varphi})[2 + (19/6)\pi + (52/35)\pi^2]\} \tag{40}$$

Besides the momentum-integral-equation, Eq. (34), with the values of $\overline{\Omega}$ and $\overline{\Sigma}$ specified above, and the skin-friction law, Eq. (38), a third equation necessary to link the three variables $\overline{R}$, $\overline{\varphi}$, π to the independent variable, $\overline{x}$, is obtained by integrating the momentum equation to some $\overline{\eta} = \overline{\eta}^* < 1$. The resulting equation is

---

* The constants A and b appearing in Equation (37) are associated with the "law of the wall" and are taken here to be A=2.43, b = 7.5.

$$\frac{\bar{\tau}^* - \bar{\tau}_w}{\bar{\rho}_e \bar{u}_e^2 \bar{R}} = \frac{d}{d\bar{\chi}} \int_o^{\bar{\eta}^*} \tilde{u}^2 d\bar{\eta} - \tilde{u} \frac{d}{d\bar{\chi}} \int_o^{\bar{\eta}^*} \tilde{u} d\bar{\eta} + \frac{d\ln \bar{U}_e}{d\bar{\chi}} \left\{ \int_o^{\bar{\eta}^*} 2\tilde{u}^2 d\bar{\eta} - \right.$$

$$\left. - \tilde{u} \int_o^{\bar{\eta}^*} \tilde{u} d\bar{\eta} - \bar{\eta}^* \right\} + \frac{d\ln \bar{R}}{d\bar{\chi}} \left\{ \int_o^{\bar{\eta}^*} \tilde{u}^2 d\bar{\eta} - \tilde{u} \int_o^{\bar{\eta}^*} \tilde{u} d\bar{\eta} \right\} \tag{41}$$

where $\bar{\tau}^*$ is the value of shear at $\bar{\eta} = \bar{\eta}^*$.

At this point, following Ref. 28, a modified form of the Clauser eddy viscosity model is introduced to describe the shear, $\bar{\tau}$, in terms of the three dependent variables $\bar{R}$, $\bar{\varphi}$, π. As for the right-hand side of Eq. (41) it can be expressed in terms of the same variables with the help of Eq. (37). The modified form of the eddy viscosity model is

$$\epsilon + \nu = \beta \bar{u}_e \bar{\delta}^* \frac{\bar{H}_{F.P.}}{\bar{H}(\bar{\chi})} = \beta' u_e \bar{\theta} \tag{42a}$$

and attempts to account somewhat for the effect of upstream history by the choice of the length scale, $\delta^* \bar{H}_{F.P.}/\bar{H}(\chi)$, rather than the usual scale $\bar{\delta}^*$. With the originally quoted value of the Clauser constant, β, changed from 0.018 to 0.016 (see Refs. 22 and 23), and with the flat-plate value of the form factor, $\bar{H}_{F.P.}$, taken as approximately 1.32 then the eddy-viscosity law becomes

$$(\epsilon + \nu)/\bar{u}_e \bar{\theta} = 0.021 \tag{42b}$$

Noteworthy is that the law used by Moses, Ref. 26, estimates a slightly greater value in that the eddy viscosity assumes the form

$$(\epsilon + \nu)/\bar{u}_e \bar{\theta} = 0.0225 + 125/(\bar{R}\bar{U}_e) \tag{42c}$$

Accordingly, substituting Eq. (37) and (42b) into Eq. (41) and performing the necessary integration and differentiation yields

$$\{\bar{\eta}^*(A/\bar{\varphi})[-4(A/\bar{\varphi})(q_2+2\pi q_3+2\pi^2 q_4)-(\tilde{u}|_{\eta^*}-2)(q_5+2\pi q_6)]\}(\ln\bar{\varphi})' +$$

$$\{\int_0^{\bar{\eta}^*_2}\tilde{u}d\bar{\eta} - \tilde{u}\int_0^{\bar{\eta}^*}\tilde{u}d\bar{\eta}\}(\ln\bar{R})'+\{\bar{\eta}^*(A/\bar{\varphi})[4(A/\bar{\varphi})(q_3+2\pi q_4)-2q_6(\tilde{u}|_{\eta^*}-2)]\}(\pi)'$$

$$+\{2\int_0^{\bar{\eta}^*}\tilde{u}d\bar{\eta} - \tilde{u}\int_0^{\bar{\eta}^*}\tilde{u}d\bar{\eta}-\bar{\eta}^*\}(\ln\bar{U}_e)'-(1/\bar{R})\{\beta'(1+\pi)(A/\bar{\varphi})^2\bar{\eta}^*[(1/\bar{\eta}^*)^2 +$$

$$12\pi(1-\bar{\eta}^*)]-(1/\bar{\varphi})^2\} = 0 \qquad (43)$$

where the integrals and the quantities $q_{1,2,\ldots}$ are defined in Appendix A.

For convenience in the numerical analysis Eq. (38) can be differentiated yielding:

$$(1+\bar{\varphi}/A)(\ln\bar{\varphi})' - (\ln\bar{R})'-2(\pi)'-(\ln\bar{U}_e)' = 0 \qquad (44)$$

In this manner the requisite CP solution is described by the three equations, i.e., Eq. (34), (43), and (44) for the three dependent variables $\bar{\varphi}$, π, $\bar{R}$ with the streamwise Reynolds number $\bar{\chi}$ as the independent variable.

Extensive comparisons of this integral method formulation with experiments appear in References 22, 26 and 28 and indicate good agreement. For completeness, a comparison is also included here between this approach and a representative finite-difference result due to Cebeci and Smith (Ref. 27). As may be seen in Figures 1, 2 and 3 the agreement is quite adequate.

Returning to the general problem, it is seen that the CP formulation has added three additional differential equations i.e., Eq. (34), (43), and (44) to the overall problem and in addition increased the number of dependent variables by one. This additional parameter, π, has been included to reflect the dependence of the velocity profile representation on the varying external pressure distribution. Thus, as it was implied before, assuming that the $\tilde{\rho}\tilde{\mu}$ dependence on $\tilde{u}$ is known and that $u_e(x)$ is specified, the system of six simultaneous differential equations involves a total of eight variables, with $\bar{\chi}$ considered as the independent one.* Since the information which can be extracted from the transformation itself, with regard to a rigorous mathematical correspondence, has been depleted it is necessary to invoke some phenomenological concept as will be now described to complete the system of equations.

E. Determination of the Transformation Parameter $\tilde{\sigma}$ - The Sublayer Hypothesis

As indicated in the introduction the main virtue of the transformation technique used here is that it minimizes empiricism and in particular restricts its use for the most part to the CP flow regime. For the latter type of flow some confidence in earlier heuristic theories has been provided by a substantial body of experimental results. The single exception to this rule is the hypothesis which will now be introduced to determine the stretching parameter $\tilde{\sigma}$ thereby completing the transformation.

The hypothesis involves the assumption that there exists some Reynolds number characterizing the VP boundary layer which is invariant under the transformation. The

---

* It is noted here that had the more general transformation procedure been adopted which accounts concurrently for mass transfer and pressure gradient, then proper implementation of this approach would require a suitable CP formulation in which the above effects occur simultaneously. Since such a formulation is not currently available, mass transfer has been assumed zero in both planes.

particular choice of Reynolds number made by Coles in his initial application was the so-called sub-structure Reynolds number wherin transport properties were evaluated at an average temperature within the fully turbulent law-of-the-wall region of the boundary layer. Crocco (Ref. 10) in a critique of this approach indicates that the particular choice of Reynolds number is not too critical, at least for the adiabatic, zero pressure gradient case. On the other hand, Baronti and Libby (Ref. 11) found that the use of sub-structure Reynolds number gave anomalous results with respect to the transformation of the VP velocity profiles. In particular, for external Mach numbers exceeding approximately 2.0 they found that the "law of the wall" was not recovered upon transformation of the profiles to CP form. Improved correlation of the profiles was obtained by introduction of a new hypothesis which postulates the invariance of the sublayer Reynolds number; i.e., a Reynolds number based on properties at the interface between the sublayer and the "law of the wall" region. Evidently this later hypothesis also has appeal on physical grounds since this Reynolds number can be loosely interpreted as a minimum Reynolds number below which laminar flow prevails. Further evidence of the appropriateness of this hypothesis was presented in Ref. 15 in connection with a study of constant pressure VP flows involving mass addition.

In view of these developments the sublayer hypothesis is utilized in this current formulation. It is expressed by the relation

$$\frac{\rho_s u_s y_s}{\mu_s} = \frac{\overline{\rho u}_s \bar{y}_s}{\bar{\mu}} \tag{45}$$

where subscript s corresponds to sublayer values. If the transformation is applied to Eq. (45) there results

$$\tilde{\sigma} = \left(\frac{\tilde{\rho}_s}{\bar{\mu}_s}\right) \frac{1}{\bar{y}_s} \int_0^{\bar{y}_s} \frac{d\bar{y}}{\tilde{\rho}} = \frac{\tilde{\rho}_s}{\bar{\mu}_s} \frac{1}{\bar{y}_s^+} \int_0^{\bar{y}_s^+} \frac{d\bar{y}^+}{\tilde{\rho}} \tag{46}$$

Although Eq. (46) provides the final relation required to complete the system of equations it should be noted that once again there is required a knowledge of the thermodynamic behavior of the VP fluid. Determination of this behavior and a development of the final form of the working equations are presented in the following sections.

F. Description of the Thermodynamic Behavior and Final Form of the Working Equations

1. Simplified Approach

Before proceeding with the development of a more accurate description of the thermodynamic behavior of means of a finite-difference solution of Eq. (3) it is worthwhile to consider the simplifications afforded by, and the ramifications associated with, the use of a Crocco integral as the necessary equation for relating $\tilde{\rho}$, $\tilde{\mu}$, etc. to the velocity distribution $\tilde{u}$. Of course, severe limitations must be placed on any analysis utilizing such an approach since the validity of the Crocco integral as a solution of Eq. (3) is restricted to rather specialized cases. Among those which may be cited are the requirements of unity Prandtl number and constancy of edge and wall conditions. Nevertheless, some success in describing boundary layer behavior has been achieved by utilization of this approach even for problems involving substantial violations of the restrictions mentioned above. Since its implementation requires relatively little effort a numerical program based on exploitation of the approach was deemed appropriate. Accordingly, a numerical computer program based on the following considerations has been developed.

The Expressions for $\tilde{\rho}$, $\tilde{\mu}$, $\tilde{\sigma}$

It is assumed that the total enthalpy ratio within the viscous layer can be represented by the relation

$$g = g_w + (1-g_w)\tilde{u} \tag{47}$$

Then for a perfect gas, the density-velocity relation is simply

$$(1/\tilde{\rho}) = \tilde{H}_e\,[g_w + (1-g_w)\tilde{u}] + (1-\tilde{H}_e)\,\tilde{u}^2 \qquad (48)$$

where $\tilde{H}_e$ is defined as the ratio between edge total and static enthalpy. Then the integral

$$I_3(\bar{\eta}) \equiv \int_o^{\bar{\eta}} \left(\frac{1}{\tilde{\rho}} - 1\right) d\bar{\eta}$$

and the term

$$\left[\frac{\partial}{\partial \bar{y}} \ln\bar{\rho}\right]_w$$

can be expressed in terms of the dependent variables. In particular, it can be shown that

$$I_3(\bar{\eta}) = (\tilde{H}_e g_w - 1)\bar{\eta} + \tilde{H}_e(1-g_w) I_1(\bar{\eta}) + (1-\tilde{H}_e) I_2(\bar{\eta}) \qquad (49)$$

where

$$I_1(\eta) \equiv \int_o^{\bar{\eta}} \tilde{u}\, d\bar{\eta}$$

and

$$I_2(\eta) \equiv \int_o^{\bar{\eta}} \tilde{u}^2\, d\bar{\eta}$$

can be obtained once Eq. (37) is substituted for $\tilde{u}$. For the second term, the transformation formulae give

$$\left(\frac{\partial \ln\tilde{\rho}}{\partial \bar{y}}\right)_w = -\frac{(1-g_w)}{g_w}\,\frac{\bar{U}_e}{\bar{\varphi}^2}\,(\tilde{\sigma}_o/\tilde{\eta}_o)\,(u_{e,0}/\nu_{e,0}) \qquad (50)$$

For the terms involving viscosity, two choices are utilized. One of these is a power law variation such that

$$\tilde{\mu} = (1/\tilde{\rho})^n \qquad (51a)$$

implying that

$$\left(\frac{\partial}{\partial y}\ln\tilde{\mu}\right)_w = +\,n\,\frac{(1-g_w)}{g_w}\left(\bar{U}_e/\bar{\varphi}^2\right)\left(\tilde{\sigma}_o/\tilde{\eta}_o\right)\left(u_{e,0}/\nu_{e,0}\right)$$

In this case the term $[\partial/\partial\bar{y}\ \ln\tilde{\rho}\tilde{\mu}]_w$ appearing in Eq. (26) becomes

$$[\partial/\partial\bar{y}\ \ln\tilde{\rho}\tilde{\mu}]_w = -(1-n)\ \frac{(1-g_w)}{g_w}\left(\bar{U}_e/\bar{\varphi}^2\right)\left(\tilde{\sigma}_o/\tilde{\eta}_o\right)\left(u_{e,0}/\nu_{e,0}\right) \tag{52a}$$

Also the term ρ_s/μ_s which appears in Eq. (46) can be written

$$\Theta \equiv \frac{\tilde{\rho}_s}{\tilde{\mu}_s} = (\tilde{\rho}_s)^{1+n} \tag{53a}$$

In the second case, the Sutherland law is used. In terms of the variables used here this can be expressed as

$$\tilde{\mu} = \frac{\left(1 + \frac{198.6}{T_{t_e}}\tilde{H}_e\right)\left(\frac{1}{\tilde{\rho}}\right)^{3/2}}{(1/\tilde{\rho}) + \frac{198.6}{T_{t_e}}\tilde{H}_e} \tag{51b}$$

Then instead of Eq. (52a) the following equation can be substituted into Eq. (26):

$$\left[\frac{\partial}{\partial\bar{y}}\ln\tilde{\rho}\tilde{\mu}\right]_w = \frac{(1-g_w)}{g_w}\left(\frac{\bar{U}_e}{\bar{\varphi}^2}\right)\left(\frac{\tilde{\sigma}_o}{\tilde{\eta}_o}\right)\left(\frac{u_{e,0}}{\nu_{e,0}}\right)\left\{\frac{3}{2} - \frac{g_w}{g_w + 198.6/T_{t_e}}\right\} \tag{52b}$$

while, in lieu of (53a) there is obtained

$$\epsilon \equiv \frac{\tilde{\rho}_s}{\tilde{\mu}_s} = \left(\frac{1}{\tilde{\rho}_s}\right)^{(1/2)} \frac{\frac{1}{\tilde{\rho}_s} + \frac{198.6}{T_{t_e}} \tilde{H}_e}{1 + \frac{198.6}{T_{t_e}} \tilde{H}_e} \tag{53b}$$

To complete the formulation $\tilde{\rho}_s$ and the integral appearing in Eq. (46), namely

$$\Gamma \equiv \frac{1}{\bar{y}_s^+} \int_0^{\bar{y}_s^+} \frac{d\bar{y}^+}{\tilde{\rho}}$$

must be expressed in terms of the basic dependent variables. Here it should be noted that the integration is to be performed only up to the edge of the laminar sublayer. Within this region the velocity profile takes on the form

$$\tilde{u} = \frac{\bar{u}}{\bar{u}_\tau} \frac{1}{\tilde{c}} = (\bar{y}^+/\bar{\varphi})$$

where $\bar{y}^+$ defines a Reynolds number based upon the shearing velocity, $\bar{u}_\tau$, i.e.,

$$\bar{y}^+ \equiv \bar{u}_\tau \bar{y}/\bar{\nu}$$

For the particular values of the law-of-the-wall constants which are used in this formulation $\bar{y}^+$ takes on the value 10.6 at the laminar sublayer edge. Then the density at this height is obtained from

$$(1/\tilde{\rho})_s = \tilde{H}_e[g_w + 10.6(1-g_w)/\bar{\pi}] + 112.36\ (1-\tilde{H}_e)/\bar{\varphi}^2$$

while integration yields

$$\Gamma = \frac{1}{\bar{y}_s^+} \int_0^{\bar{y}_s^+} (1/\tilde{\rho})\, d\bar{y}^+ = \tilde{H}_e[g_w + 5.3(1-g_w)/\bar{\varphi}] + 37.45(1-\tilde{H}_e)/\bar{\varphi}^2 \tag{54}$$

Accordingly, Eq. (46) may be written

$$\ln \tilde{\sigma} = \ln \Gamma + \ln \Theta \tag{55a}$$

where Γ is given by Eq. (54) while Θ is expressed by either (53a) or (53b) depending on the choice of viscosity-temperature variation. It is important to note from these relations that the quantity $\tilde{\sigma}$ has the functional form

$$\tilde{\sigma} = \tilde{\sigma}\ (\chi, \bar{\varphi})$$

where the dependence on χ, enters through the possible variation of both $\tilde{H}_e$ and g_w.

2. Final Form of the Working Equations

In this section the various equations which are required for determination of the VP boundary layer behavior are presented in final form suitable for numerical integration. In this system the basic dependent variables are taken to be $\bar{\varphi}$, π, $\bar{R}$, $\bar{U}_e$, $\tilde{\sigma}$, $\tilde{\eta}$, χ with the CP Reynolds number $\bar{\chi}$ considered as the independent variable. Once these have been evaluated, θ, δ^*, c_f, etc. follow from the various auxiliary equations which have been derived. Also for numerical convenience the algebraic equation for $\tilde{\sigma}$ is differentiated. Thus, considering the definitions of Γ and Θ which go into the expression for $\tilde{\sigma}$ and considering their relation to the dependent variables, it can be shown that formally

$$(\ln\tilde{\sigma})' - \left[\frac{1}{\Gamma}\frac{d\Gamma}{d\chi} + \frac{1}{\Theta}\frac{d\Theta}{d\chi}\right](\chi)' - \left[\frac{\bar{\varphi}}{\Gamma}\frac{d\Gamma}{d\bar{\varphi}} + \frac{\bar{\varphi}}{\Theta}\frac{d\Theta}{d\bar{\varphi}}\right](\ln\bar{\varphi})' = 0 \tag{55b}$$

can be used instead of Eq. (55a). In addition to the above equation, the complete system of differential equations,

includes Eqs. (22),(26),(34),(36),(43), and (44). The matric representation of this system is

$$\begin{bmatrix} A_{11} & A_{12} & A_{13} & A_{14} & 0 & 0 & 0 \\ A_{21} & A_{22} & A_{23} & A_{24} & 0 & 0 & 0 \\ A_{31} & A_{32} & A_{33} & A_{34} & 0 & 0 & 0 \\ 0 & 0 & 0 & A_{44} & 0 & 0 & 0 \\ A_{51} & 0 & 0 & 0 & A_{55} & 0 & A_{57} \\ 0 & 0 & 0 & A_{64} & A_{65} & A_{66} & A_{67} \\ 0 & 0 & 0 & 0 & A_{75} & A_{76} & A_{77} \end{bmatrix} * \begin{bmatrix} (\ln\bar{\sigma})' \\ (\pi)' \\ (\ln\bar{R})' \\ (\ln\bar{U}_e)' \\ (\ln\tilde{\sigma})' \\ (\ln\tilde{\eta})' \\ (\bar{\chi})' \end{bmatrix} = \begin{bmatrix} 0 \\ C_2 \\ C_3 \\ C_4 \\ 0 \\ 0 \\ C_7 \end{bmatrix} \tag{56}$$

Explicit expressions for the elements of the matrix are given in Appendix A.

3. Boundary and Initial Conditions

External Conditions - Since the perfect gas assumption is implicitly employed in this simplified formulation (cf, Eq. (48)) specification of the external Mach number distribution $M_e(x)$ suffices for the determination of all external flow parameters by utilization of the appropriate isentropic relations. For conversion of these distributions to the variable χ it is also necessary to specify the initial value of unit Reynolds number $(u_e/\nu_e)_o$. If the Sutherland viscosity representation is utilized it is also necessary to specify the total temperature of the external stream (cf, Eq. (51)) which is, of course, taken as constant in this analysis.

Wall Conditions - The wall conditions are completely characterized by specification of g_w which, in view of the perfect gas assumption is equivalent to specification of the wall temperature. The adiabatic wall condition of course corresponds to setting $g_w \equiv 1$ since the Prandtl number has been taken as unity. Although not strictly valid it is of course possible to specify, that g_w is a variable. This would be accounted for in the calculations by proper

interpretation of the partial derivatives $\partial\Gamma/\partial\chi$ and $\partial\Theta/\partial\chi$ appearing in Eq. (55b).

4. Initial Conditions

It is noted that in the differential coefficients, A_{ij}, of the system (56) no explicit dependence on χ or $\bar{\chi}$ occurs; accordingly these initial values are arbitrary and may conveniently be taken to be zero; furthermore, insofar as $\tilde{\eta}$ is concerned it can be shown that this variable appears only in the combination $\tilde{\eta}/\tilde{\eta}_o$ implying again that the initial value $\tilde{\eta}_o$ is arbitrary and can be taken as unity. Since the four dependent variables $\bar{\varphi}$, π, $\bar{R}$ and $\tilde{\sigma}$ are related by the two algebraic equations (38) and (55a) only two of these need be specified. It will become apparent in the ensuing development that the most convenient choice corresponds to specification of initial values of $\bar{\varphi}$ and π. The initial value of $\bar{U}_e$ is by definition unity.

One method of specifying these initial values makes use of a prescribed velocity profile in the VP flow. In this case the choice of $\bar{\varphi}$ and π follow unambiguously from the following consideration. Let

$$R_{\bar{y}} \equiv (\bar{u}_e/\bar{\nu}_e)\bar{y} \quad ; \quad R_y = (u_e/\nu_e)y$$

Then from the transformation laws it can be shown that

$$\frac{R_{\bar{y}}}{\tilde{\sigma}} = \int_o^{R_y} \tilde{\rho} dR_y \tag{57a}$$

$$\frac{\bar{R}}{\tilde{\sigma}} = \int_o^{R_\delta} \tilde{\rho}\, dR_y \tag{57b}$$

Since the velocity profiles $\tilde{u}(R_y)$ have been specified, a plot of $\tilde{u}$ versus $R_{\bar{y}}/\tilde{\sigma}$ can be generated. This can be compared with a series of theoretical velocity profiles within the "law of the wall" region* corresponding to various choices of $\bar{\varphi}$**. The

* The velocity profile representation within the "law of the wall" region follows from the latter of Eq. (37) by setting π=0. There results $\tilde{u} = (A/\bar{\varphi}) \ln(bR_{\bar{y}}/\bar{\varphi})$

** The value of $\tilde{\sigma}$ associated with this choice of $\bar{\varphi}$ follows from Eq. (55).

profile which best correlates the data determines the corresponding initial value of φ for the given profile. The associated value of $\bar{\pi}$ follows from Eq. (38) with $U_e = 1$ and $\bar{R}$ evaluated "experimentally" from Eq. (57b).

This procedure was first developed in Ref. 11 and subsequently also utilized in Ref. 12. It may be thought of as a generalization of the "Clauser Plot" technique (Ref. 29) which accounts for the effect of compressibility.

The initialization technique described above, since it requires specification of velocity profiles at some streamwise location has application in connection with experimental results. In the absence of such data it is necessary to initialize the computational procedures at a leading edge. In this case the same procedure is utilized for both the simplified analysis and the finite-difference approach, and thus will be discussed after the details of the latter have been described.

5. Finite Difference Approach

We consider now a more accurate treatment of the conservation of energy equation, Eq. (3). One possible approach would be to transform this equation into the same imcompressibility field as was done to the momentum equation in Section II. In this case it would be necessary to derive transformation rules which would govern the correspondence of the dependent variable, g, and the parameter, P_e, to their respective counterparts. In fact this approach was examined by Crocco (Ref. 10) who found that the correspondence between P_e and $\bar{P}_e$ was of such complexity as to render the numerical solution of the energy equation impractical.

Accordingly, the approach taken here will essentially be similar to that taken in Ref. 32 and 33, which treat the behavior of the turbulent boundary layer with mass addition and heat transfer at constant pressure. In these formulations the transformation is formally applied to the independent variables x, y and the velocity components. A modified von Mises transformation is then used to reduce the energy equation to a general form of a diffusion equation. Standard finite-difference-techniques are then applied to effect a solution.

Working Form of the Energy Equation

According to the compressibility transformation utilized herein the following differentiation rules apply:

$$\frac{\partial}{\partial y} = \eta \frac{\rho}{\bar{\rho}} \frac{\partial}{\partial \bar{y}}$$

$$\rho u \frac{\partial}{\partial x} + \rho v \frac{\partial}{\partial y} = \left(\frac{\xi \eta}{\sigma} \right) \left(\frac{\rho}{\bar{\rho}} \right) \left\{ \left[\overline{\rho u} \frac{\partial}{\partial x} + \overline{\rho v} \frac{\partial}{\partial \bar{y}} \right] + \right.$$

$$\left. + \left[\frac{\bar{\psi}}{\xi} \frac{d \ln \sigma}{dx} \right] \frac{\partial}{\partial \bar{y}} \right\}$$

Applying these rules to the energy equation yields

$$\overline{\rho u} \frac{\partial g}{\partial \bar{x}} + \overline{\rho v} \frac{\partial g}{\partial \bar{y}} + \left(\bar{\psi} \frac{d \ln \sigma}{d \bar{x}} \right) \frac{\partial g}{\partial \bar{y}} = \frac{\sigma \eta}{\xi} \frac{\partial}{\partial \bar{y}} \left\{ \rho (\rho \epsilon + \mu) \left[\frac{1}{P_e} \frac{\partial g}{\partial y} + \right. \right. \tag{3a}$$

$$\left. \left. + \frac{u_e^2}{2 H_e} \left(1 - \frac{1}{P_e} \right) \frac{\partial \tilde{u}}{\partial \bar{y}} \right] \right\}$$

A modified von Mises transformation is now introduced such that

$$\bar{x}, \bar{y} \rightarrow \bar{\chi}, \tilde{\psi}$$

where

$$\tilde{\psi} \equiv \bar{\psi} / \bar{\mu}$$

then

$$\frac{\partial}{\partial x} = \frac{\overline{\rho u}_{e,0}}{\bar{\mu}} \frac{\partial}{\partial \bar{\chi}} - \frac{\overline{\rho v}}{\bar{\mu}} \frac{\partial}{\partial \tilde{\psi}}$$

and

$$\frac{\partial}{\partial \bar{y}} = \frac{\overline{\rho u}}{\bar{\mu}} \frac{\partial}{\partial \bar{\psi}}$$

Substituting the above transformation rules into Eq. (3a) and recalling the definition of $\tilde{\sigma}$ and $\tilde{\eta}$ and the fact that

$$1/\xi = dx/d\bar{x} = \frac{(\overline{\rho u}_{e,0}/\bar{u})}{(\rho_e u_e/\mu_e)_o} \frac{d\bar{x}}{d\bar{x}}$$

yields the desired expression, i.e.,

$$\frac{\partial g}{\partial \bar{x}} = \frac{\partial}{\partial \bar{\psi}} \{ [\tilde{\rho}\tilde{u}\tilde{\sigma}^2 \frac{(\rho_e/\rho_{e,0})(u_e/u_{e,0})}{(\mu_e/\mu_{e,0})} \frac{(\rho\epsilon+\mu)}{\mu_e}][\frac{1}{P_e} \frac{\partial g}{\partial \bar{\psi}} + \frac{u_e^2}{2H_e}(1 - \frac{1}{P_e}) \frac{\partial \tilde{u}^2}{\partial \bar{\psi}}](\frac{d\bar{x}}{d\bar{x}}) \} - \{\bar{\psi}[\frac{d\ln\tilde{\sigma}}{d\bar{x}} - \frac{d\ln \mu_e}{dx}](\frac{dx}{d\bar{x}})\} \frac{\partial g}{\partial \bar{\psi}} \quad (3b)$$

At this point it is necessary to specify the form of the eddy-viscosity variation $(\rho\epsilon+\mu)$. This is provided by the transformation itself in terms of the CP variables. Thus, no additional empirical statement in this regard is required. The desired variation is obtained in a manner similar to that used to derive Eq. (41), i.e., the momentum equation (2) is integrated with respect to the normal coordinate but with the upper limit of integration considered a variable. Application of the transformation rules then yields

$$\frac{\tau-\tau_w}{\rho_e u_e^2} = \frac{\bar{R}}{(\tilde{\eta}/\tilde{\eta}_o)(\tilde{\sigma}_o)}\left\{\{\int_o^{\bar{\eta}} \tilde{u}^2 d\bar{\eta} - \tilde{u}\int_o^{\bar{\eta}} \tilde{u} d\bar{\eta}\}\{\frac{(\ln\bar{R})'}{(\bar{x})'} - \frac{(\ln\tilde{\eta})'}{(\bar{x})'} + \right.$$

$$\left.\frac{d\ln[(u_e/u_{e,0})(\rho_e/\rho_{e,0})]}{d\bar{x}}\} + \frac{1}{(\bar{x})'}\{\frac{d}{d\bar{x}}\int_o^{\bar{\eta}} \tilde{u}^2 d\bar{\eta} - \tilde{u}\frac{d}{d\bar{x}}\int_o^{\bar{\eta}} \tilde{u} d\bar{\eta}\} + \right.$$

$$\left. + \frac{d(u_e/u_{e,0})}{d\bar{x}}\{\int_o^{\bar{\eta}} \tilde{u}^2 d\bar{\eta} - \int_o^{\bar{\eta}} \frac{1}{\tilde{\rho}} d\eta\}\right\} \qquad 0 \le \bar{\eta} \le 1 \qquad (58)$$

Thus, since

$$\tilde{\rho}\tilde{\mu}\tilde{\sigma}^2 \frac{(\rho\epsilon+\mu)}{\mu_e} = \left(\frac{\tau}{\tau_w}\right)\left(\frac{C_f}{2}\right)(\tilde{\sigma})\left(\frac{\partial\tilde{u}}{\partial\bar{\psi}}\right)^{-1}$$

the terms in the first square bracket in Eq. (3b) can be related to properties of the transformation and the CP solution. It is noted also that

$$\bar{\psi} = \int_o^{\bar{y}} \frac{\bar{\rho}\bar{u}}{\bar{\mu}} d\bar{y} = \bar{R}\,\bar{U}_e \int_o^{\bar{\eta}} \tilde{u} d\bar{\eta} \qquad (59)$$

which provides the correspondence between $\bar{\psi}$ and $\tilde{u}$.

Finite Difference Form of the Energy Equation

To generate a solution of Eq. (3b) an implicit-central-finite-difference scheme is utilized with a variable step size in the $\bar{\psi}$ direction (c.f., Figure 4). Let

$$f_1 \equiv \tilde{\sigma}(\chi)' (\rho_e/\rho_{e,0})(u_e/u_{e,0})(\mu_e/\mu_{e,0})^{-1}$$

$$f_2 \equiv u_e^2/2H_e$$

$$f_3 \equiv (\ln\tilde{\sigma})' - (d\ln\mu_e/d\chi)(\chi)' \tag{60}$$

$$\Phi_1 \equiv (1/P_e)(\tau/\tau_w)(c_f''/2)/(\partial\tilde{u}/\partial\tilde{\psi})$$

$$\Phi_2 \equiv (1-1/P_e)(\tau/\tau_w)(c_f/2)\ 2\tilde{u}$$

Then Equation (3b) can be written

$$\frac{\partial g}{\partial \chi} = f_1 \frac{\partial}{\partial \tilde{\psi}}\left[\Phi_1 \frac{\partial g}{\partial \tilde{\psi}} + f_2\ \Phi_2\right] - f_3\ \tilde{\psi}\ \frac{\partial g}{\partial \tilde{\psi}} \tag{61}$$

and in accordance with the aforementioned procedure the following set of algebraic equations evolves:

$$\frac{g_m^{n+1} - g_m^n}{\Delta\chi} = \frac{f_1^n}{(\Delta\tilde{\psi})^2(\bar{\alpha}+1)\bar{\alpha}^{2m-3}}\{g_{m+1}^{n+1}[(\Phi_1)_{m+1}^n + (\Phi_1)_m^n]$$

$$+ g_m^{n+1}[(\Phi_1)_{m+1}^n + (\bar{\alpha}+1)(\Phi_1)_m^n + \bar{\alpha}\ (\Phi_1)_{m-1}^n]$$

$$+ g_{m-1}^{n+1}[(\Phi_1)_m^n + (\Phi_1)_{m-1}^n]\} + \frac{f_2 f_1^n}{\Delta\tilde{\psi}(\bar{\alpha}+1)\bar{\alpha}^{m-2}}[(\Phi_2)_{m+1}^n -$$

$$-(\Phi_2)_{m-1}^n] - \frac{f_3^n\ \tilde{\psi}_m}{\Delta\tilde{\psi}\ (\bar{\alpha}+1)\bar{\alpha}^{m-2}}\ [g_{m+1}^{n+1} - g_{m-1}^{n+1}]$$

or

$$A_m^n\ g_{m-1}^{n+1} + B_m^n\ g_m^{n+1} + C_m^n\ g_{m+1}^{n+1} = F_m^n \tag{62}$$

where

$$C_m^n \equiv \left\{ \frac{f_1}{b_m} (\Phi_1)_{m+1} + (\Phi_1)_m \right] - f_3 \frac{\bar{\psi}_m}{a_m} \Big\}^n$$

$$B_m^n = -\left\{ \frac{f_1}{b_m} \left[(\Phi_1)_{m+1} + (\alpha+1)(\Phi_1)_m + \alpha(\Phi_1)_{m-1} \right] + \frac{1}{\Delta\bar{x}} \right\}^n$$

$$A_m^n = \left\{ \frac{f_1}{c_m} \left[(\Phi_1)_m + (\Phi_1)_{m-1} \right] + \frac{f_3 \bar{\psi}_m}{a_m} \right\}^n$$

$$F_m^n = -\left\{ \frac{f_1 f_2}{a_m} \left[(\Phi_2)_{m+1} - (\Phi_2)_{m-1} \right] + \frac{g_m}{\Delta\bar{x}} \right\}^n$$

$$a_m \equiv \Delta\bar{\psi} (\bar{\alpha}+1) \bar{\alpha}^{m-3} \quad ; \quad b_m = (\Delta\bar{\psi})^2$$

$$c_m \equiv \frac{b_m}{\bar{\alpha}}$$

where the order of the truncation error is $0(\Delta\bar{x}, \Delta\bar{\psi}^2)$ for all $m \geq 3$.*

Here n denotes a generic streamwise station while m is an index for the mesh in the "normal" direction $\bar{\psi}$ which runs up to a value M which is determined in a manner consistent with the edge boundary condition on g as is discussed below. Note that all of the coefficients appearing in Eq. (62), which essentially involve only the fluid mechanic behavior, are evaluated at a previous station n relative to the g-field which is to be determined at the station n+1. That is, the thermodynamics, represented here by g_m^{n+1}, "lags" the fluid mechanics as reflected by the A_m^n, B_m^n, etc.

*At m=2 it can be shown that Eq. (62) is not valid to order $(\Delta\bar{\psi})^2$ by virtue of the behavior of g in the vicinity of the wall, i.e., $\partial g/\partial\bar{\psi} \to \infty$ as $\bar{\psi} \to 0$. Accordingly, a special form of difference equations is required at m=2. This special form is discussed below.

Consider now applications of the boundary conditions to these finite-difference equations. At m = M, Eq. (62) yields

$$A_M^n g_{M-1}^{n+1} + B_M^n g_M^{n+1} + C_M^n g_{M+1}^{n+1} = F_M^n$$

The "exact" boundary conditions $\partial g/\partial \psi \to 0$ as $\psi \to \infty$ are imposed in an approximate way by taking

$$g_{M-1}^{n+1} = g_{M+1}^{n+1} .$$

Accordingly, the proper form of the difference equation for m = M becomes

$$\bar{A}_M^n g_{M-1}^{n+1} + B_M^n g_M^{n+1} = F_M^n \qquad (63)$$

where

$$\bar{A}_M^n = A_M^n + C_M^n .$$

To impose the boundary conditions at the wall the proper form of difference equation for m = 2 must first be developed. The details of the derivation will be given in Appendix B. Basically, the required equation is obtained by recognizing that in the vicinity of the wall g can be represented by the finite series*

$$g = \sum G_j(\chi)\psi^{j/2} \quad , \; j = 0, 1, 2, \ldots \qquad (64)$$

*The series is truncated at j=3 to be consistent with the order of the truncation error associated with the basic finite-difference scheme.

Evidently, in view of the boundary condition on g (cf., Eq. (10)) the leading coefficient of the series (64) is simply g_w. The remaining three coefficients are evaluated by a forward-three-point-difference scheme as described in Appendix B. Thus, taking into account Equations (63) and (64), Equation (51) from 2....M, can be written in the tridiagonal matrix form

$$\begin{bmatrix} \bar{B}_2 & \bar{C}_2 & & & & \\ A_3 & B_3 & C_3 & & & \\ & A_4 & B_4 & C_4 & & \\ & & \ddots & \ddots & \ddots & \\ & 0 & & A_{M-1} & B_{M-1} & C_{M-1} \\ & & & & \bar{A}_{M_g} & B_{M_g} \end{bmatrix}^{n} \begin{bmatrix} g_2 \\ g_3 \\ g_4 \\ \vdots \\ g_{M-1} \\ g_M \end{bmatrix}^{n+1} = \begin{bmatrix} \bar{F}_2 \\ F_3 \\ F_4 \\ \vdots \\ F_{M-1} \\ F_M \end{bmatrix}^{n} \qquad (65)$$

where $\bar{B}_2$, $\bar{C}_2$, and $\bar{F}_2$ are functions of the G_j's as given in Appendix B.

The above M-1 algebraic expressions when coupled to the seven ordinary differential equations previously described yield a system of M+6 equations for the unknowns $\bar{\varphi}$, π, $\bar{R}$, $\bar{U}_e$, $\tilde{\sigma}$, $\tilde{\eta}$, χ and g ($\bar{\alpha}$, $\Delta\psi$, m) where m = 2,3,...M.

6. Boundary and Initial Conditions for the General Problem

In this case, the linear relation between stagnation enthalpy and velocity, alluded to in the previous section as a curve fit between the wall and external stream conditions need not be applicable. Consequently boundary conditions to be evaluated at the wall, e.g., $[\partial/\partial\bar{y}\ln\tilde{\rho}\tilde{\mu}]_w$ cannot be expressed analytically but must be compatible with the finite-difference formulation.

Wall Conditions - Two cases are considered; for the adiabatic case $(\tilde{\rho}\tilde{\mu})_w$ and g_w are unknown and must be calculated as the solution proceeds. For the second case, with heat transfer the wall temperature is prescribed. Then g_w and $(\tilde{\rho}\tilde{\mu})_w$ can be calculated from appropriate thermodynamic relations. To evaluate derivatives for the non-adiabatic case requires special attention similar to that used to obtain the finite-difference equation at the first mesh point above the wall. In this connection it can be shown that the product $\tilde{\rho}\tilde{\mu}$ in the neighborhood of the wall can be considered to behave in a similar fashion to g. That is, we take

$$\tilde{\rho}\tilde{\mu} = \sum_{j=0}^{3} R_j(\bar{x})\bar{\psi}^{j/2} \tag{66}$$

from which

$$\left(\frac{d\ln\tilde{\rho}\tilde{\mu}}{d\bar{y}}\right)_w = \frac{[R_1(\bar{x})]}{[R_o(\bar{x})]}\left(\frac{\sqrt{2}}{2}\right)\left(\frac{\tilde{\sigma}}{\tilde{\eta}\bar{\varphi}}\right)\left(\frac{u_e}{\nu_e}\right) \tag{67}$$

where

$$R_o = (\tilde{\rho}\tilde{\mu})_w$$

and we have utilized the relations

$$\left(\frac{\partial\tilde{u}}{\partial\bar{y}}\right)_w = \frac{\tilde{\sigma}}{\tilde{\eta}}\,\frac{(u_e/\nu_e)}{\bar{\varphi}^2}$$

$$\left(\frac{\partial\bar{\psi}}{\partial\tilde{u}}\right)_w = \frac{\sqrt{2}}{2}\,\bar{\varphi}$$

which follow in a straight forward manner from the previous formulation. To evaluate the coefficient R_1 consider the power series to be valid at the first three generic points above the wall, i.e., m = 2,3,4. Then, in terms of the values of $\tilde{\rho}\tilde{\mu}$ at these points, a system of three algebraic equations evolves for R_1, R_2, and R_3. In particular

$$R_1 = R_{11}(\tilde{\rho}\tilde{\mu})_{m=4} + R_{12}(\tilde{\rho}\tilde{\mu})_{m=3} + R_{13}(\tilde{\rho}\tilde{\mu})_{m=2} + R_{14}(\tilde{\rho}\tilde{\mu})_w \tag{68}$$

where the coefficients R_{ij} are only functions of $\Delta\bar{\psi}$ and $\bar{\sigma}$. For the adiabatic wall case we take $(\partial g/\partial\bar{y})_w=(\partial \ln\tilde{\rho}\tilde{\mu}/\partial\bar{y})_w=0$. To determine g_w consider Eq. (64) with $G_1=0$ since for $\partial g/\partial\bar{y} \to 0$, $(\partial g/\partial\bar{\psi})\tilde{u} \to 0$. Thus in the neighborhood of the wall

$$g = G_0 + G_2\bar{\psi} + G_3\bar{\psi}^{3/2}$$

where

$$G_o = g_w$$

Consequently, by considering the above $(g, \bar{\psi})$ dependency to be valid at the first three mesh points above the wall, again a system of three algebraic equations results which when solved for G_o (or g_w) yields

$$g_w = G_{10}g_{m=4} + G_{11}g_{m=3} + G_{12}g_{m=2} \tag{69}$$

where the coefficients G_{1j} can be shown to be functions of $\Delta\bar{\psi}$ and α.

External Conditions - For the general problem, the external stream need not be considered as a perfect gas with constant specific heats. However, theinitial state of the gas must be prescribed together with the external velocity and presuming that a suitable equilibrium chemistry is available all other external quantities and their requisite derivatives are readily obtainable.

Initial Conditions - To start the solution, the state of the gas must be prescribed at each generic point of the $\bar{\psi}$ mesh. Hence $g(\bar{\psi}, \chi_o)$ and $\tilde{u}(\bar{\psi}, \chi_o)$ must be considered known from the wall to the edge of the boundary layer. Knowledge of these profiles and the appropriate "chemistry" model then initially fixes all other profiles of thermodynamic properties, e.g., $\tilde{\rho}(\bar{\psi})$ and $\tilde{\mu}(\bar{\psi})$. The procedure in determining the initial values of the seven dependent variables, $\bar{\varphi}, \bar{\pi}, \bar{R}$, etc., is then identical to that discussed in Section II.F.4 except that the parameter $\tilde{\sigma}$ is evaluated by numerical integration utilizing the basic relation (46).

One special consideration arises here in connection with the parameter $(\ln\tilde{\sigma})'$ which appears in Equation (3b) Since the Crocco integral is not valid in this formulation an explicit value of $(\ln\tilde{\sigma})'$ cannot be computed at the initial station. Two alternatives may be considered to initialize the computational scheme. First, a value of $(\ln\tilde{\sigma})'$ can be initially assumed and an iterative procedure performed at this first numerical station to obtain a more accurate starting value. Or, initially, a Crocco integral and a $\tilde{\rho}$, $\tilde{\mu}$ dependency is assumed, thereby making $(\ln\sigma)'$ calculable from Equation (55b). In either case, the subsequent values of $(\ln\tilde{\sigma})'$ can be approximated by a numerical finite-difference technique.

III. RESULTS AND DISCUSSIONS

A. The Available Prediction Methods

As a preface to the subsequent comparisons with experiments, it would seem worthwhile to acquaint the reader with the other available prediction methods. The results of the present approach will be compared to the results of seven other investigations. Two points of view are taken here. One, is to compare with other methods that utilize the transformation of Coles but resort to different closure rules than those specified herein. In this regard, the works of Lewis et al, Ref. 34, the procedure of Camarata and McDonald, Ref. 35, as reported by McDonald, Ref. 36, will comprise this contingent.

The second viewpoint is to compare with analyses which resort to different computational procedures than the transformation. Consequently, comparisons will be made with the integral methods of Sasman and Cresci, Ref. 37, Flaherty, Ref. 38, and the eddy-viscosity model of Fish and McDonald, Ref. 39, as are also reported by McDonald, Ref. 36, who notes that the latter approach is somewhat similar to the development made by Herring, Ref. 40.

With regard to the procedures resorting to the transformation, the method of Ref. 35 reported by McDonald assumes that the (σ/η) scale be proportional to the static temperature. This assumption was required as McDonald points out since

> ... extreme sensitivity, indeed singular behavior was a consequence of deriving the transformation scale ξ by simultaneously satisfying the energy and momentum equations at the wall using a laminar Prandtl number invariant under the transformation. ....

In the current method, this difficulty does not exist since the energy equation has not been transformed and as such no postulates or empiricisms are deemed necessary in relating the Prandtl number in both planes. Rather, the energy equation is solved in the physical plane with one less empiricism however. The eddy-viscosity distribution required in the formulation is not a priori stated but inferred from the solution since the transformation has shown to produce a correspondence between the local physical shear distribution and the CP parameters.

Four basic differences in the method of Lewis, Kubota and Webb, Ref. 34, exist when compared to the method herein. One difference, although not fundamental, is their choice of a suitable incompressible formulation; another is the choice of the "substructure hypotheses" of Coles rather than the "sublayer hypothesis" used within. However, the following two are considered fundamental differences between the two approaches. Foremost is the necessity imposed by their solutions with regard to satisfying the laws of "corresponding stations" whereas in this approach strict adherence is given to the correspondence of skin friction. The requirement that zero-pressure-gradient flows must map into their zero-pressure-gradient counterparts constitutes the last difference.

The integral method of Sasman-Cresci is one which uses a modification to the standard Mager-type transformation thereby eliminating the need of assuming that the turbulent shear stress remain invariant under the transformation. Use of the moment of momentum equation and an approximation to the integral of shear are coupled to the momentum equation in the usual way. Assuming a Crocco integral and a power-law velocity profile, two equations result with incompressible form factor and a momentum-thickness-Reynolds-number parameter as the two dependent variables. A major criticism to this approach and similar ones is the lack of a more realistic velocity-profile representation and the possible restrictions imposed by the assumed shear distribution. In this context it is noted here that good agreement between theory and experiment for gross boundary-layer properties is not sufficient justification for stating the suitability of a particular method. In addition, it is deemed necessary that the method reproduce very accurately profile development, or, at least, the rationale used can be subsequently extended to encompass a broader problem-solving range.

For comparisons with a finite-difference formulation, the present approach will be compared to that of Ref. 39. This procedure evolved by Fish and McDonald, does contain an extended turbulence model. The results from using this method have been taken from Ref. 36 which also reports that the Herring, Ref. 40, eddy-viscosity relationship has been coupled to this approach. It had been noted, therefore, any differences that might arise between the predictions of the Herring procedure

and that which has been reported can only be attributable to the difference in numerical technique.

Also, the eddy-viscosity and mixing-length distributions which can be deduced from the present formulation will be compared to those obtained from the generalized velocity-profile-concept of Maise and McDonald, Ref. 41.

B. The Experimental Data

Perhaps one of the best sets of experimental information to date on compressible-turbulent-boundary layers has been reported by Winter, Smith, and Rotta (Ref. 42). In this study both boundary-layer velocity profiles and skin friction have been measured. The very large scale of the model used (5 feet) and the high unit Reynolds of $2(10)^6$/ft. is of particular consequence. Although tests were conducted at six free-stream Mach numbers, comparisons with only one are discussed here.

In Ref. 43, McLafferty and Barber have reported a series of measurements, made in a relatively small wind tunnel, along a series of highly curved two-dimensional ramps. Rather severe adverse pressure gradients were imposed which indicated large normal static-pressure gradients. Although these investigators have not measured skin friction directly, skin-friction coefficients have been deduced herein from the six reported velocity profiles according to the previously discussed "Clauser Plot" method.

The flat-plate experiments of Matting, Ref. 44, and those of Bertram and Neal, Ref. 45, are also considered mainly to show the remarkably improved agreement that accrues as a result of incorporating the wake correlation of Reference 15, into the analysis.

Finally, some numerical experiments are performed whereby the pressure gradient is maintained constant but non-zero. Thus effects of pressure gradient and heat transfer on, for example, eddy-viscosity-distribution and mixing length are reported and wherever possible compared with other existing theories.

C. Zero Pressure Gradient Flows

Under this heading of "Zero Pressure Gradient Flows" two concepts need some clarification before comparisons with experiments can be made. The first deals with implementation of the correlation of Reference 13 which was discussed in Section I, while the latter concerns itself with the choice of initial values when the solution commences from the leading edge.

1. Correlation of the Wake Parameter

As discussed in Section I, analysis of experimental results obtained for high speed flows with uniform external pressure indicated a systematic distortion of the wake portion of the velocity profile as reflected by reduced values of the Coles' wake parameter, π. In Ref. 13 an empirical correlation was developed which modifies this parameter in such a way that the resulting predictions give better agreement with experiment. This correlation takes the form*

$$(\pi)_{corr} = (\pi)_o + 0.425 \ln P \qquad (70)$$

where $(\pi)_{corr}$ denotes the correlated value of the wake parameter, $(\pi)_o$ corresponds to the nominal value which would apply in the absence of compressibility and/or heat transfer effects and P is defined by

$$P \equiv g_w \tilde{\rho}_{min}$$

* Further reexamination of the available experimental data has led to the conclusion that a more appropriate correlation is obtained if the multiplicative factor .425 is replaced by .53. The latter value has been incorporated in the computer program developed under this contract for use with the "PI CORRELATION" option (c.f., Part III, p. 16). It is also noted here that Eq. (72) exhibits singular behavior at values of $\pi = 2/3, -1$. Accordingly, Eq. (70) is considered to apply only for values of P such that $\pi \geq -0.25$. For P less than this limit the corresponding value for $(\pi)_{corr}$ is taken to be $(\pi)_{corr} \equiv -.25$.

The quantity $\tilde{\rho}_{min}$ represents the minimum density ratio within the boundary layer and, if a Crocco integral is utilized, it can be expressed as

$$\tilde{\rho}_{min} = \{ g_w \tilde{H}_e + \frac{\tilde{H}_e^2 (1-g_w)^2}{4(\tilde{H}_e - 1)} \}^{-1} \qquad (71)$$

Thus, for $g_w \to 1$ and $M_e \to 0$, $P \to 1$ in which case the wake parameter takes on the nominal value, $(\pi)_o$, which corresponds to the CP value associated with the zero pressure gradient case.

In order to apply this correlation in a consistent manner, it is necessary to examine the properties of the CP formulation when applied to the zero pressure gradient case. In particular, for any given value of $\pi=(\pi)_{corr}$ the remaining parameters appearing in this formulation (i.e., β, $\bar{\varphi}$, and $\bar{\eta}^*$) must be selected in a manner which assures that $d\pi/d\bar{\chi} = 0$ when $d\bar{U}_e/d\bar{\chi}=0$. Since this condition must hold for all $\bar{\chi}$ it is appropriate to impose it at the "leading edge" where the corresponding value of $\bar{\varphi}$ will be denoted by $\bar{\varphi}_{LE}$. The desired relation is obtained by setting $\pi' = \bar{U}_e' = 0$ in Equations (34), (43), and (44). There results

$$B(\beta, \pi, \bar{\varphi}, \bar{\eta}^*) = 0 \qquad (72)$$

Accordingly, with $\bar{\varphi} = \bar{\varphi}_{LE}$ and $\bar{\eta}^* = 0.5$, Equation (72) provides the relation between β and π which is shown in Figure 5. All of the calculations which have been generated utilizing the wake correlation and which are presented in the subsequent discussion have incorporated this relationship. Selection of a particular value for the parameter $\bar{\varphi}_{LE}$ is discussed below.

2. Initial Conditions for the Leading Edge

There remains now specification of the CP skin friction parameter $\bar{\varphi}_{LE}$. At an actual leading edge, of course, the skin friction becomes arbitrarily large. However, by the same token the existence of laminar boundary layer regime followed by a transition region must also be recognized. Evidently, these features cannot be included in a rigorous way within the context of the present formulation.

Accordingly, this initial condition is imposed in an approximate manner. For this purpose we follow Coles, Ref. 9 and take

$$\varphi_{LE} \equiv \left(\sqrt{2/C_f}\right)_o = 18.4$$

It is noted that Lewis, et al., Ref. 34 also associate the value 18.4 with the "leading edge" of a fully developed turbulent boundary layer.

3. Experimental Comparisons

The improvement in the prediction of skin-friction with momentum-thickness variation by use of the present transformation together with the above correlation is clearly indicated in Figure 6. In Figure 7, the velocity profiles generated from the solution are compared with the experiments while in Figure 8, comparison is made with some of the profiles generated without the use of the wake correlation. Again, the improvement is clearly indicated. Figures 9 and 10 compare respectively the momentum-thickness-Reynolds number and skin-friction coefficient with Reynolds number with and without the use of the correlation law. In addition to the good agreement afforded by the use of the correlation, these two figures additionally show that the procedure previously discussed of picking an initial value of $(\bar{\varphi})$ as well as (π) is well posed.

D. Two-Dimensional Pressure Gradient

For pressure-gradient flows comparison is offered between the present method and the four selected procedures of Ref. 36. In fact, Figure 11 is a reproduction of Figure 11 of this reference with the results of the present theory added. This figure compares the results of several approaches with one of the sets of the McLafferty and Barber experiments. Slight improvement is afforded by the present approach when compared to the method of Ref. 39. However, the results from this method, as indicated in Figure 11 of Ref. 36, and herein

terminate approximately at station $x = 0.21$ feet while the present approach continues; hence, further comparison cannot be made.

An important note to be considered in drawing conclusions, when comparing these various results, is the fact that the present solution starts at station $x = 0$ and uses the experimental profile there to generate the initial starting values while the other four analyses are initiated further upstream. In addition to the momentum-thickness and form-factor comparisons to the McLafferty-Barber experiments, made in Figure 11, Figure 12, compares the present results with the integral method of Ref. 37 and the transformation method of Ref. 34. The "experimental" values of skin friction shown have been obtained by the use of the "Clauser Plot" method which has been previously discussed. Clearly, all three methods predict, rather poorly, the skin-friction development over the entire portion of the model. For the first half of the model however, the present approach is significantly an improvement over the other transformation method. Again, it is believed that closer correspondence between the two transformation methods can be achieved by imposing identical initial conditions. Figure 13 draws attention to the ability of the transformation approach to reproduce more accurately the velocity-profile development than other integral approaches. Notable also is the improvement afforded when the wake correlation is coupled to the transformation. Again, it must be reiterated that this correlation is strictly an empiricism. However, its indicated improvement lends further credence to the idea of a multiple stretching formulation of say the y-coordinate where one transformation law is valid for some range while beyond that range another stretching law becomes applicable.

E. Axi-symmetric Flow with Pressure Gradient

To investigate turbulent-boundary-layer growth under the influence of both favorable and adverse pressure gradients the experiments performed by Winter, Smith and Rotta were chosen. These data, although complete and carefully taken and in some instances when the pressure gradients not too severe, does include effects not considered in the analysis. For example, the change in lateral curvature which can produce strong convergence or divergence of the streamlines is not part of the formulation. Notwithstanding, the candidate experiment for

the theoretical comparison was that performed at M_∞=2 and a unit Reynolds number of $2(10)^6$/ft. The governing differential equations used were those obtained by the formal applications of the Mangler transformation and are discussed in Appendix C. Figure 14 compares the results generated using the present approach with the theoretical method of Herring and Mellor, Ref. 40. The circles indicate the experimental values obtained directly from the profiles, and the squares indicate the values calculated with the von Karmen momentum-integral equation beginning with the initial experimental value of θ and the experimental values of c_f and δ^*/θ. The darker squares indicate the values of skin friction which were obtained from the "Clauser Plot" method. Initial conditions were obtained by examining the velocity profile at x = 20 inches from which a suitable value of φ and π were inferred.

In general both theories agree well with experiment with slight improvement indicated by the method of Ref. 39 which attempts to account for the convergence and divergence of the stream-line. Also both methods tend to bracket the experimental c_f distribution with the present approach underestimating the experimental results.

F. Eddy-Viscosity Distributions

Perhaps the most significant feature of the approach employed is that the compressible, kinematic eddy viscosity, $\epsilon(x,y)$, can be obtained as part of the solution. In this instance the analytic procedures were coupled to a Crocco-integral energy solution and the eddy-viscosity behavior in high-speed flows with and without heat transfer and pressure gradients was studied.

1. Zero Pressure Gradient; Adiabatic Case

Before discussing the high-speed results, Figure 15 compares the low-speed formulation with the flat-plate experiments of Klebanoff, Ref. 47. As indicated the agreement is excellent. For high-speed, zero-pressure-gradient, zero-heat-transfer cases, Figure 16 shows the variation of eddy viscosity through the boundary layer for one momentum-thickness-Reynolds-number and three Mach numbers.

Comparison is made with the theoretical approach of Maise and McDonald, Ref. 41, and as can be seen the agreement is rather favorable. The corresponding shear distribution together with the M_e = 0 and 5 results of the above reference are shown in the next figure. Clearly, Figure 17 shows that the distributions are independent of Mach number at least up to M_e=2. For the M_e=5 case, the shear distribution generated by the two methods differs to some extent only within the lower half of the boundary layer. However, the agreement between the two methods is much more improved here than that shown in Figures 4 and 12 of the aforementioned reference. In those figures a comparison is made between shear and eddy-viscosity distributions obtained using the Coles transformation and the generalized-velocity-profile method reported therein and shows the results of both methods to be considerably different. The application of the transformation method which was used there, relies on the Coles substructure hypothesis together with a Spalding-Chi skin-friction law and the Crocco energy relationship and is considerably different from that which is employed here. Thus the closer correspondence between the two methods indicated therein in contradistinction to that shown by Maise and McDonald disproves to some extent their conclusions as to the suitability of the transformation for predicting compressible shear-stress profiles. In fact, the conclusion that, at least up to Mach number of 5, the incompressible distribution of mixing length can be used in a compressible formulation is in disagreement with the findings of the present results as attested to by examining Figure 18. It is the contention here that the agreement between the two methods only up to a Mach number of 2 indicates that the generalized-velocity-profiles used therein are only applicable up to that Mach number, beyond which the generalization used becomes too restrictive.

By examining Figure 19 it is noted that the dependency of eddy viscosity normalized with respect to displacement thickness becomes less dependent on momentum-thickness-Reynolds-number as the Mach number decreases and that up to a Mach number of 5 its dependency with Reynolds number beyond a value of $(10)^5$ is severely reduced.

2. Zero Pressure Gradient, Non-Adiabatic Cases

The next five figures tend to exemplify the effects of heat transfer on shear, eddy-viscosity , and mixing-length distributions. First, Figure 20 indicates that for a given Mach number and Reynolds number, the effect of heat transfer on shear-stress distribution is rather small showing at most a 2% variation between the adiabatic case and that for which the wall temperature is half the external total temperature. However, comparing Figure 21 with Figure 16 indicates that although the variations of the parameter, $\epsilon/u_e\delta^*$, with η are similar, the effect of heat transfer is shown to substantially increase the value of this parameter throughout most of the boundary layer. In addition, the effect of heat transfer, on its maximum value, is seen in Figure 22 to diminish with Mach number for a given R_θ . It is recalled here that these are deduced from results generated by using a Crocco-integral formulation and not the most general approach which has been derived. Thus, evidence of a decreasing dependence of Mach number and heat transfer rate on the eddy-viscosity distribution as the Mach number increases should be substantiated by the more general approach derived since it can include "real gas" effects and appropriate models of laminar and turbulent heat transport coefficients. Heuristically speaking however, it is felt that a reduced heat-transfer-rate dependence on eddy-viscosity can be shown to exist if, as Maise and McDonald, at the suggestion of Herring and Mellor, have shown for the adiabatic case, that a reduction of Mach number dependence on ϵ occurs when the eddy viscosity is normalized with respect to a thickness based upon velocity defect rather than mass defect.

With regard to mixing length, Figures 18 and 23 tend to show that no uniformly valid correlative properties which will tend to reduce the Mach number dependency for flows beyond a Mach number of 2, are likely to exist. However, Figure 24 which shows the effect of heat-transfer rate on mixing-length distribution for a given M_e and R_θ does intimate to some extent a similarity in profile development with heat-transfer rate. Further study is required, however, before these conclusions can be substantiated.

3. Pressure Gradient Cases

In addition to the numerical experiments performed with zero pressure gradient, several "solutions" have been generated which have taken into account pressure gradient as well as heat transfer. In this connection the pressure gradient has been imposed by considering flows wherein the parameter

$$(1/p_t)(dp/dx)$$

is considered constant. Considering a perfect gas with constant specific heats and the fact that the unit Reynolds number can be made a function of Mach number, total temperature and total pressure, then it can be easily shown that similar solutions result if the parameter

$$d(p/p_t)\ d\chi$$

is kept constant.

Figure 25 summarizes the results with regard to the variation of $(\epsilon/u_e\delta^*)_{max}$ with initial Mach number $M_{e,0}$ which have been obtained by imposing constant values of the pressure gradient parameter under both adiabatic and non-adiabatic wall conditions. Preliminary examination of this figure indicates that for initial Mach numbers less than approximately 2, the eddy-viscosity behavior is somewhat insensitive to moderate pressure variations. However, this degree of insensitivity is reduced considerably with heat transfer. Accordingly, the possibility of developing conclusions to describe the details of turbulent-boundary-layer flow development when a pressure gradient prevails from laws generated from flat-plate results appears to exist only for low to moderate Mach numbers. Indications are that the maximum value of (ℓ/δ), for a given Mach number, decreases with increasing pressure gradient and the result that this variation increases with the increasing Mach number is shown in the next figure, i.e., Figure 26. Figure 27 compares the variation of the shear-stress integral with pressure gradient and compares it to the empirical law of Ref. 37 in which the shear integral, plotted

in the manner shown, is considered invariant with pressure gradient and Mach number. Figures 28, 29, 30 and 31 tend to quantize the effect of initial Mach number and momentum-thickness Reynolds-number on shear, eddy-viscosity and mixing-length distributions. Consequently, the results indicated are depicted for only one value of $(1/p_t)(dp/dx)$ with the additional effect of heat transfer on such behavior being further portrayed by Figures 32 and 33. Thus by examining Figures 28, 29 and 30 it appears that for a given value of the pressure gradient parameter and R_θ no ordered variation of (τ/τ_w), $(\epsilon/u_e\delta^*)$ or (ℓ/δ) with $M_{e,0}$ exists. However, Figure 31 shows that the eddy-viscosity distributions are more sensitive to changes in R_θ than the mixing lengths are. As far as heat transfer is concerned, increasing the heat-transfer-rate reduces the shear-stress distribution while concomitantly increasing the mixing-length distribution as Figures 32 and 33 depict.

G. Extensions to Statistical Turbulent Studies

The possibility of relating statistical turbulent concepts to transformation properties has also been examined briefly. It is concluded that no direct relation can be obtained by the use of the transformation. The reason is inherent in the form of the transformation since it has only been applied to temporal-mean quantities thereby producing no correspondence between these fluctuating terms in both planes. However, some indirect information which can possibly provide a deeper insight into the turbulent mechanism can be obtained by studying the ramifications of the transformation with regard to the concepts of intermittancy. It is noted that the low-speed formulation described herein has the capability of generating the parameter since the intermittancy, γ, is defined as the ratio of $\overline{\epsilon}$ with $(\overline{\epsilon})_{max}$. To deduce the corresponding behavior for the high-speed case, it is assumed that the intermittancy is related to the eddy-viscosity by the relation

$$\gamma \equiv \tilde{\rho}\epsilon/(\tilde{\rho}\epsilon)_{max} \tag{73}$$

the results of which are shown in Figure 34.

Insofar as turbulent kinetic energy is concerned, several investigators (c.f., Ref. 48, 49) have treated the low-speed problem by solving a system of equations which includes the conservation of turbulent kinetic energy. The proponents of this approach generally believe "that the connection between

the turbulent shear stress and other properties of the turbulence is very much closer than the connection between the turbulent shear stress and velocity field". In fact, it is asserted in Ref. 49, that improved results are obtained by assuming that the turbulent kinetic energy is directly proportional to the local shear stress.

If such an approach does indeed provide improved prediction capability for low-speed flows, it would evidently be useful to have available a transformation which can be applied to this additional auxiliary equation.

At this time all of the ramifications of the concept described above have not been examined in detail. Nevertheless, it can be said that this approach is likely to prove useful and further exploitation is recommended.

IV. CONCLUDING REMARKS

The results cited demonstrate that by suitable implementation of the compressibility transformation and by proper interpretation of their implications a wide variety of variable-property-turbulent-boundary-layer problems can be analyzed with a minimum of empiricism. The results have shown that a suitable constant-property-solution has been coupled to the overall formulations; however, the conceptual ideas of the transformation and the implications pertaining thereto, do not preclude the possibility of a "marraige" of the transformation with any other "suitable" CP formulation. Furthermore, there has been removed the usual necessity of prescribing in some manner the compressible-eddy-viscosity distribution, since the analysis replaces this restrictive requirement with a much simpler task of assuming the form of the well-known incompressible velocity field. In addition, no restrictions have been posed on the energy field. Noteworthy here is the fact that if a suitable constant property solution involving mass transfer and pressure gradient existed then the above approach can also be coupled to species-conservation equation and as such the study of turbulent compressible flow with mass and heat transfer as well as pressure gradient could be formally effected without the requirement of knowing how the Lewis number or turbulent Schmidt number have to be transformed.

It is evident from the comparisons between experiments and other theories that the present approach must be included in the list of suitable methods for predicting compressible-turbulent-boundary layer development. Its de-emphasis on certain empiricisms used in other methods, e.g., compressible eddy-viscosity laws, mixing length hypothesis, shear-integral distributions and generalized-velocity profiles is considered to make this type of an approach more suitable for studying other complex flow structures.

Unfortunately, however, further justification of the above conclusions cannot be made because of the dearth of suitable experiments which are wholly devoted to the study of the compressible-turbulent mechanism.

Comparisons with "available" experiments shown and the conclusions obtained therefrom lack definitiveness because most "present-day suitable-experiments" inherently contain either three-dimensional effects, transverse curvature effects and/or the existance of normal pressure gradients; three factors not included in this and the comparable theories. Also, knowledge of the thermodynamic behavior within these experimental boundary layers is either completely unknown and a priori assumed or subject to question.

Nevertheless, an optimistic viewpoint has been taken and several forms of numerical experiments have been performed. As such, the preceding analysis has indicated, heuristically, the effects of pressure gradient and heat transfer on eddy viscosity, shear and mixing length distributions. A correlative study showing the effect of pressure gradients on these properties has been attempted by considering flows wherein the pressure gradient is held constant and non-zero.

These results have shown that for the adiabatic case, at least, most theories which do not account for pressure gradient in their empirical laws are to some degree only applicable to flows up to Mach number of two. With heat transfer, the variations of eddy-viscosity and mixing length diverge strongly from the norm - the zero pressure case - before a Mach number of two is attained. This divergence increases as the pressure gradient increases.

APPENDIX A

THE PROFILE PARAMETERS $I_{1,2,3}$ AND ELEMENTS OF MATRIX A_{ij}

Velocity Profile

$$\tilde{u} = \begin{cases} \tilde{u}_I = \overline{RU}_e \bar{\eta}/\bar{\varphi}^2 & 0 < \eta \leq \eta_s \\ \tilde{u}_{II} = 1 + (A/\bar{\varphi})[\ln\bar{\eta} - 2\pi(2\bar{\eta}^3 - 3\bar{\eta}^2 + 1)] & \eta_s < \eta \leq 1 \end{cases}$$

Integral $I_1(\bar{\eta}) \equiv \int_o^{\bar{\eta}} \tilde{u} d\bar{\eta}$

$$I_1(\bar{\eta}) = \begin{cases} \overline{RU}_e(\bar{\eta}^2/2)(1/\bar{\varphi}^2) & 0 < \eta \leq \eta_s \\ \eta[1+(A/\varphi)(q_5+2\pi q_6)] - I_1(II,\eta_s) + I_1(I,\bar{\eta}_s) & \eta_s < \eta \leq 1 \end{cases}$$

Integral $I_2(\bar{\eta}) \equiv \int_o^{\bar{\eta}} \tilde{u}^2 d\tilde{\eta}$

$$I_2(\bar{\eta}) = \begin{cases} (\overline{RU}_e)^2(\bar{\eta}^3/3\bar{\varphi}^4) & 0 < \eta \leq \eta_s \\ \bar{\eta}[1+2(A/\bar{\varphi})^2(q_2+2\pi q_3+2\pi^2 q_4)+2(A/\bar{\varphi})(q_5+2\pi q_6)] \\ \quad -I_2(II,\bar{\eta}_s)+I_2(I,\bar{\eta}_s) & \eta_s < \eta \leq 1 \end{cases}$$

$$I_3(\bar{\eta}) = (\tilde{H}_e G_w - 1)\bar{\eta} + \tilde{H}_e(1-G_w)\ I_1(\bar{\eta}) + (1-\tilde{H}_e) I_2(\bar{\eta})$$

In addition to the above integrals we also require their derivatives with respect to $(\bar{\chi})$. Accordingly,

$$(I_1)' = \begin{cases} I_1[\ln\bar{R})' + (\ln\bar{U}_e)' - 2(\ln\bar{\varphi})'] & 0 < \eta \leq \eta_s \\ \eta[-(A/\bar{\varphi})(q_5+2\pi q_6)(\ln\bar{\varphi})' + (A/\varphi)(2q_6)(\pi)'] & \\ \quad -I_1'(II,\bar{\eta}_s) + I_1'(I,\bar{\eta}_s) & \eta_s < \eta \leq 1 \end{cases}$$

$$(I_2)' = \begin{cases} I_2[2(\ln R)' + 2(\ln U_e)' - 4(\ln\bar{\varphi})'] & 0 < \eta \leq \eta_s \\ \bar{\eta}\ \{-(2A/\bar{\varphi})^2(\ln\bar{\varphi})'[q_2+2\pi q_3+2\pi^2 q_4] & \\ \quad +2(A/\bar{\varphi})^2[2q_3(\pi)'+4q_4\pi(\pi)'] & \\ \quad -2(A/\bar{\varphi})(\ln\bar{\varphi})'(q_5+2\pi q_6)+4(A/\bar{\varphi})(q_6)(\pi)'\} & \\ \quad -I_2'(II,\bar{\eta}_s) + I_2'(I,\bar{\eta}_s) & \eta_s < \eta \leq 1 \end{cases}$$

Where the connotation of $I_1'(II,\bar{\eta}_s)$, $I_2'(II,\bar{\eta}_s)$ ... etc., is similar to that used for $I_1(II,\bar{\eta}_s)$, $I_2(II,\bar{\eta}_s)$,... respectively.

where

$$I_1(I,\bar{\eta}_s) = \int_0^{\bar{\eta}_s} \tilde{u}_I d\bar{\eta} = \overline{RU}_e(\bar{\eta}_s^2/2)(1/\bar{\varphi}^2)$$

$$I_1(II,\bar{\eta}_s) = \int_0^{\bar{\eta}_s} \tilde{u}_{II} d\bar{\eta} = \bar{\eta}_s\,[1+(A/\bar{\varphi})(q_{5,s}+2\pi q_{6,s})]$$

$$I_2(I,\bar{\eta}_s) = \int_0^{\bar{\eta}_s} \tilde{u}_I^2 d\bar{\eta} = \bar{R}^2\bar{U}_e^2\,(\bar{\eta}_s^3/3)(1/\bar{\varphi}^4)$$

$$I_2(II,\bar{\eta}_s) = \int_0^{\bar{\eta}_s} \tilde{u}_{II}^2 d\bar{\eta} = \bar{\eta}_s[1+2(A/\bar{\varphi})^2(q_{2,s}+2\pi q_{3,s}+2\pi^2 q_{4,s})$$

$$+ 2(A/\bar{\varphi})(q_{5,s}+2\pi q_{6,s})]$$

where

$$q_2 = 1/2(\ln\bar{\eta})^2 - (\ln\bar{\eta}) + 1$$

$$q_3 = (\ln\bar{\eta})[-(\bar{\eta}^3/3)+\bar{\eta}^2-1] + (\bar{\eta}^3/8)-(\bar{\eta}^2/2) + 1$$

$$q_4 = (4/7)\,\bar{\eta}^6 - 2\bar{\eta}^5 + (9/5)\,\bar{\eta}^4 + \bar{\eta}^3 - 2\bar{\eta}^2 + 1$$

$$q_5 = \ln\bar{\eta} - 1$$

$$q^6 = -(1/2)\bar{\eta}^3 + \bar{\eta}^2 - 1$$

and $q_{j,s}$ with $j = 2,3,4,5,6$ implies that the above expressions are evaluated at $\bar{\eta}_s$. Although it is not formally required here, an additional parameter is needed in the analysis, namely,

$$q_1 = 2 + (19/6)\pi + (52/35)\pi^2$$

$$\text{Integral } I_3(\bar{\eta}) = \int_0^{\bar{\eta}} (1/\tilde{\rho} - 1)d\bar{\eta}$$

If a Crocco integral is used then $\tilde{\rho} = \rho(\tilde{u})$ and I_3 becomes

Non-zero elements of matric A_{ij}

$$A_{1,1} = 1 + \bar{\varphi}/A$$

$$A_{1,2} = 1.0$$

$$A_{1,3} = 2.0$$

$$A_{1,4} = -1.0$$

$$A_{2,1} = 2q_1(A/\bar{\varphi}) - (1+\pi)$$

$$A_{2,2} = (1+\pi) - q_1(A/\bar{\varphi})$$

$$A_{2,3} = 1 - (A/\bar{\varphi})[(19/6) + (104/35)\pi]$$

$$A_{2,4} = 3(1+\pi) - 2q_1(A/\bar{\varphi})$$

$$A_{3,1} = \bar{\eta}^*(A/\bar{\varphi})\{-4(A/\bar{\varphi})(q_2+2\pi q_3+2\pi^2 q_4)+[(\tilde{u})_{\bar{\eta}^*}-2)](q_5+2\pi q_6)\}$$

$$A_{3,2} = I_2(\bar{\eta}^*) - (u)_{\bar{\eta}^*} I_1(\bar{\eta}^*)$$

$$A_{3,3} = (\bar{\eta}^*)(A/\bar{\varphi})[4(A/\bar{\varphi})(q_3+2\pi q_4) - 2q_6(\tilde{u}_{\bar{\eta}^*}-2)]$$

$$A_{3,4} = 2I_2(\bar{\eta}^*) - (\tilde{u})_{\bar{\eta}^*} I_1(\bar{\eta}^*) - \bar{\eta}^*$$

$$A_{4,4} = 1$$

$$A_{5,1} = -[d\ln\Gamma/d\ln\bar{\varphi} + d\ln\Theta/d\ln\bar{\varphi}]$$

$$A_{5,5} = 1$$

$$A_{5,7} = -[d\ln\Gamma/d\chi + d\ln\Theta/d\chi]$$

$$A_{6,4} = -1$$

$$A_{6,5} = 1$$

$$A_{6,6} = -1$$

$$A_{6,7} = d/d\chi[\ln(u_e/\nu_e)]$$

$$A_{7,5} = -(2+\bar{\Omega}/\bar{\Sigma})$$

$$A_{7,6} = (1 + \bar{\Omega}/\bar{\Sigma})$$

$$A_{7,7} = \left(\frac{d\ln u_e}{d\chi}\right)\left[\frac{\delta^*}{\theta} - \frac{\bar{\Omega}}{\bar{\Sigma}}\right] + \left(\frac{d\ln\mu_e}{d\chi}\right)\left[2 + \frac{\bar{\Omega}}{\bar{\Sigma}}\right] - \left(\frac{d\ln\rho_e}{d\chi}\right)\left[1 + \frac{\bar{\Omega}}{\bar{\Sigma}}\right]$$

$$- (\bar{\varpi}^2\overline{R\Sigma})^{-1}(\tilde{\sigma}\ \tilde{\sigma}_o)(\tilde{\eta}/\tilde{\eta}_o)(\tilde{\rho}\tilde{\mu})_w$$

$$C_2 = 1/(\overline{R\varpi}A)$$

$$C_3 = (1/\bar{R})\{\beta'(1+\pi)(\bar{\Sigma}/\bar{\Omega})(A/\bar{\varphi})^2(\bar{\eta}^*)[(1/\bar{\eta}^*)^2 + 12\pi(1-\bar{\eta}^*)]$$

$$- (1/\bar{\varphi})^2\ \}$$

$$(C_4) = (\tilde{\eta}/\tilde{\sigma})_o(1/\tilde{\rho})_w(1/\tilde{\rho}\tilde{\mu})_w(1/\tilde{\sigma}\tilde{\eta})(d\ln u_e/d\chi) +$$

$$(\tilde{\eta}/\tilde{\sigma})_o(1/\bar{\varphi})^2(\nu_e/u_e)_o[\partial/\partial\bar{y}\ \ln\tilde{\rho}\tilde{\mu}]_w$$

$$C_7 = -1/(\bar{\varphi}^2\overline{R\Sigma})$$

APPENDIX B

DERIVATION OF THE EQUATION $\overline{C}_2 g_3^{n+1} + \overline{B}_2 g_2^{n+1} = F_2$

The finite-difference equation associated with the first $\tilde{\psi}$-mesh point above the wall, i.e., at $\tilde{\psi} = \tilde{\psi}_2 = \Delta\tilde{\psi}$, must have coefficients $\overline{C}_2$, $\overline{B}_2$, and $\overline{F}_2$ properly interpreted to reflect the singular behavior of $(\partial q/\partial\tilde{\psi})$ and $(\partial\tilde{u}/\partial\tilde{\psi})$ at the wall. However, because of the "physics", g must be a regular function of $\tilde{u}$ and hence can be expanded in a power series. In the neighborhood of the wall and within the laminar sublayer it can be shown that

$$\tilde{u} = \sqrt{2\tilde{\psi}/\varphi} \tag{B1}$$

Accordingly, a power series of g with $\tilde{u}$ necessarily requires a power series of g with $\tilde{\psi}$ to be of the form

$$g = \sum_{j=0}^{n} G_j(\chi)\, \tilde{\psi}^{j/2} \tag{B2}$$

where only the first four terms are required to be consistent with the order of the truncation error. Thus, in the vicinity of the wall g behaves like

$$g = G_o + G_1\tilde{\psi}^{\frac{1}{2}} + G_2\tilde{\psi} + G_3\tilde{\psi}^{3/2} \tag{B3}$$

where

$$G_o = g_w$$

Considering that the first three mesh points above the wall, i.e., where

$$\begin{aligned} \tilde{\psi}_2 &= \Delta\tilde{\psi} \equiv a^2 \\ \tilde{\psi}_3 &= \tilde{\psi}_2 + \alpha\,\Delta\tilde{\psi} = \Delta\tilde{\psi}\,(1+\overline{\alpha}) \equiv (ab)^2 \\ \tilde{\psi}_4 &= \Delta\tilde{\psi}\,(1+\overline{\alpha}+\overline{\alpha}^2) \equiv (ac)^2 \end{aligned} \tag{B4}$$

to be within the laminar sublayer and applying Eq. (B3) to the points m = 2,3,4, yields a system of three algebraic equations for the three unknown coefficients, G_1, G_2, G_3. Solving for $G_{1,2,3}$ yields formally

$$G_i = \sum_{j=0}^{3} G_{ij}\, g\,(4-j) \qquad i = 1,2,3 \tag{B5}$$

where

$$G_{10} = b^2 a^5 (b-1)/\Delta$$

$$G_{11} = c^2 a^5 (1-c)/\Delta$$

$$G_{12} = b^2 c^2 a^5 (c-b)/\Delta$$

$$G_{13} = -(a^5/\Delta)[b^2(b-1)+c^2(1-c)+b^2c^2(c-b)]$$

with

$$\Delta = a^6 bc\,[(b^2-c^2) + bc\,(c-b) + (c-b)]$$

and

$$G_{20} = -\,G_{10}\,(1+b)/ab$$

$$G_{21} = -G_{11}(1+c)/ac$$

$$G_{22} = -G_{12}(c+b)/abc$$

$$G_{23} = -(a^4/\Delta)[(b^2-c^2)bc+b(1-b^2) +c(c^2-1)]$$

$$G_{30} = G_{10}/(a^2 b)$$

$$G_{31} = G_{11}/(a^2 c)$$

$$G_{32} = G_{13}/(a^2 bc)$$

$$G_{33} = -(a^3/\Delta)[b(b-1) +c(1-c) + bc(c-b)]$$

Differentiating Eq. (B3) and evaluating at the first mesh-point above the wall yields after substituting Eq. (B5)

$$\left(\frac{\partial g}{\partial \bar{\psi}}\right)_2 = \sum_{j=0}^{3} \bar{G}_{2j}\, g^{(4-j)} \tag{B6}$$

where

$$\bar{G}_{2j} = (1/2a)\, G_{1j} + G_{2j} + (3/2)a\, G_{3j}$$

Likewise for the second derivative, it can be shown

$$\left(\frac{\partial^2 g}{\partial \bar{\psi}^2}\right)_2 = \sum_{j=0}^{3} \tilde{G}_{2j}\, g^{(4-j)} \tag{B7}$$

where

$$\tilde{G}_{2j} = -\,(1/4a^3)\, G_{1j} + (3/4a)\, G_{3j}$$

Now substituting (B6) and (B7) into the energy equation with $(\partial g/\partial \bar{\chi})$ replaced by its finite difference form and collecting terms yields the expression

$$\sum_{j=0}^{3} \tilde{\bar{G}}_{2j}\, g^{(4-j)} = 0 \tag{B8}$$

where

$$\tilde{\bar{G}}_{2j} = [f_1(\partial \bar{\Phi}/\partial \psi) - f_3 \psi]_2\, \bar{G}_{2j} + f_1\, (\Phi_1)_2\, \tilde{G}_{2j}$$

for j = 0 and 1. While for the index 2 and 3 a slightly different expression is required

$$\tilde{\bar{G}}_{22} = [f_1(\partial \Phi/\partial \bar{\psi}) - f_3 \bar{\psi}]_2\, \bar{G}_{22} + f_1(\Phi_1)_2\, \tilde{G}_{22} - (1/\Delta \bar{\chi})$$

and

$$\tilde{\bar{G}}_{23} = \left\{ \left[f_1 (\partial \Phi / \partial \psi) - f_3 \tilde{\psi} \right]_2 \bar{G}_{23} + f_1 (\Phi_1)_2 \tilde{G}_{23} + \left[\frac{(g)_2}{(g_w)} \right]^n + \left[\frac{f_1 f_2}{g_w} \left(\frac{\partial \Phi_2}{\partial \tilde{\psi}} \right) \right] \right\}$$

Substituting Eq. (B8) into the finite-difference form of the energy equation for the $\tilde{\psi} = \tilde{\psi}_3$ mesh point, thereby eliminating $(g)_4$ yields the desired equation for the $\tilde{\psi} = \tilde{\psi}_2$ mesh point, i.e.,

$$\bar{C}_2 g_3^{n+1} + \bar{B}_2 g_2^{n+1} = \bar{F}_2 \tag{B9}$$

where

$$\begin{aligned} \bar{C}_2 &= C_3 \tilde{\bar{G}}_{21} - B_3 \tilde{\bar{G}}_{20} \\ \bar{B}_2 &= C_3 \tilde{\bar{G}}_{22} - A_3 \tilde{\bar{G}}_{20} \\ \bar{F}_2 &= C_3 \tilde{\bar{G}}_{23} - F_3 \tilde{\bar{G}}_{20} \end{aligned} \tag{B10}$$

It is noted further, that additional modification is required for Eq. (B9) and hence Eq. (B10) for the adiabatic wall case since, as will be shown below, $G_1 \equiv 0$ in this case.

Adiabatic wall implies that

$$\left(\frac{\partial g}{\partial y} \right)_w = \left(\frac{\partial G}{\partial \tilde{\psi}} \right)_w \left(\frac{\partial \tilde{\psi}}{\partial \tilde{u}} \right)_w \left(\frac{\partial \tilde{u}}{\partial y} \right)_w = 0$$

or

$$\left[\left(\frac{G_1}{2} \right) (\tilde{\psi})^{-\frac{1}{2}} \left(\frac{\partial \tilde{\psi}}{\partial \tilde{u}} \right) \left(\frac{\partial \tilde{u}}{\partial y} \right) \right]_w = 0$$

But since

$$\left(\tilde{\psi}^{-\frac{1}{2}} \frac{\partial \tilde{\psi}}{\partial u}\right)_w = 2\bar{\varphi}$$

and since

$$\left(\frac{\partial \tilde{u}}{\partial y}\right)_w \neq 0$$

then adiabatic wall requires $G_1 \equiv 0$. Now to arrive at an equation of a form similar to Eq. (B9) the procedure is the same except that $G_1 \equiv 0$. In this case the same formation as above can be applied; however, it can easily be shown that the following modifications are required.

Thus for adiabatic flow set

$$G_{2j} = 0 \quad j = 0,1,2,3$$

and re-define

$$\begin{aligned} G_{21} &= -aG_{31} - a^3/\Delta \\ G_{22} &= -abG_{32} = b^3a^3/\Delta \\ G_{23} &= aG_{33} = -(a^3/\Delta)(b^3-1) \\ \Delta &= a^5b^2(b-1) \end{aligned} \tag{B11}$$

Also, for adiabatic flow g_w cannot be prescribed but must be an outcome of the solution. Considering $G_1 = 0$, and now G_o as the unknown wall enthalpy value, then in a manner similar to that in obtaining Eq. (B5), it can be shown that

$$G_o = g_w = \sum_{j=0}^{2} G_{1j}\, g(4-j) \tag{B12}$$

with G_{1j}'s defined as those shown below, Eq. (B5).

To complete the formulation for the wall region also requires expressions for $(\partial\Phi_1/\partial\tilde{\psi})$ and $(\partial\Phi_2/\partial\tilde{\psi})$ at the first mesh point above the wall. Repeating the same arguments as above, the shear distribution τ/τ_w can be considered regular and hence expanded into a power series of $\tilde{u}$. Now near the wall $\tilde{u} \sim \tilde{\psi}^{\frac{1}{2}}$ hence

$$(\Phi_1) \sim (\tau/\tau_w)/(\partial\tilde{u}/\partial\tilde{\psi}) = \sum_{j=1}^{n} P_{ij}\,\tilde{\psi}^{\,j/2} \tag{B13a}$$

Likewise since

$$(\Phi_2) \sim (\tau/\tau_w)(\tilde{u}) = \sum_{j=1}^{n} P_{2j}\,\tilde{\psi}^{\,j/2} \tag{B13b}$$

Truncating the power series after the second term and assuming that the expression is valid at the two mesh points above the wall yields two algebraic equations for each of the P_{ij}'s and P_{2j}'s. Thus

$$P_{m1} = (a^2/\Delta)\ \{b^2(\Phi m)_2 - (\Phi_m)_3\} \tag{B14a}$$

$$P_{m2} = (a/\Delta)\ \{(\Phi_m)_3 - b(\Phi_m)_2\} \tag{B14b}$$

where m = 1,2, and

$$\Delta = a^3 b(b-1)$$

These four expressions are all that are required to evaluate the derivatives of Φ_1 or Φ_2 at $\tilde{\psi}_2$ since

$$\left(\frac{\partial\Phi_m}{\partial\tilde{\psi}}\right)_{/2} = \left(\frac{1}{2a}\right) P_{m1} + P_{m2} \tag{B15}$$

with m = 1,2.

APPENDIX C

REDUCTION OF THE AXISYMMETRIC EQUATIONS TO THE TWO-DIMENSIONAL FORM

The equations of mass, momentum, and energy for a turbulent boundary layer over a body of revolution with the boundary layer thickness considered to be much smaller than both the lateral and longitudinal radii of curvature are instead of Eq. (1), (2) and (3), the following:

$$\frac{\partial}{\partial x_a}(r_w \rho u) + \frac{\partial}{\partial y_a}(r_w \rho v) = 0 \tag{C1}$$

$$\rho u \frac{\partial u}{\partial x_a} + \rho v \frac{\partial u}{\partial y_a} = -\frac{dp}{dx_a} + \frac{\partial}{\partial y_a}\left[(\rho\epsilon+\mu)\frac{\partial u}{\partial y_a}\right] \tag{C2}$$

$$\rho u \frac{\partial g}{\partial x_a} + \rho v \frac{\partial g}{\partial y_a} = \frac{\partial}{\partial y_a}\left[\frac{(\rho\epsilon+\mu)}{P_e}\left(\frac{\partial g}{\partial y_a}\right) + (u_e^2/2H_e)(\rho\epsilon+\mu)(1-1/P_e)\left(\frac{\partial \tilde{u}^2}{\partial y_a}\right)\right] \tag{C3}$$

where the subscript "a" infers that the coordinates x and y are respectively along and normal to the surface of the axisymmetric body, r_w is the radius of the body of revolution and is considered as a function of x_a only.

The procedure taken here is to formally apply Manglers transformation to the above three equations, thereby reducing them to their corresponding two-dimensional forms. Thus, by considering a coordinate transformation of the form

$$(x-x_o)_{2\text{-}D} = \int_{(x_a)_o}^{x'_a} (r_w/L)^2 dx_a \; ; \qquad y_{2\text{-}D} = \int_o^{y'_a} (r_w/L) dy_a \tag{C4}$$

where L is some reference length which is to be determined. There the above three equations can be formally transformed into

their two-dimensional counterparts. The implication of the transformation also require the shear, momentum thickness and displacement thickness, for example, to transform as

$$(\tau)_a = \tau_{2-D}(r_w/L) \tag{C5}$$

$$(\theta)_a = \theta_{2-D}/(r_w/L) \tag{C6}$$

$$(\delta^*)_a = (\delta^*)_a/(r_w/L) \tag{C7}$$

To complete the problem and to properly effect the transformation back into the physical axisymmetric plane requires specification of the reference length, L. To determine L consider that at some point on the body, i.e., $(x_a)_o$ all profile information as well as all external quantities are given. And at the corresponding stretched point in the two-dimensional plane, i.e., $(x_{2-D})_o$ the skin friction, the external velocity, temperature, Mach number, and unit Reynolds number are the same as those which occur at point $(x_a)_o$ then it can be easily shown that for this correspondence to exist

$$L = (r_w)_{(x_a)_o} \tag{C8}$$

REFERENCES

1. Dorodnitsyn, A., Laminar Boundary Layer in Compressible Fluid, Comptes Rendus (Doklady) USSR, Vol. 34, 1942, p. 213.

2. Howarth, L., Concerning the Effect of Compressibility on Laminar Layers and Their Separation, Proceedings of the Royal Society (London) Series A, Vol. 194, 1948, p. 16.

3. Stewartson, K., Correlated Incompressible and Compressible Boundary Layers, Proceedings of the Royal Society (London) Series A. Vol. 200, 1949, p. 84.

4. Illingworth, C.R., Steady Flow in the Laminar Boundary Layer of a Gas, Proceedings of the Royal Society of London, Series A, Vol. 199, 1949.

5. Laufer, J., Thoughts on Compressible Turbulent Boundary Layers, paper appearing in Compressible Turbulent Boundary Layers, NASA SP-216, 1969, Editor: Mitchel Bertram. Also Rand Memo. RM-5946-PR, March 1969.

6. Mager, A., Transformation of the Compressible Turbulent Boundary Layer, Journal of Aeronautical Sciences, 25, pp 305-3011, 1958.

7. Culick, F.E.C. and Hill J.A.F., A Turbulent Analog of the Stewartson-Illingworth Transformation, Journal of Aeronautical Sciences, 25, 1958.

8. Burggraf, O.R., The Compressibility Transformation and the Turbulent-Boundary-Layer Equations, J. Aerosp. Sci. vol. 29, No. 4, April 1962, pp. 434-439.

9. Coles, Donald, The Turbulent Boundary Layer in a Compressible Fluid, Phys. Fluids, Vol. 7, No. 9, September 1964, pp. 1403-1423.

10. Crocco, L., Transformations of the Compressible Turbulent Boundary Layer with Heat Exchange, AIAA J., 1, No. 12, December 1963, pp. 2723-2731.

11. Baronti, Paola, O., and Libby, Paul, A., Velocity Profiles in Turbulent Compressible Boundary Layers, AIAA J, 4, No. 2, February 1966, pp. 193-202.

12. Economos, C., A Transformation Theory for the Compressible Turbulent Boundary Layer with Mass Transfer - AIAA J., Vol. 8, No. 4, April 1970, pp. 758-764.

13. Economos, C., On the Applicability of the Transformation Theory to Variable Property Turbulent Boundary Layers with Pressure Gradient and Heat and Mass Transfer, paper appearing in Compressible Turbulent Boundary Layers, NASA SP-216, 1969, Editor, Mitchel Bertram.

14. Bertram, M.H., Cary, A.M., Jr., and Whitehead, A.H., Jr., Experiments with Hypersonic Turbulent Boundary Layer on Flat Plates and Delta Wings, presented at the AGARD Specialists Meeting on Hypersonic Boundary Layers and Flow Fields, London, England, May 1968.

15. Libby, P.A. and Baronti, P. O., A Transformation Theory of the Turbulent Compressible Boundary Layer with Pressure Gradient and Heat Transfer, GASL TR-455, August 1964.

16. Lewis, J.E., The Compressible Boundary Layer and its Low Speed Equivalent, AIAA J., Vol. 6, No. 6, June 1968, pp. 1185-1187.

17. Bushnell, D.M., and Beckwith, I.E., Calculation of non-equilibrium Hypersonic Turbulent Boundary Layers and Comparisons with Experimental Data, AIAA Preprint No. 69-684, 1969.

18. Rotta, J.C., Turbulent Boundary Layers in Incompressible Flow, Progress in Aeronautical Sciences, Vol. 2, Ed. A. Ferri, et al., Pergamon Press, 1962.

19. Rotta, J.C., Critical Review of Existing Methods for Calculating the Development of Turbulent Boundary Layers, published in Fluid Mechanics of Internal Flow, Editor Gino Sovran, Elsevier Publishing Co. 1967.

20. Thompson, B.G.J., A Critical Review of Existing Methods of Calculating the Turbulent Boundary Layer, Aeronautical Research Council 26,109, 1964, Also, Ph.D Thesis University of Cambridge, 1964.

21. Head, M.R., (1960) Entrainment in the Turbulent Boundary Layer, Aero. Res. Counc. Rep. & Mem. 3152.

22. Moses, H.L. The Behavior of Turbulent Boundary Layers in Adverse Pressure Gradients, Gas Turbine Lab., Mass. Inst. Techn. Rep. No. 73, 1964.

23. Libby, P.A., Baronti, P.O., and Napolitano, L., Study of the Incompressible Turbulent Boundary Layer with Pressure Gradient, AIAA J, pp.445-452, 1964.

24. Mellor, G.L.. and Gibson, D.M., Equilibrium Turbulent Boundary Layers, Princeton University, Dept. Aerospace Mech. Sci. FLD No. 13, 1963.

25. Kline, S.J., Cockrell, D.G., and Morkovin, M.V., AFOSR-IFP, Stanford 1968, Conference on Turbulent Boundary Layer Prediction, Vol. I, 1968.

26. Moses, H., A Strip-Integral Method for Predicting the Behavior of Turbulent Boundary Layers, proceedings of AFOSR-IFP, Stanford 1968 Conference on Turbulent Boundary Layer Prediction, 1968, Editors, Kline, S.J., Morkovin, M.V., Sovran, G., and Cockrell, D.J., Publ. Stanford University.

27. Cebeci, T., Smith, A.M.O., A Finite-Difference Solution of the Incompressible Turbulent Boundary-Layer Equations by an Eddy-Viscosity Concept, proceedings of AFOSR-IFP, Stanford 1968 Conference on Turbulent Boundary Layer Prediction, Editors, Kline, S.J., Morkovin, M.W., Sovran, G., and Cockrell, D.J., Publ. Stanford University.

28. Baronti, P.O., An Investigation of the Turbulent Incompressible Boundary Layer, GASL TR-624, August 1966.

29. Coles, D., The Law of the Wake in the Turbulent Layer, J. Fluid Mech, 1, pp.191-226, 1956.

30. Clauser, F., The Turbulent Boundary Layer, Advances in Applied Mechanics, Vol. IV, Academic Press, New York, 1956.

31. Schubauer, G.B., Klebanoff, P.S., Investigation of Separation of the Turbulent Boundary Layer, NACA TN2133, 1950.

32. Rosenbaum, H., Turbulent Compressible Boundary Layer on a Flat Plate with Heat Transfer and Mass Diffusion, AIAA J., 9, 1548-1556 (1966). See also, General Applied Science Laboratories, Inc., Report TR 514, Compressible Turbulent Boundary Layer with Application to Hydrogen Dumping and Combustion, March 1965.

33. Lane, F., et al., Ballistic Missile Reentry Phenomenology Study Annual Report, December 1968-July 1969, prepared by General Applied Science Labs., Inc. for U. S. Army Missile Cmmd, Redstone Arsenal, Ala.. Contract No. DAAH01-69-C-0792.

34. Lewis, J., Kubota, T., and Webb, W.H., Transformation Theory for the Compressible Turbulent Boundary Layer with Arbitrary Pressure Gradient, AIAA Paper 69-160, presented at the AIAA 7th Aerospace Sciences Meeting, N.Y., January 20-29,1969.

35. Camarata, F.J., and McDonald, H., A Procedure for Predicting Characteristics of Compressible Turbulent Boundary Layers Which Includes the Treatment of Upstream History, United Aircraft Research Lab. Rept. No. G212238-3, August 1968.

36. McDonald, H., An Assessment of Certain Procedures for Computing Compressible Turbulent Boundary Layer Development, paper appearing in Compressible Turbulent Boundary Layers, NASA SP-216, 1969, Editor, Mitchel Bertram.

37. Sasman, P.K., and Cresci, R.J., Compressible Turbulent Boundary Layer with Pressure Gradient and Heat Transfer, AIAA Journal 4, pp. 19-25, January 1966.

38. Flaherty, R.J., A Method for Estimating Turbulent Boundary Layers and Heat Transfer in an Arbitrary Gradient, United Aircraft Res. Lab. Rept. No. UAR G51,1968.

39. Fish, R.W., and McDonald, H., Practical Calculations of Transitional Boundary Layers, United Aircraft Corp. Rept. UAR H48, March 1969.

40. Herring, H.J., On the Calculation of Compressible Turbulent Boundary Layers, Princeton University Ph.D. Thesis 1966. See also, NASA-CR 1144, September 1968, (Co-author: G.L. Mellor).

41. Maise, G., and McDonald, H., Mixing Length and Kinematic Eddy Viscosity in a Compressible Boundary Layer, AIAA J, 6, pp. 73-80, January 1968.

42. Winter, K.G., Smith, K.G., and Rotta, J.C., Turbulent Boundary Layer Studies on a Waisted Body of Revolution in Subsonic and Supersonic Flow, AGARDograph 97, May 1965.

43. McLafferty, G.H., and Barber, R.E., Turbulent Boundary Layer Characteristics in Supersonic Streams Having Adverse Pressure Gradients, United Aircraft Res. Dept. R-1285-11, September 1959, see also, Journal of Aeronautical Sciences, Vol. 29, pp 1-10, 1962.

44. Matting, F.W., Chapman, D.R., Nyholm, J.R., and Thomas, A., Turbulent Skin Friction at High Mach Numbers and Reynolds Numbers and Reynolds Numbers in Air and Helium, NASA TR R-82, 1961.

45. Bertram, M.H., and Neal, L.,Jr., Recent Experiments in Hypersonic Turbulent Boundary Layers, AGARD Specialists Meeting on Recent Developments in Boundary Layer Research, 1965, also NASA TM X-56335, 1965.

46. Reshotko, E., and Tucker, M., Approximate Calculation of the Compressible Turbulent Boundary Layer with Heat Transfer and Arbitrary Pressure Gradient,NACA TN 4154, 1957.

47. Klebanoff, P.S., Characteristics of Turbulence in a Boundary Layer with Zero Pressure Gradient, NACA Rept.1247, 1955.

48. Beckwith, I.E., and Bushnell, D.M., Detailed Description and Results of a Method for Computing Mean and Fluctuating Quantities in Turbulent Boundary Layers, NASA TN D4815 1968.

49. Bradshaw, P., Ferriss, D.H., and Atwell, N.P., Calculation of Boundary Layer Development Using the Turbulent Energy Equation, J. Fluid Mech. (1967), Vol. 28, Part 3.

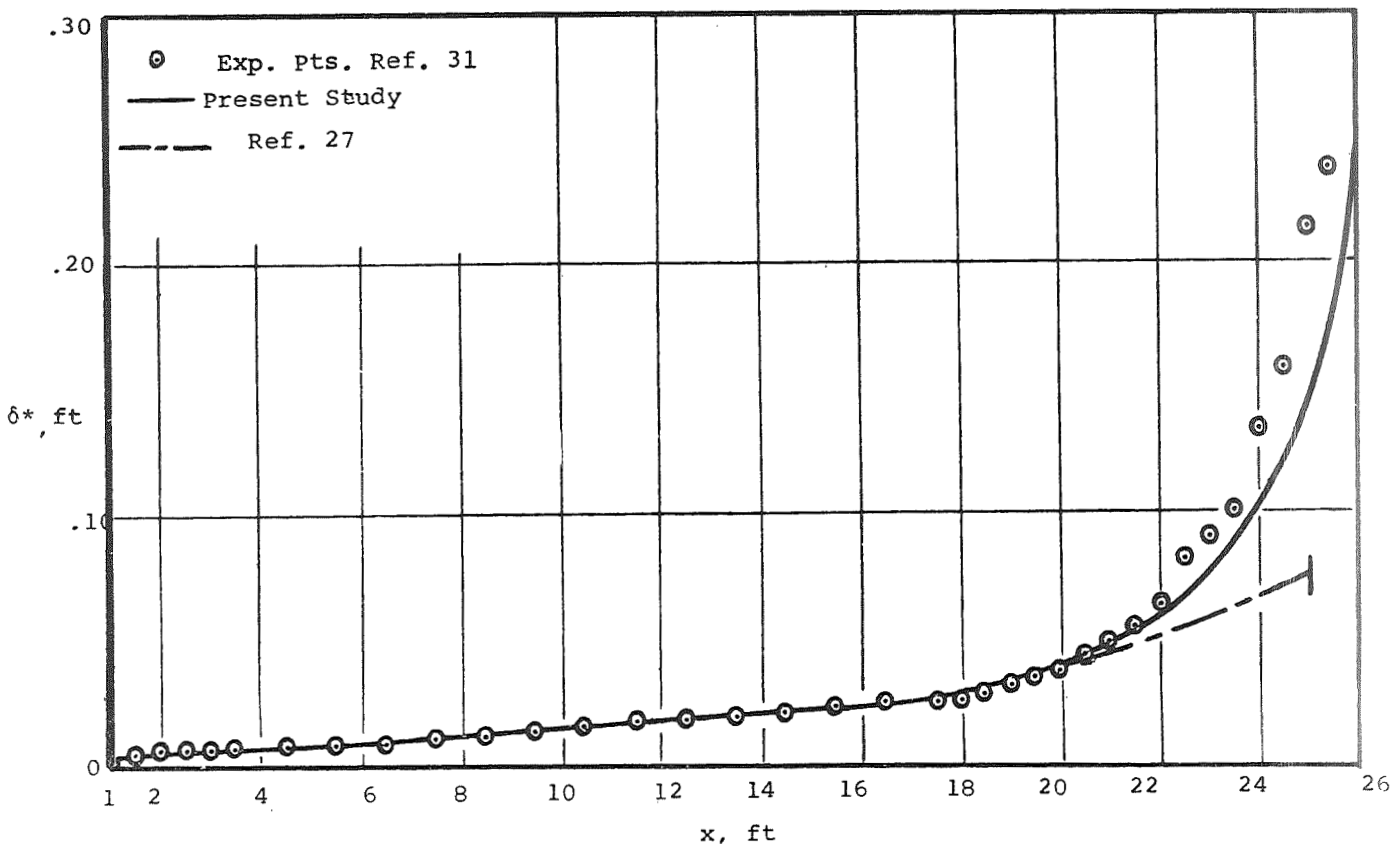

FIGURE 1 - COMPARISON OF TWO LOW SPEED FORMULATIONS WITH EXPERIMENTS - DISPLACEMENT THICKNESS

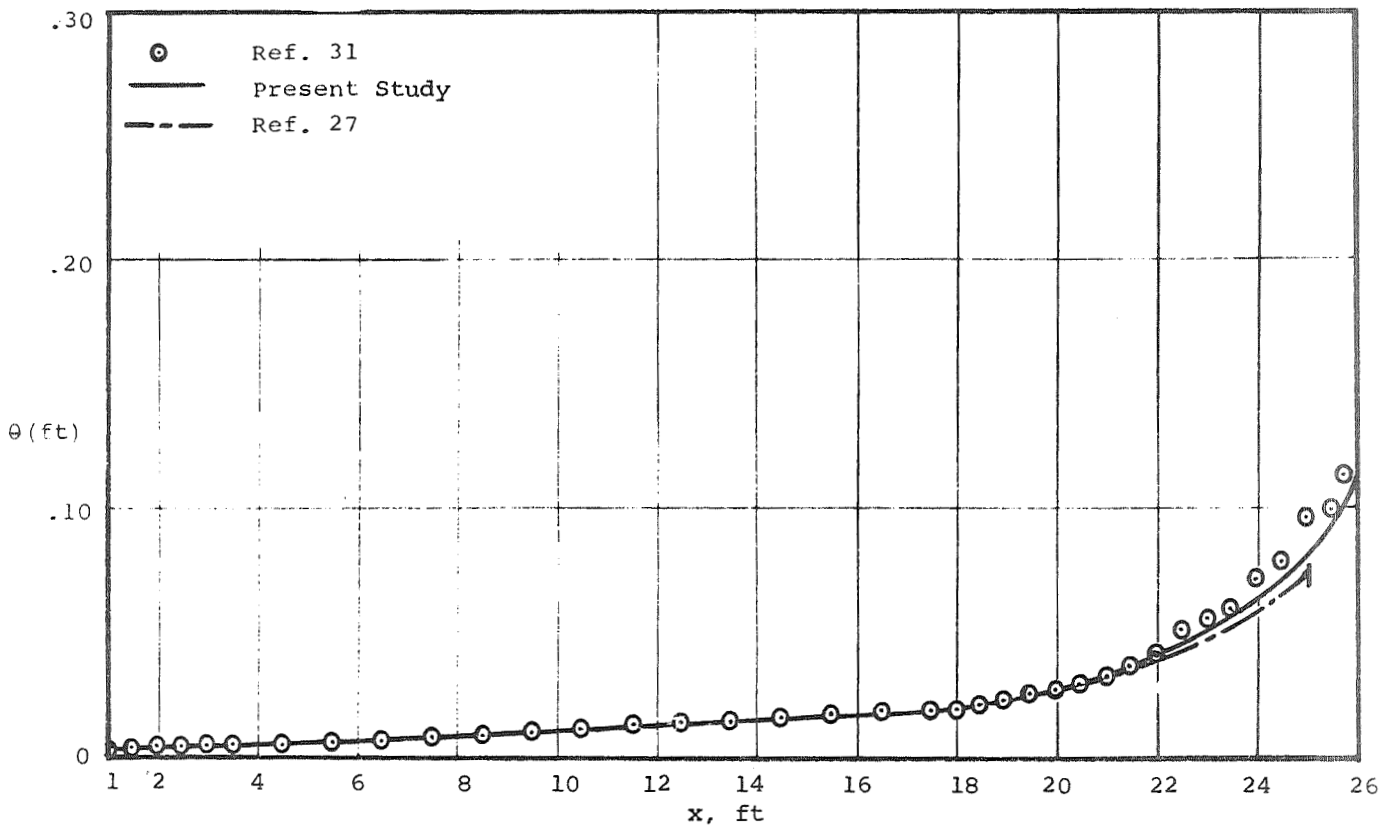

FIGURE 2 - COMPARISON OF TWO LOW SPEED FORMULATIONS WITH EXPERIMENTS - MOMENTUM THICKNESS

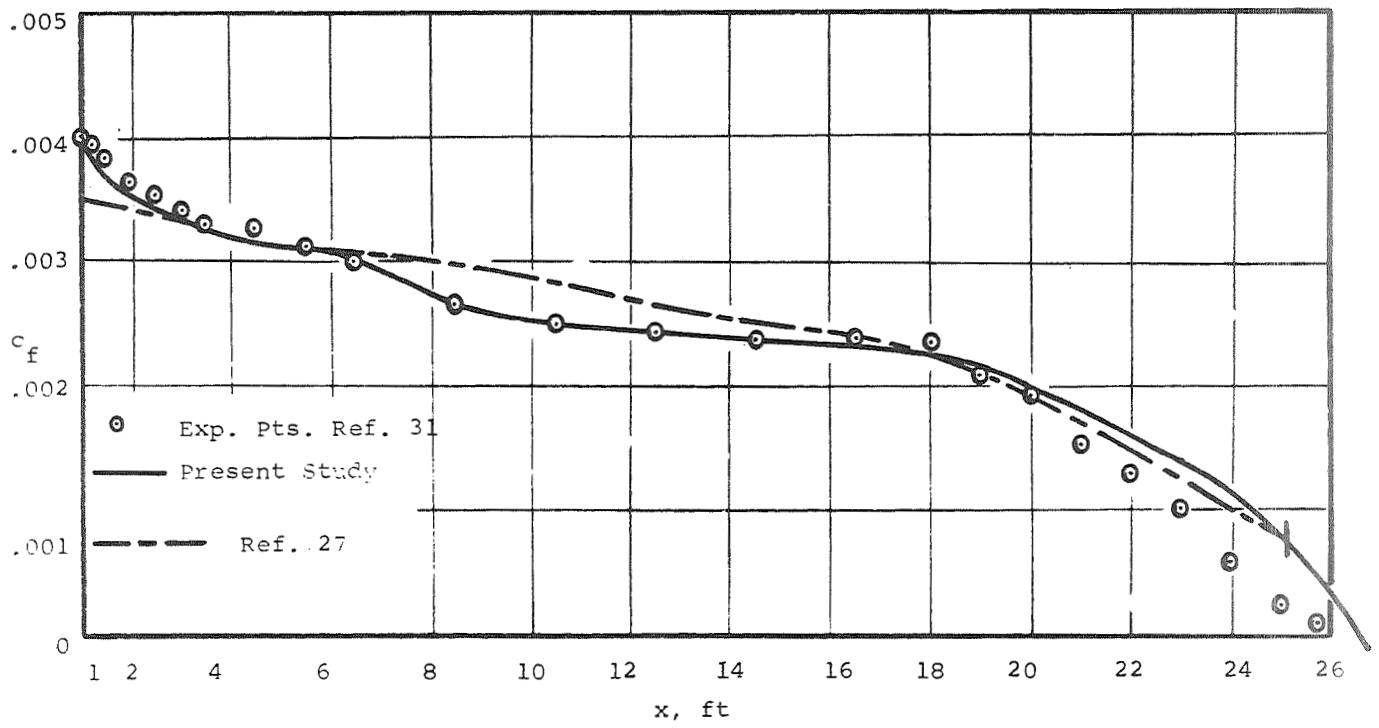

FIGURE 3 - COMPARISON OF TWO LOW SPEED FORMULATIONS WITH EXPERIMENT - SKIN FRICTION

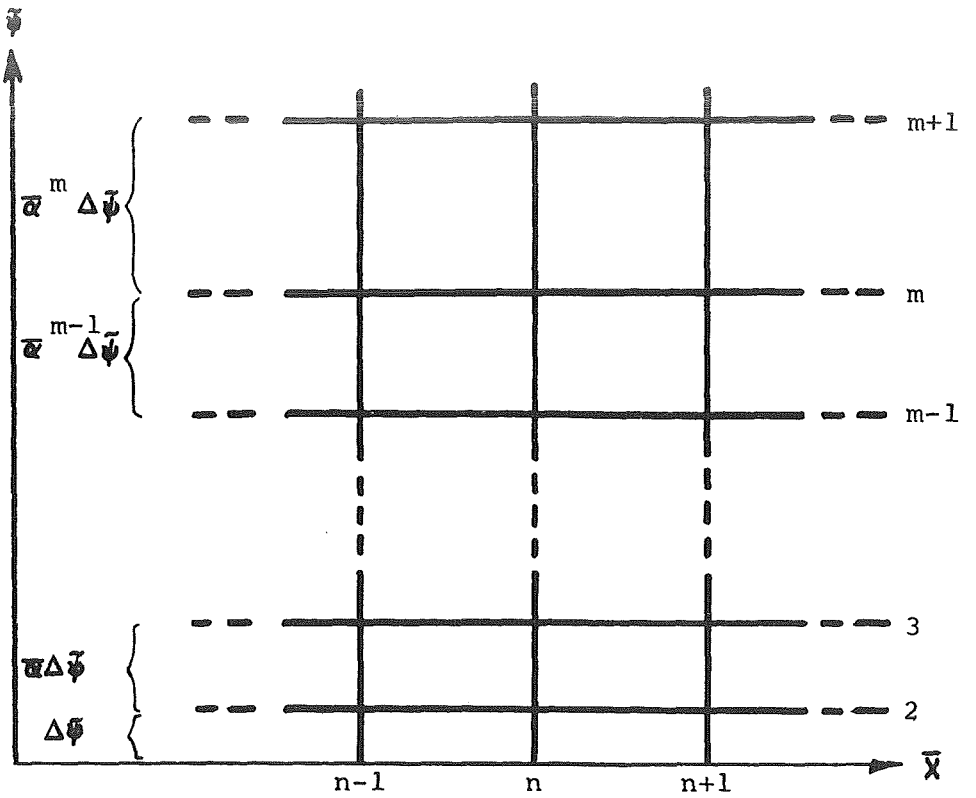

FIGURE 4 - FINITE DIFFERENCE MESH

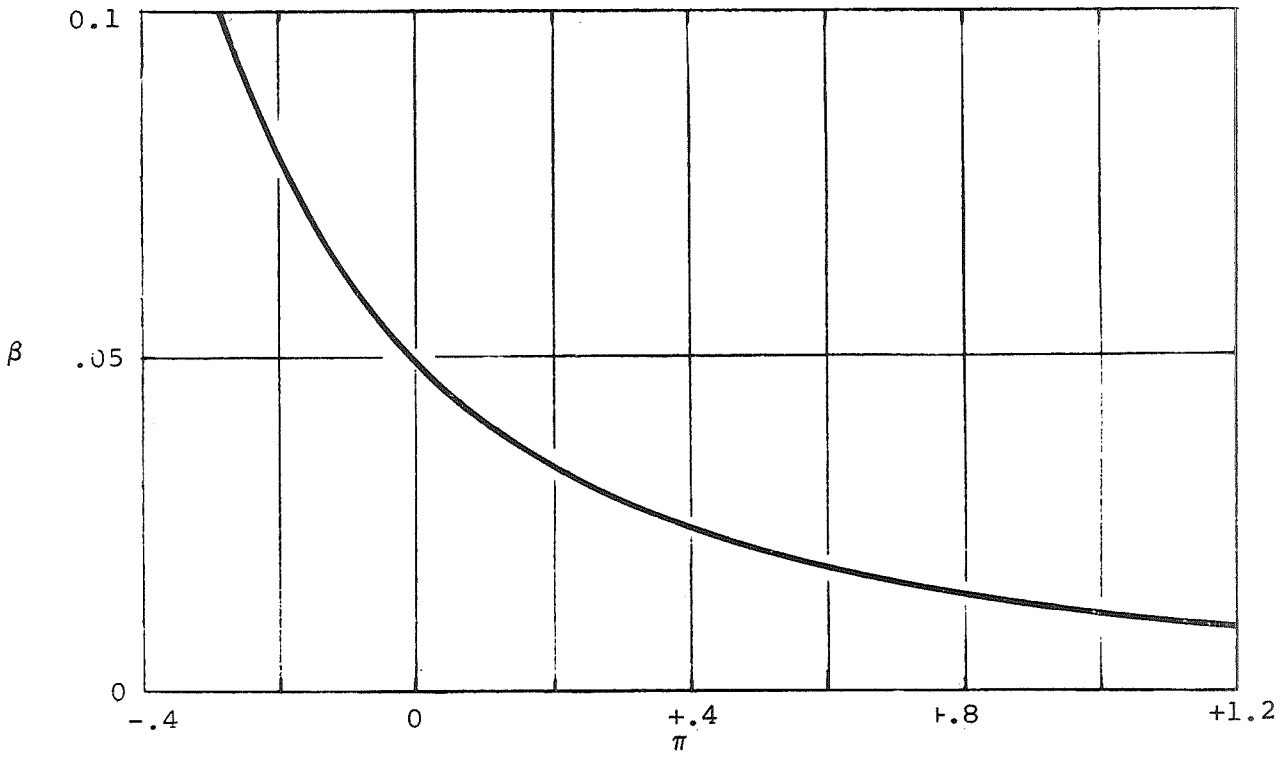

FIGURE 5 - RELATION BETWEEN THE CLAUSER EDDY VISCOSITY PARAMETER AND THE COLES WAKE PARAMETER

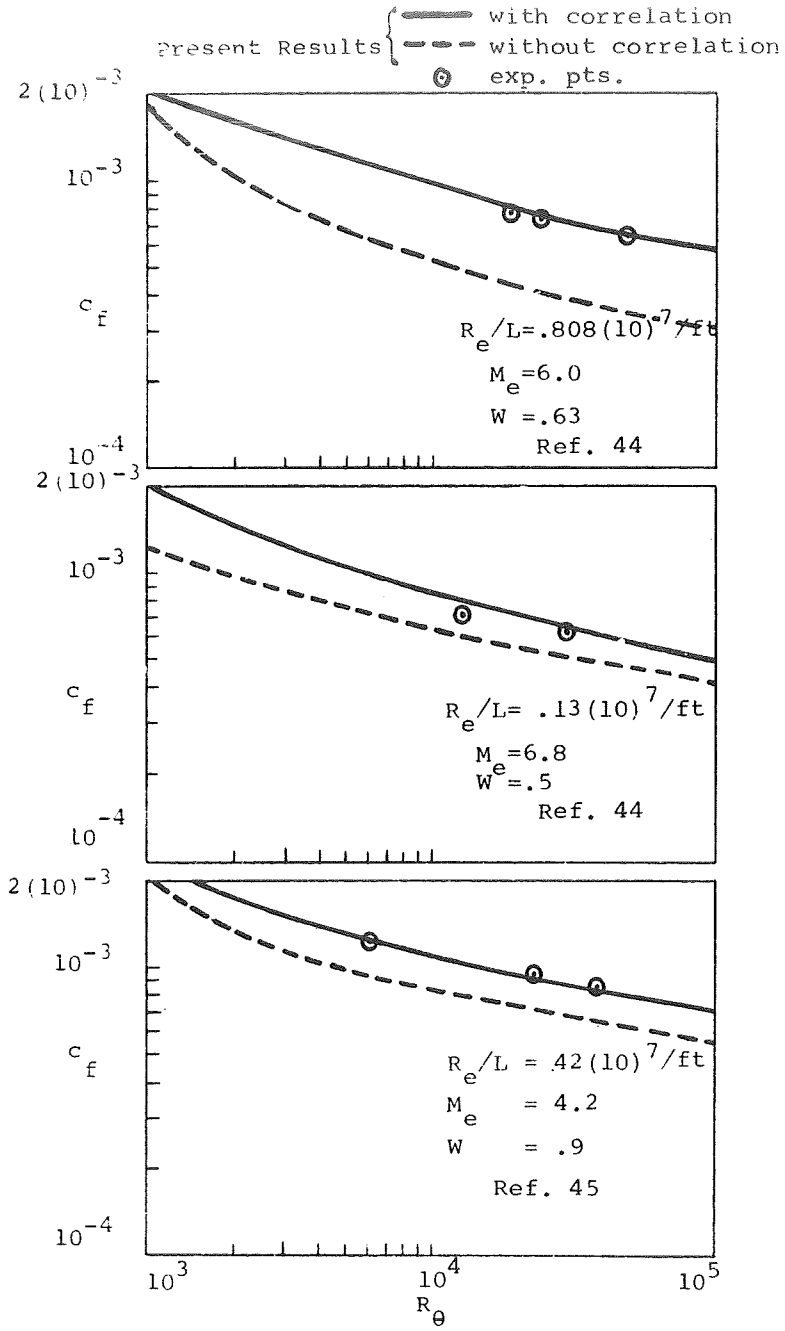

FIGURE 6 - COMPARISON OF THEORY WITH EXPERIMENT WITH AND WITHOUT THE USE OF THE WAKE CORRELATION

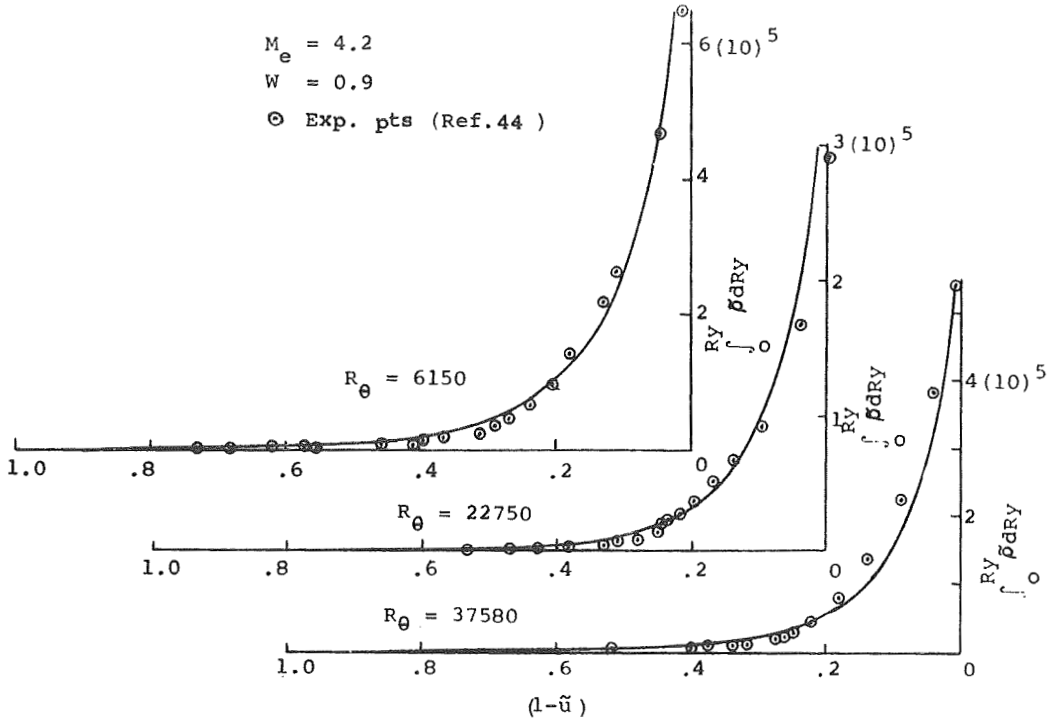

FIGURE 7a- COMPARISON OF A SERIES OF VELOCITY PROFILES WITH PRESENT METHOD (With Correlation)

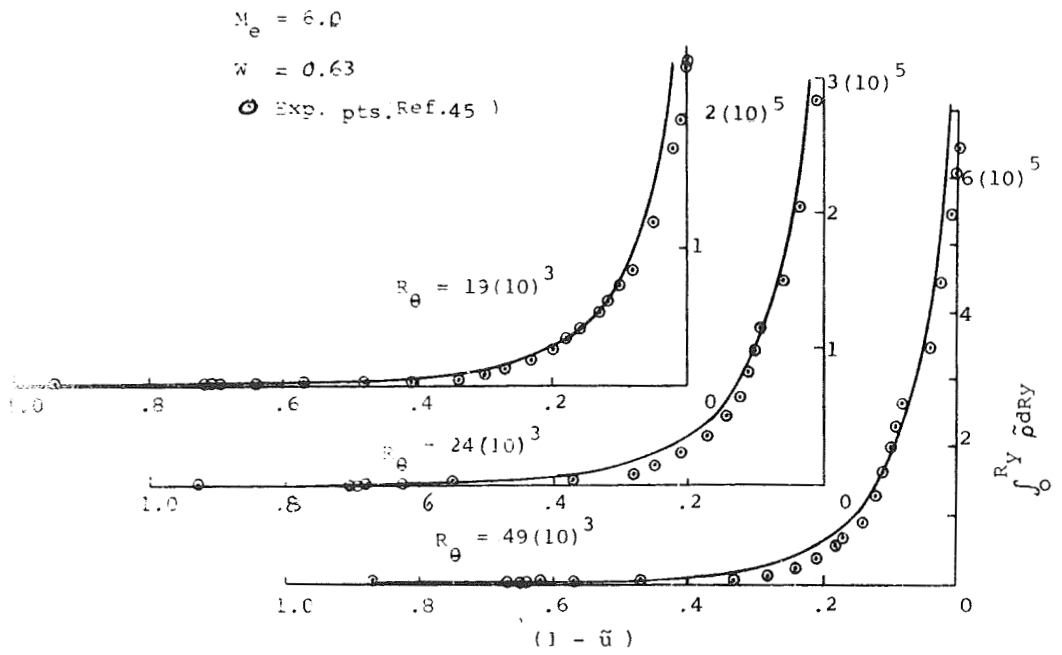

FIGURE 7b - COMPARISON OF A SERIES OF VELOCITY PROFILES WITH PRESENT METHOD
(With Correlation)

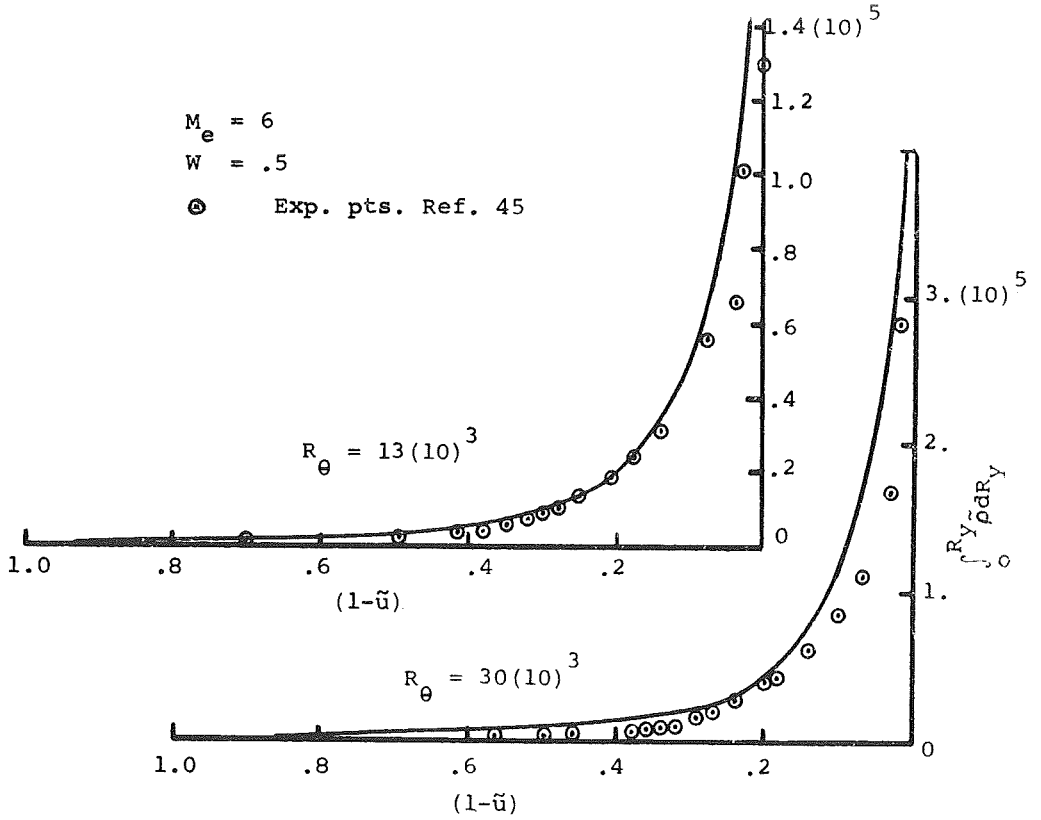

FIGURE 7c - COMPARISON OF A SERIES OF VELOCITY PROFILES WITH PRESENT METHOD
(With Correlation)

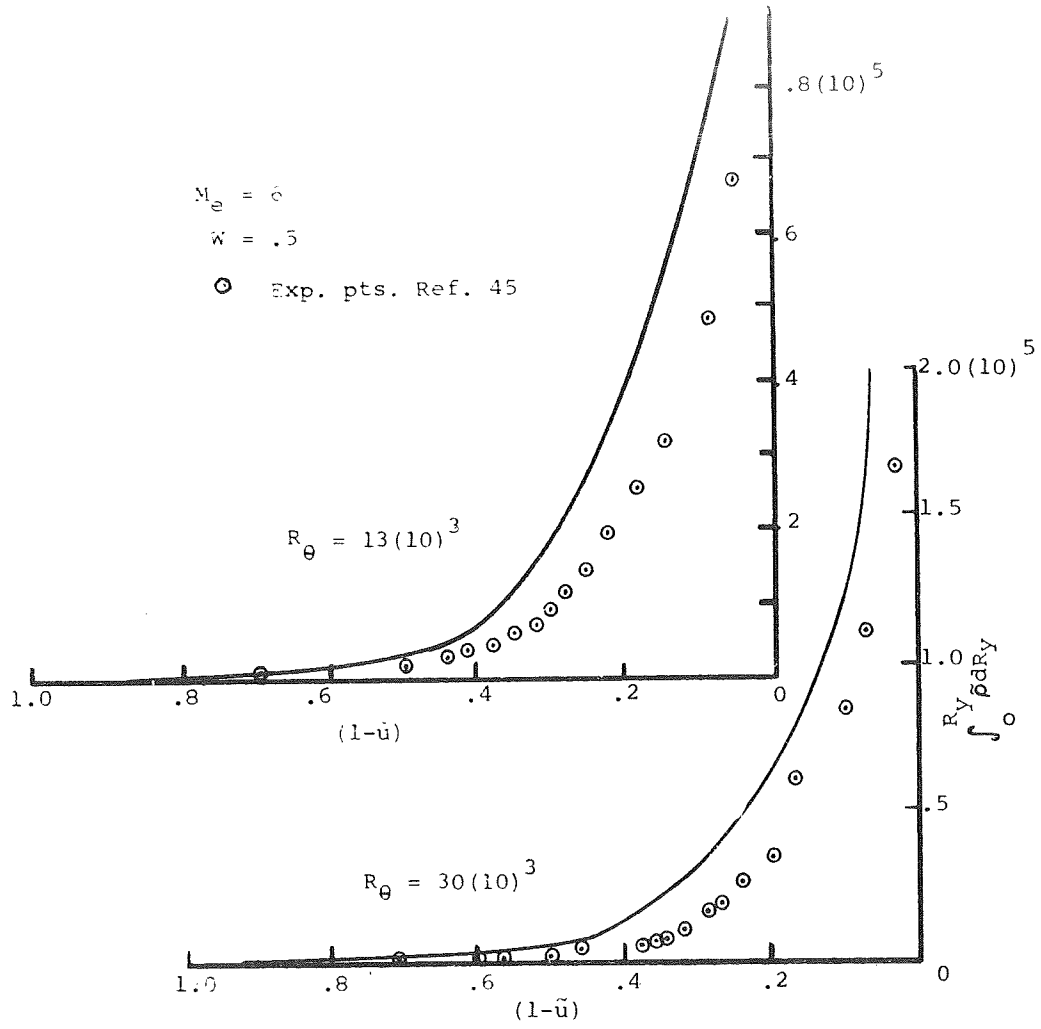

FIGURE 8a - COMPARISON OF A SERIES OF VELOCITY PROFILES WITH PRESENT METHOD
(Without Correlation)

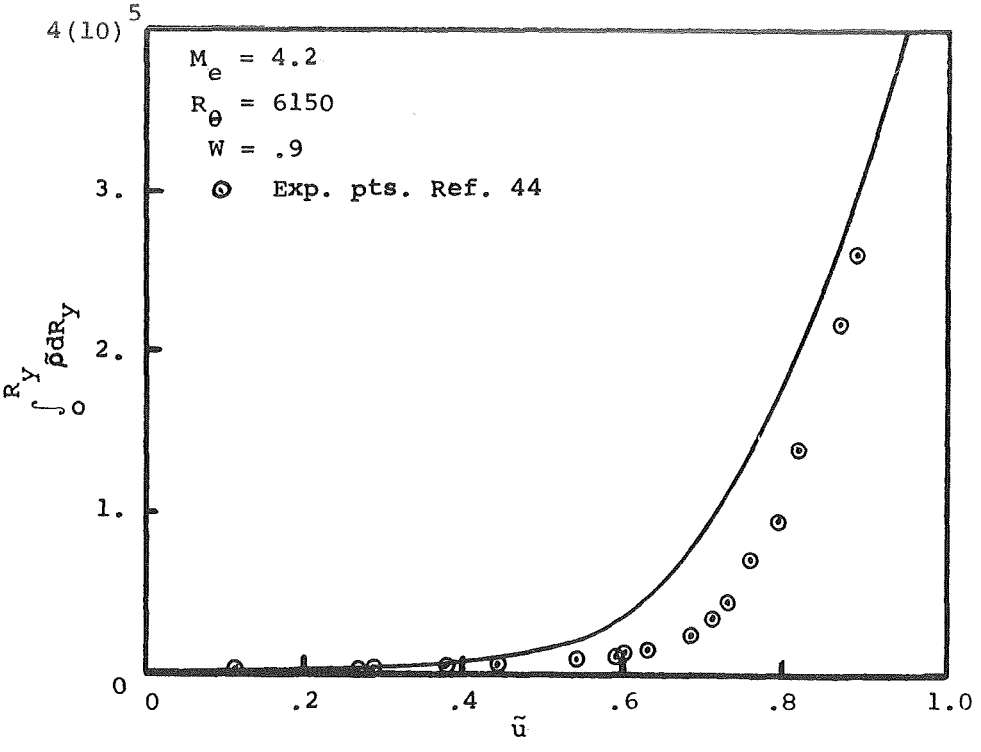

FIGURE 8b - COMPARISON OF A SERIES OF VELOCITY PROFILES WITH PRESENT METHOD (Without Correlation)

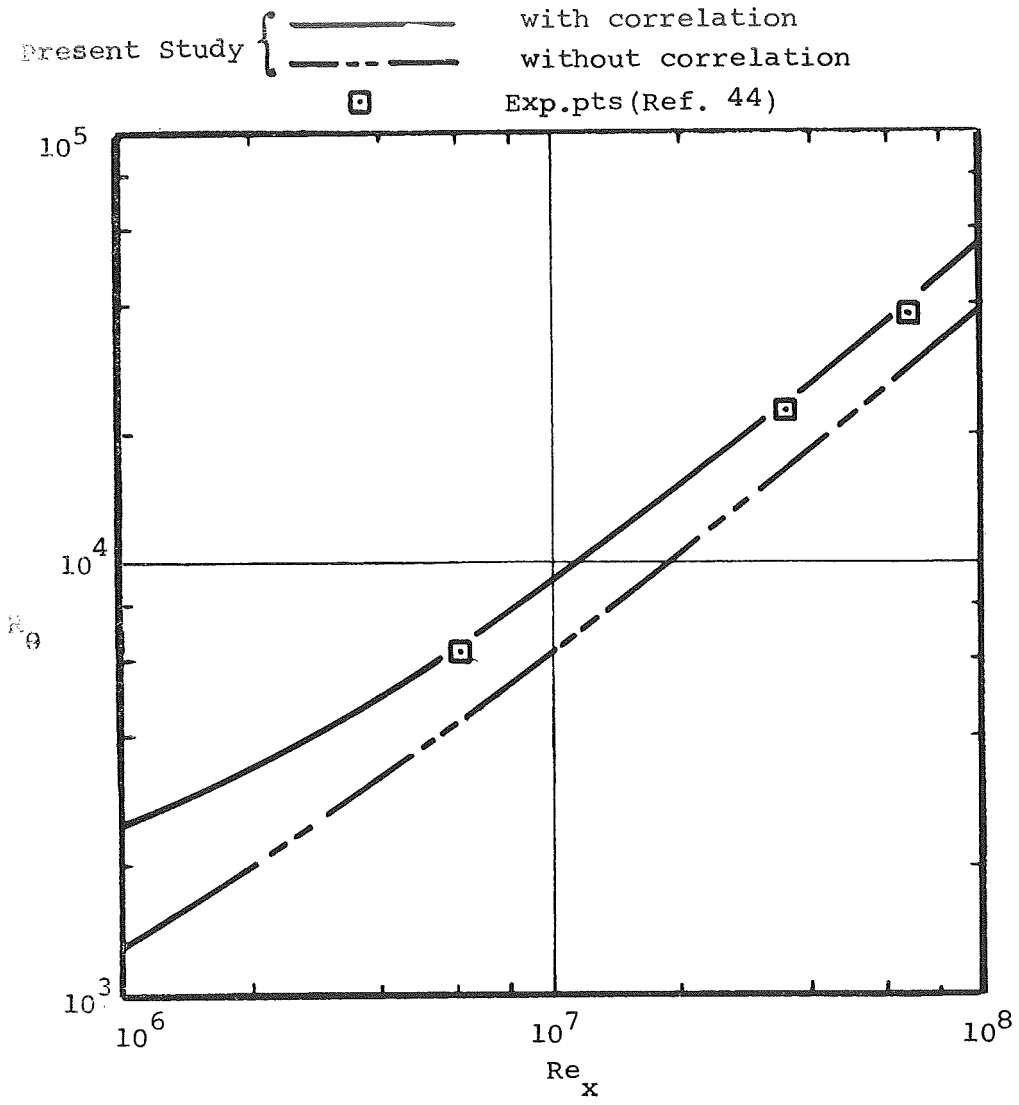

FIGURE 9 - COMPARISON OF THEORY WITH EXPERIMENT FOR STREAMWISE VARIATION OF MOMENTUM THICKNESS

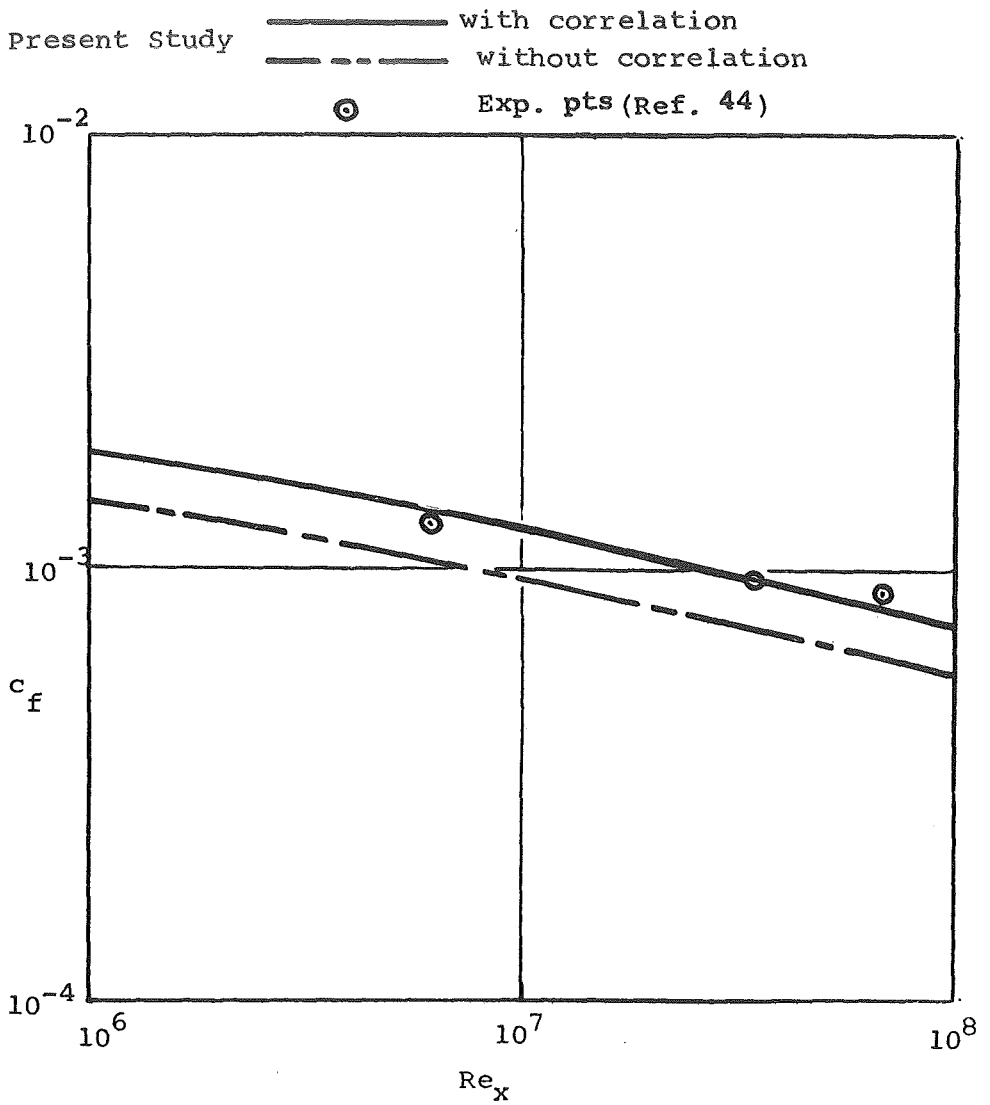

FIGURE 10 - COMPARISON OF THEORY WITH EXPERIMENT FOR STREAMWISE VARIATION OF SKIN FRICTION

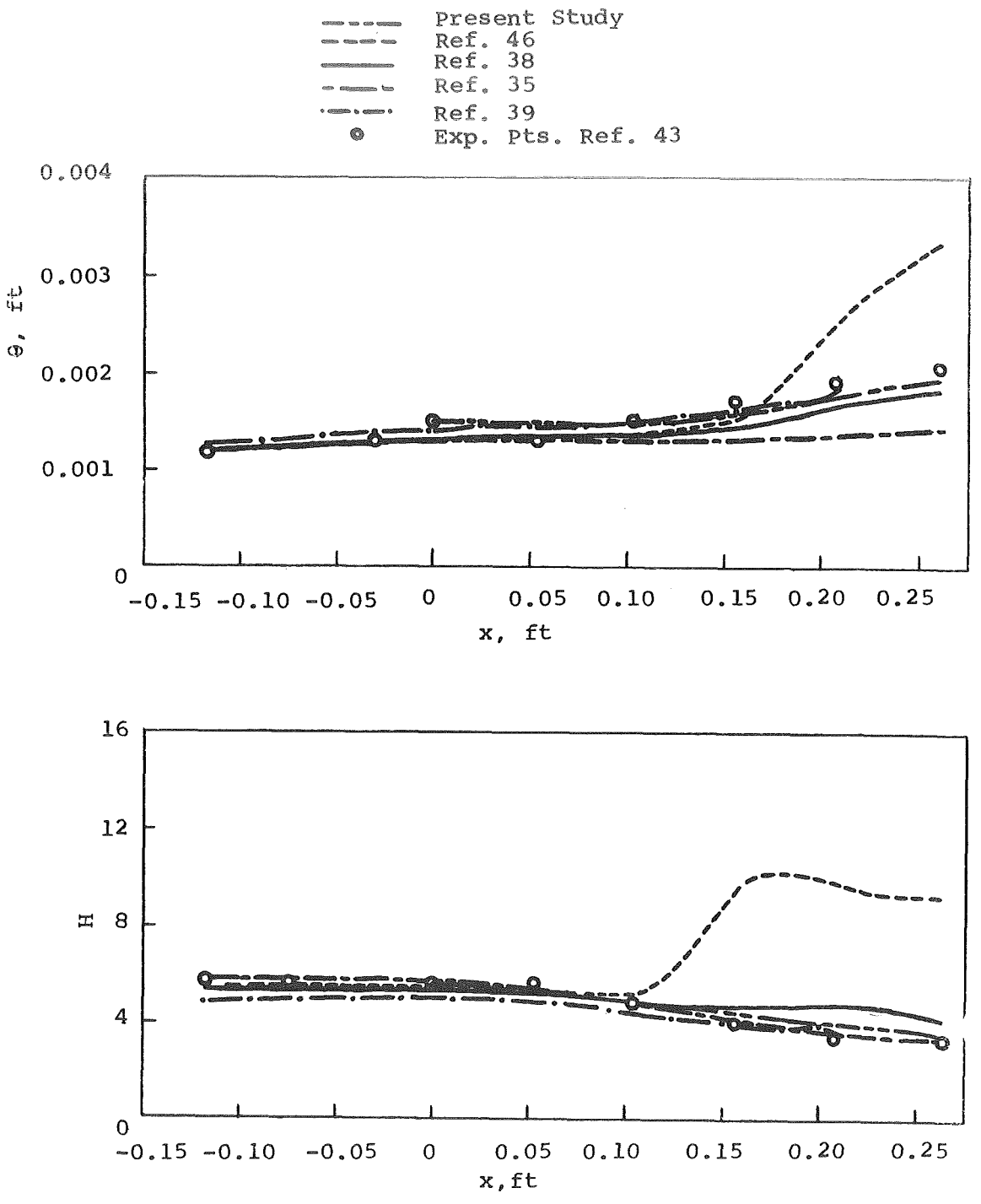

FIGURE 11 - COMPARISON BETWEEN THEORIES AND MEASUREMENTS OF McLAFFERTY AND BARBER, REF. 43, $M_\infty \approx 3.0$ FOR MOMENTUM THICKNESS AND FORM FACTOR

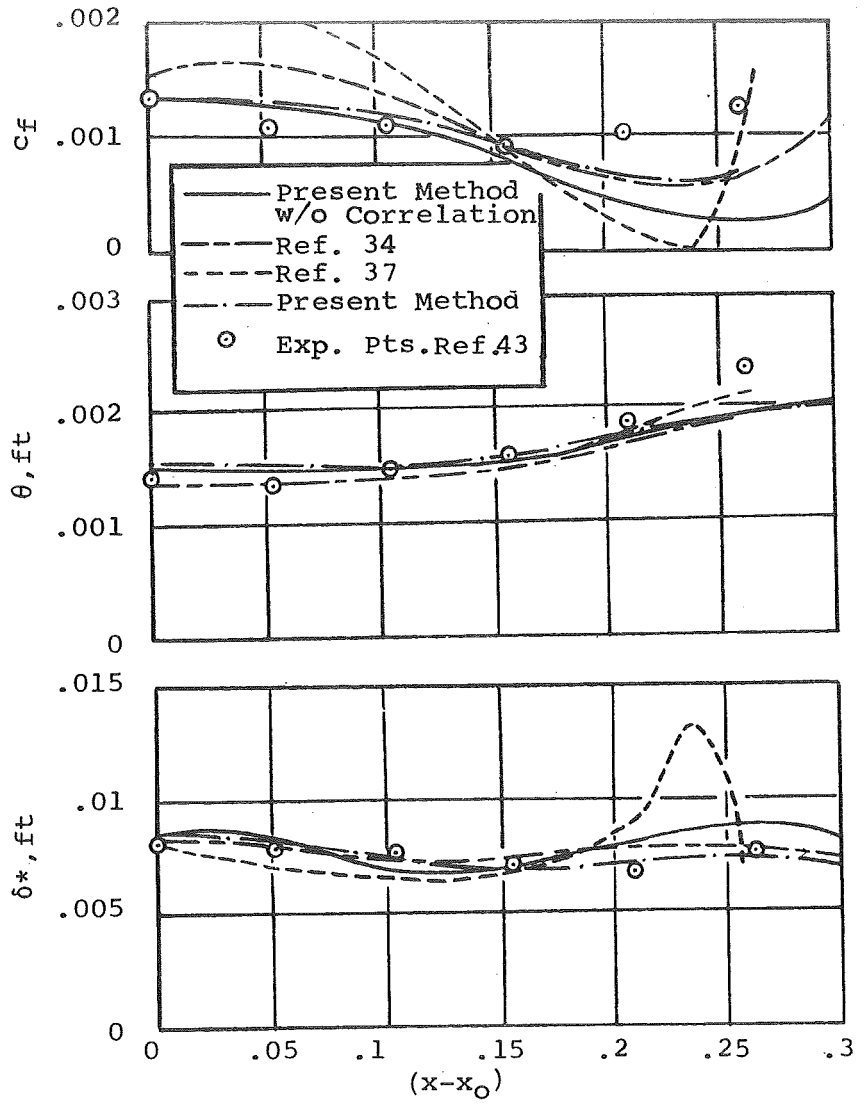

FIGURE 12 - COMPARISON BETWEEN THEORIES AND MEASUREMENTS OF McLAFFERTY AND BARBER, REF. 43, $M_{\infty} \approx 3.0$ FOR SKIN FRICTION MOMENTUM THICKNESS AND DISPLACEMENT THICKNESS

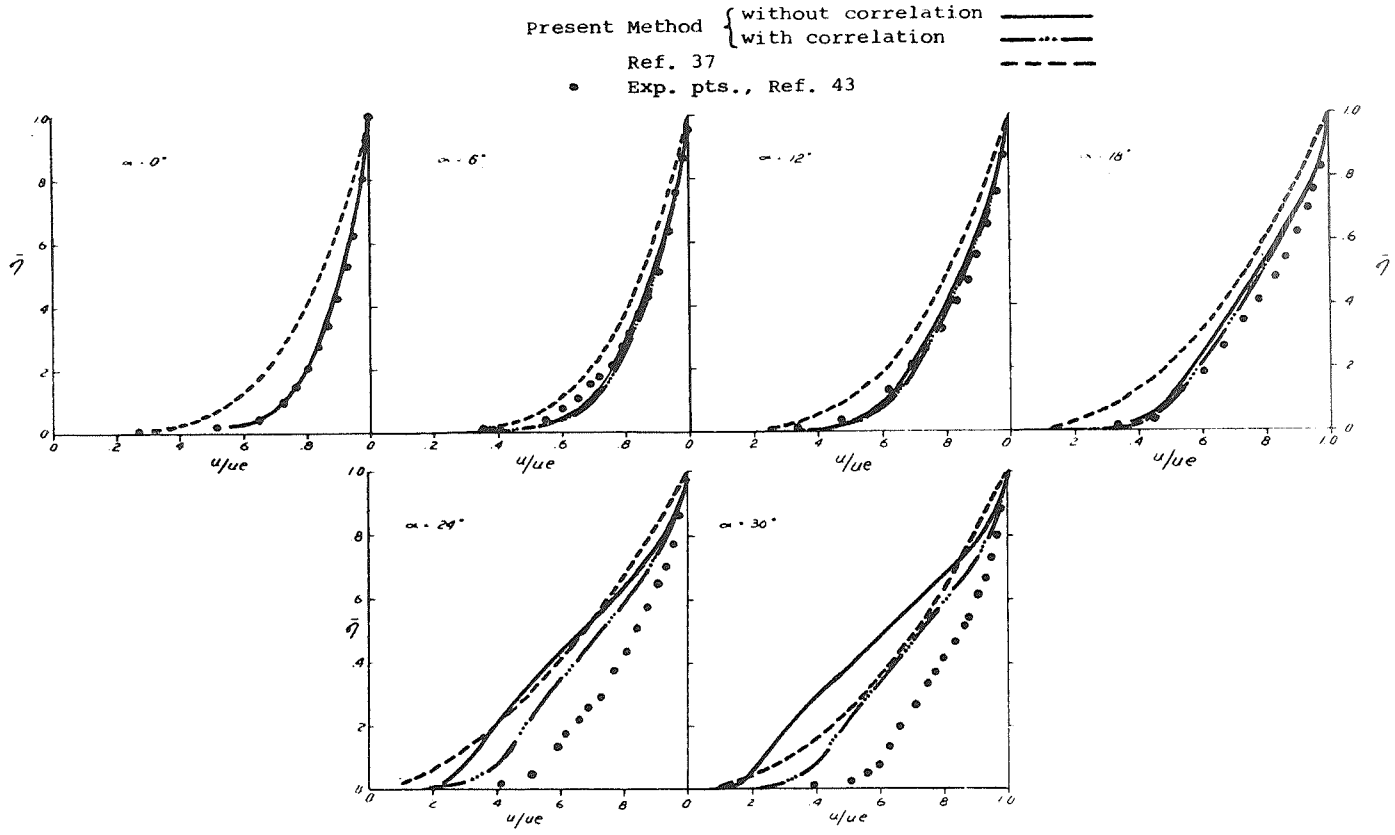

FIGURE 13 - COMPARISON OF A SERIES OF VELOCITY PROFILES WITH THEORY

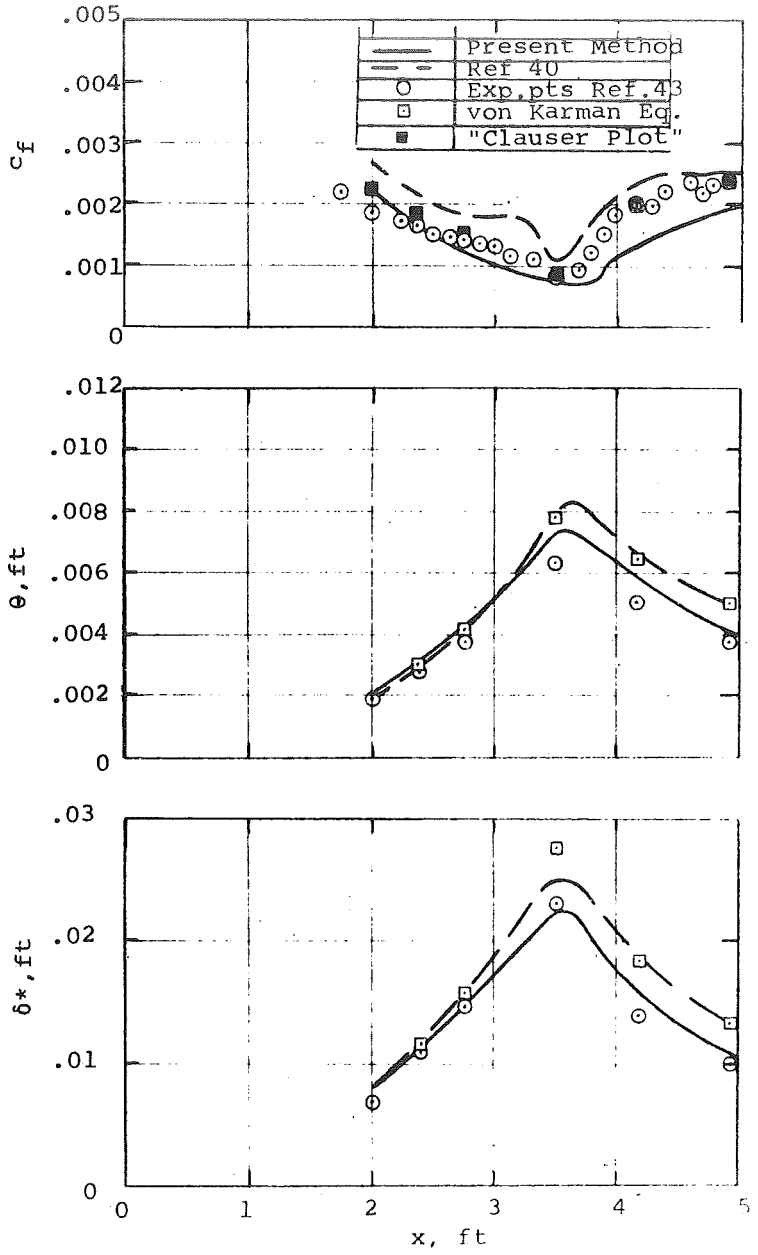

FIGURE 14 - COMPARISON BETWEEN THEORY AND MEASUREMENTS OF WINTER, SMITH AND ROTTA, REF. 42, $M_\infty = 2.0$, $(R_e/L)_\infty = 2(10)^6/ft$

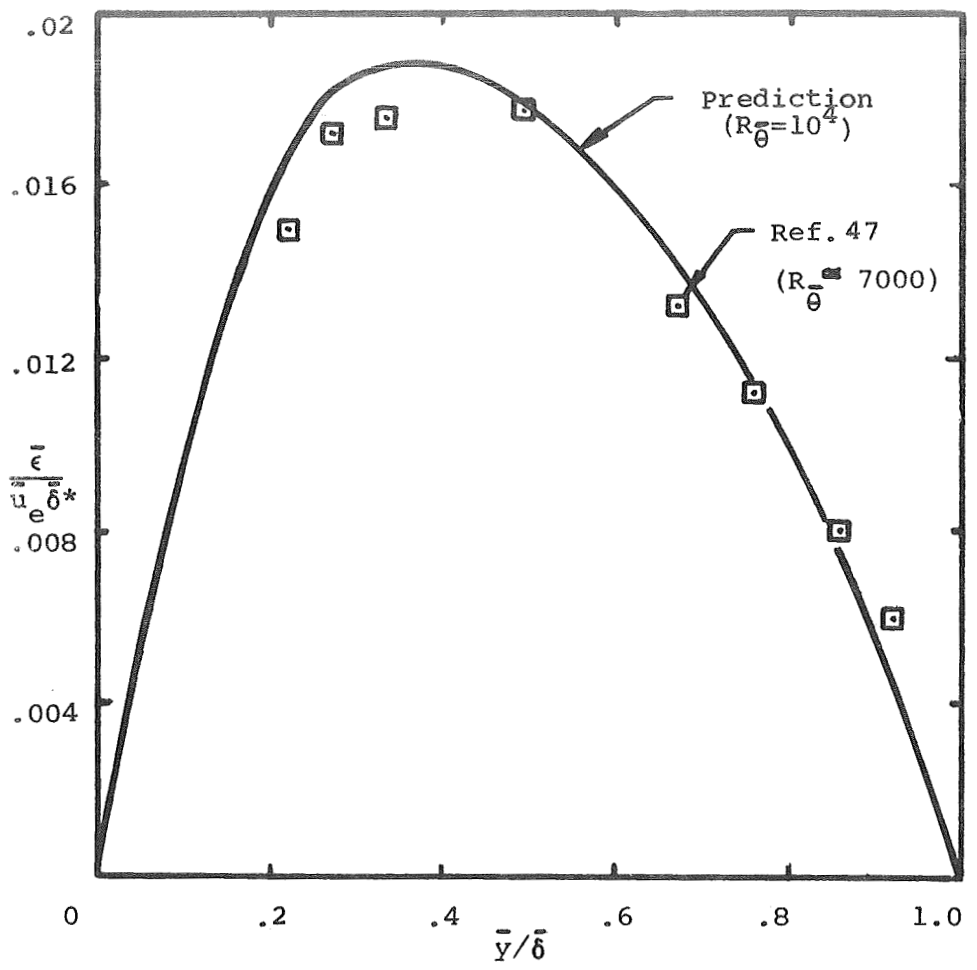

FIGURE 15 - COMPARISON OF THEORY WITH EXPERIMENT FOR EDDY VISCOSITY DISTRIBUTION

$M_e \simeq 0$; $dp/dx = 0$

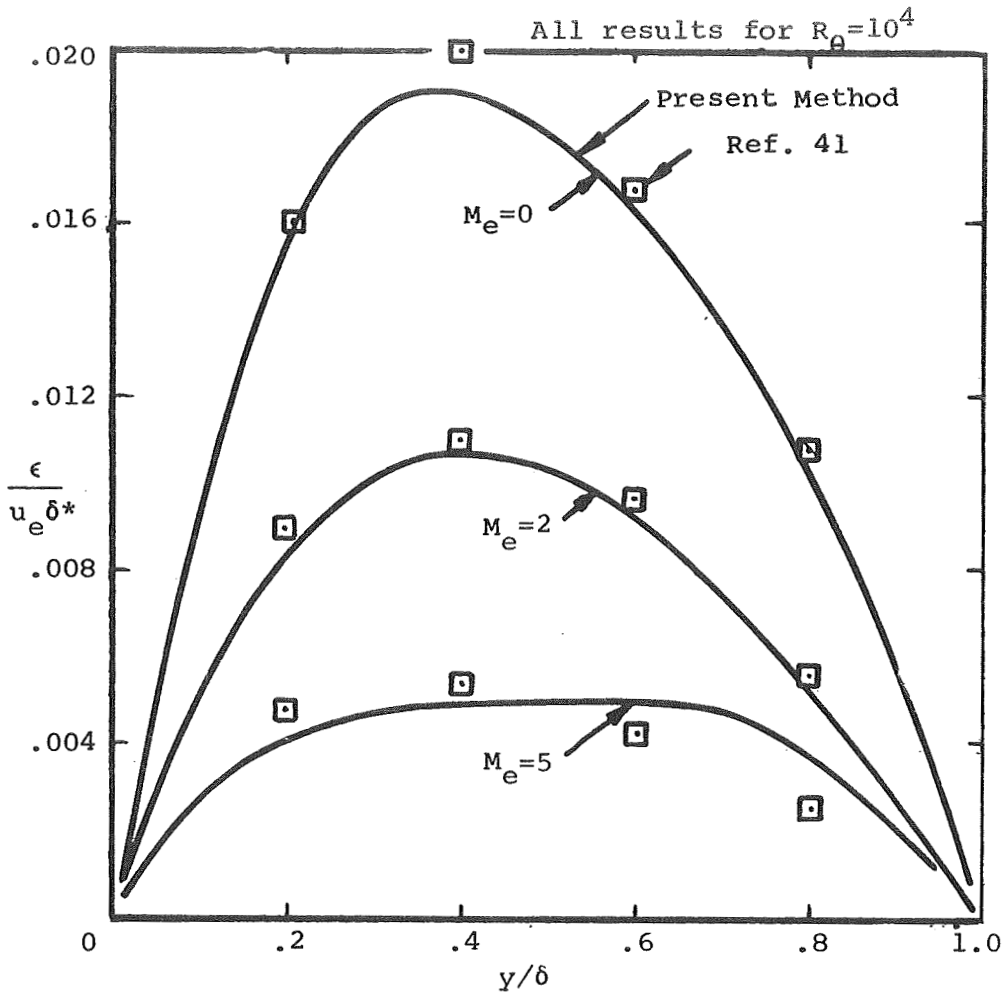

FIGURE 16 - EFFECT OF M_e ON EDDY VISCOSITY DISTRIBUTION FOR ADIABATIC FLOW
(W = 1)

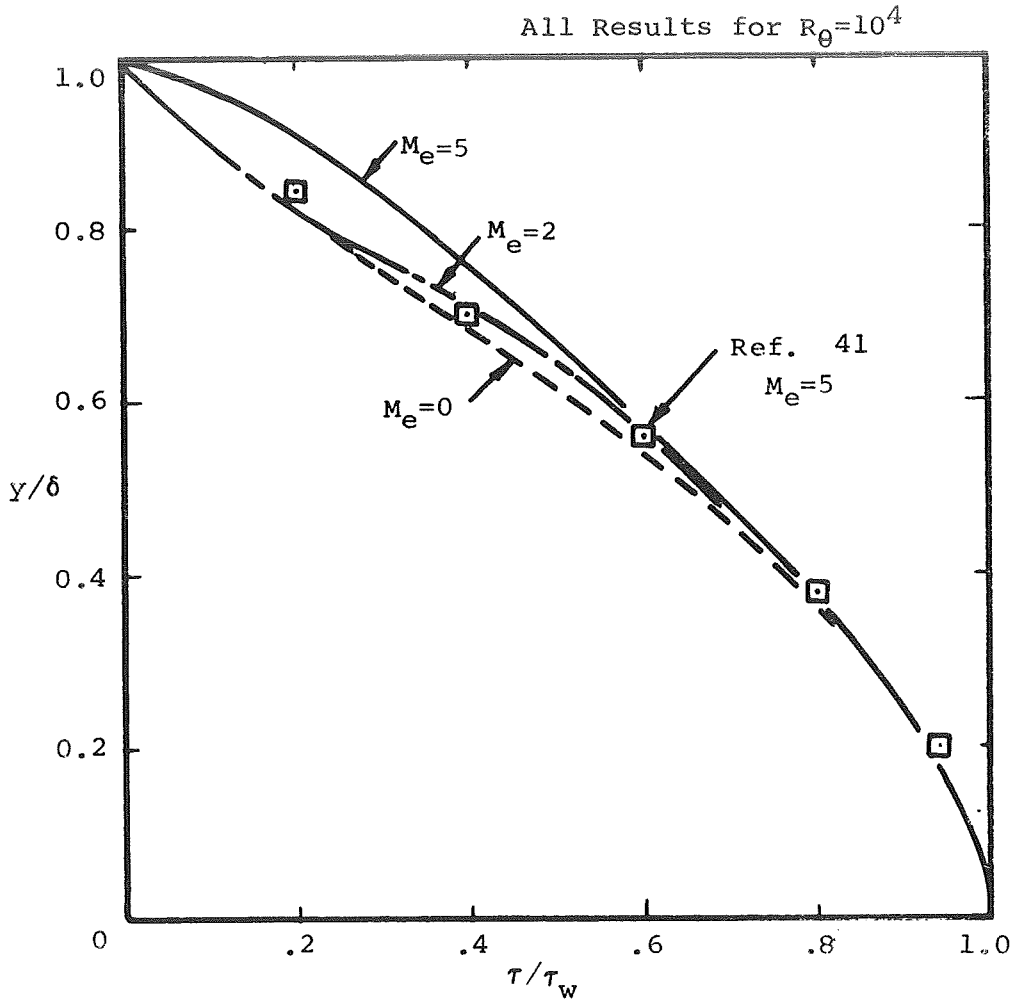

FIGURE 17- EFFECT OF M_e ON SHEAR DISTRIBUTION FOR ADIABATIC FLOW

(W = 1)

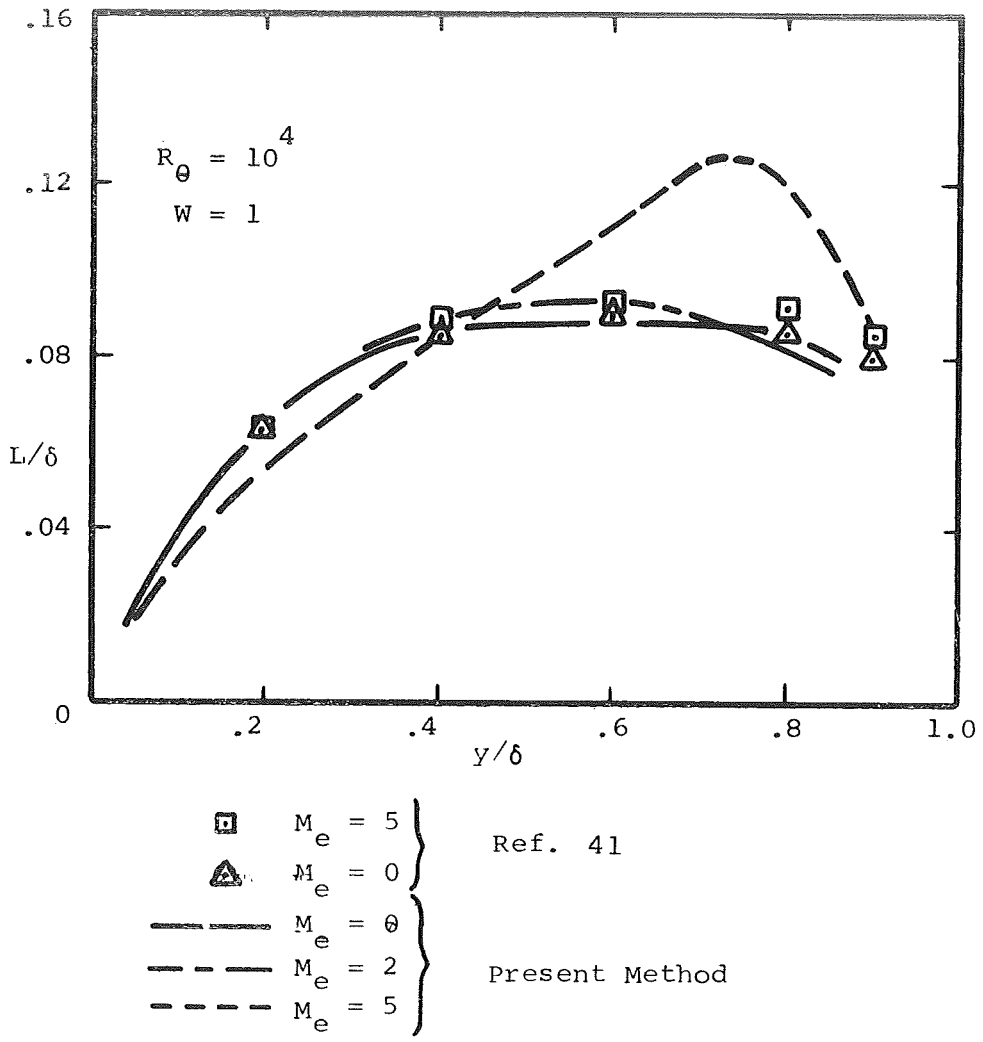

FIGURE 18 - EFFECT OF M_e ON MIXING LENGTH DISTRIBUTION FOR ADIABATIC FLOW (W = 1)

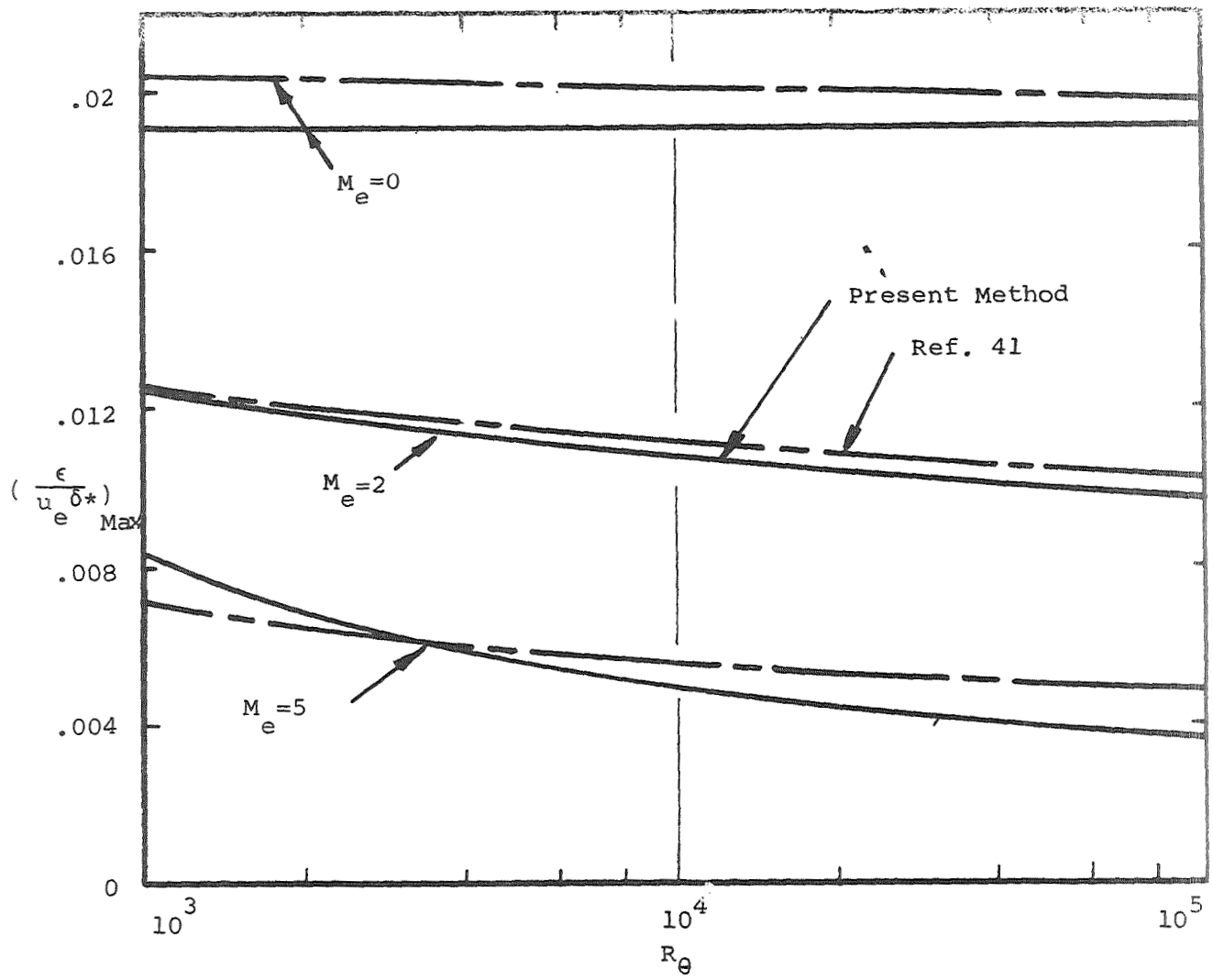

FIGURE 19- EFFECT OF M_e AND R_θ ON $(\epsilon/u_e\delta^*)_{MAX}$ FOR ADIABATIC FLOW (W=1)

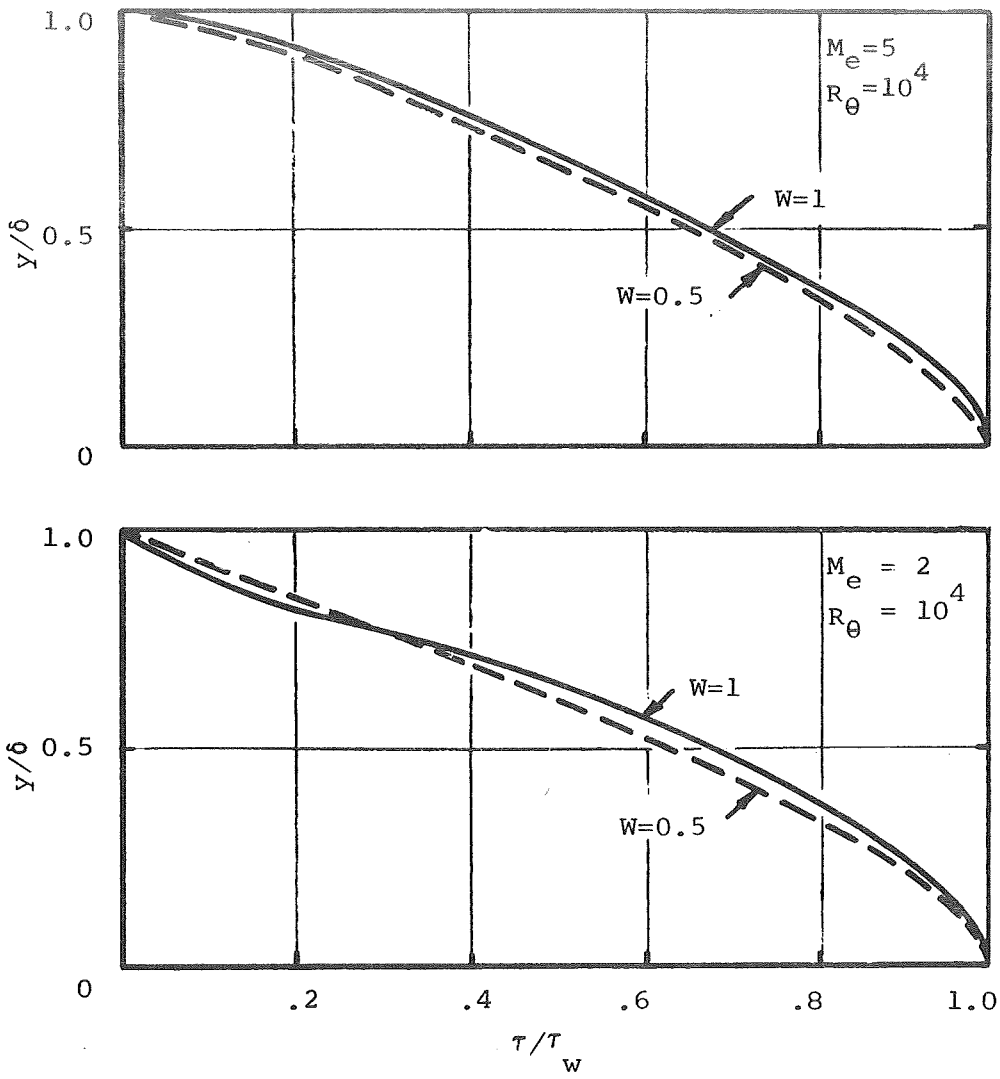

FIGURE 20 - EFFECT OF W ON SHEAR DISTRIBUTION

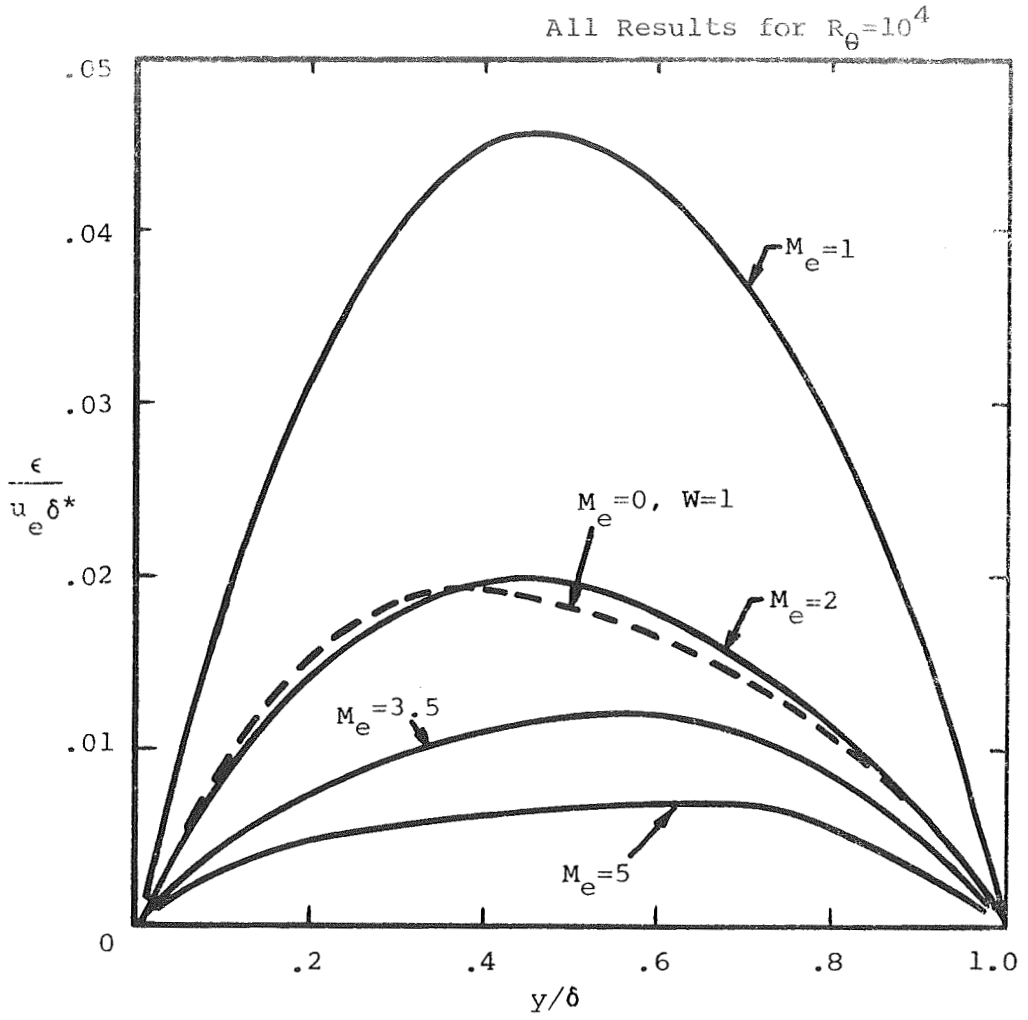

FIGURE 21- EFFECT OF M_e ON EDDY VISCOSITY DISTRIBUTION FOR NON-ADIABATIC FLOW (W = .5)

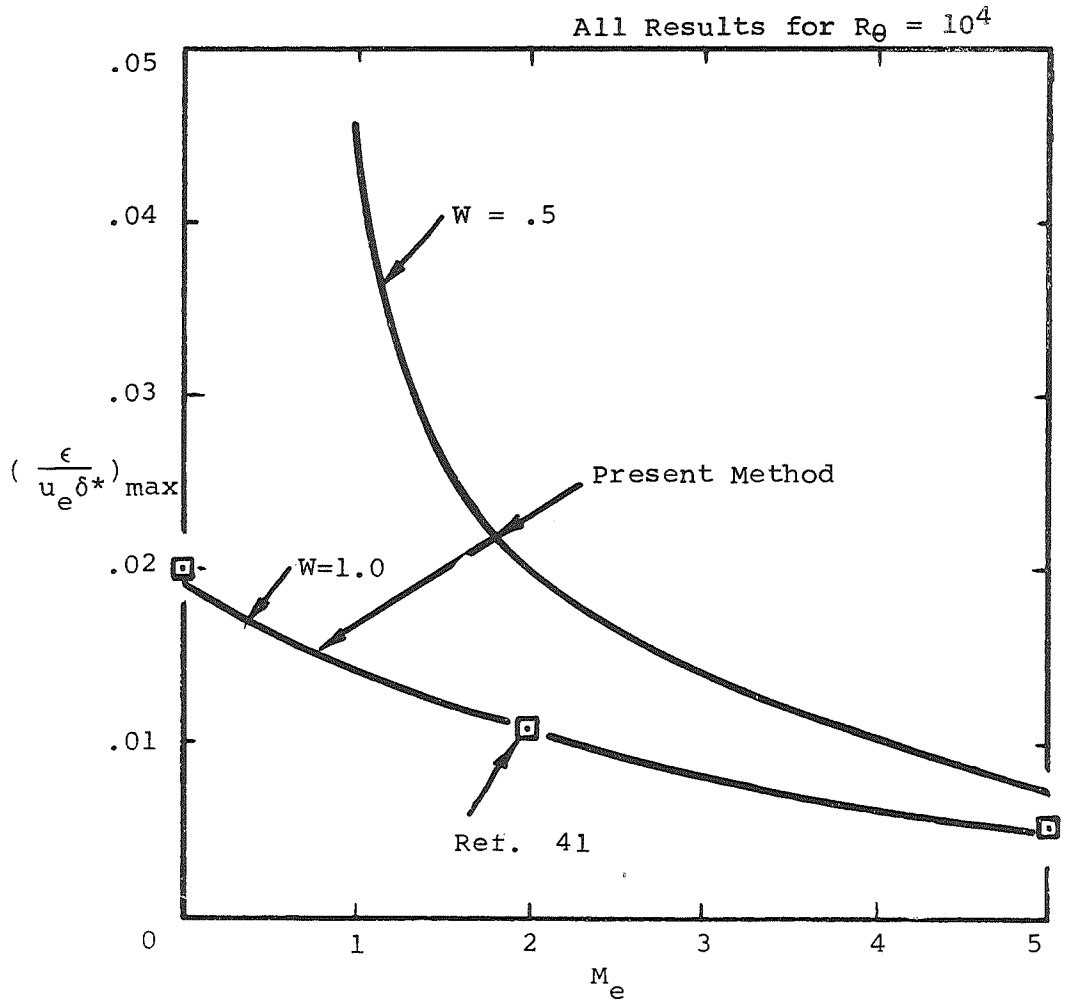

FIGURE 22- EFFECT OF M_e AND W ON $(\epsilon/u_e\delta^*)_{MAX}$

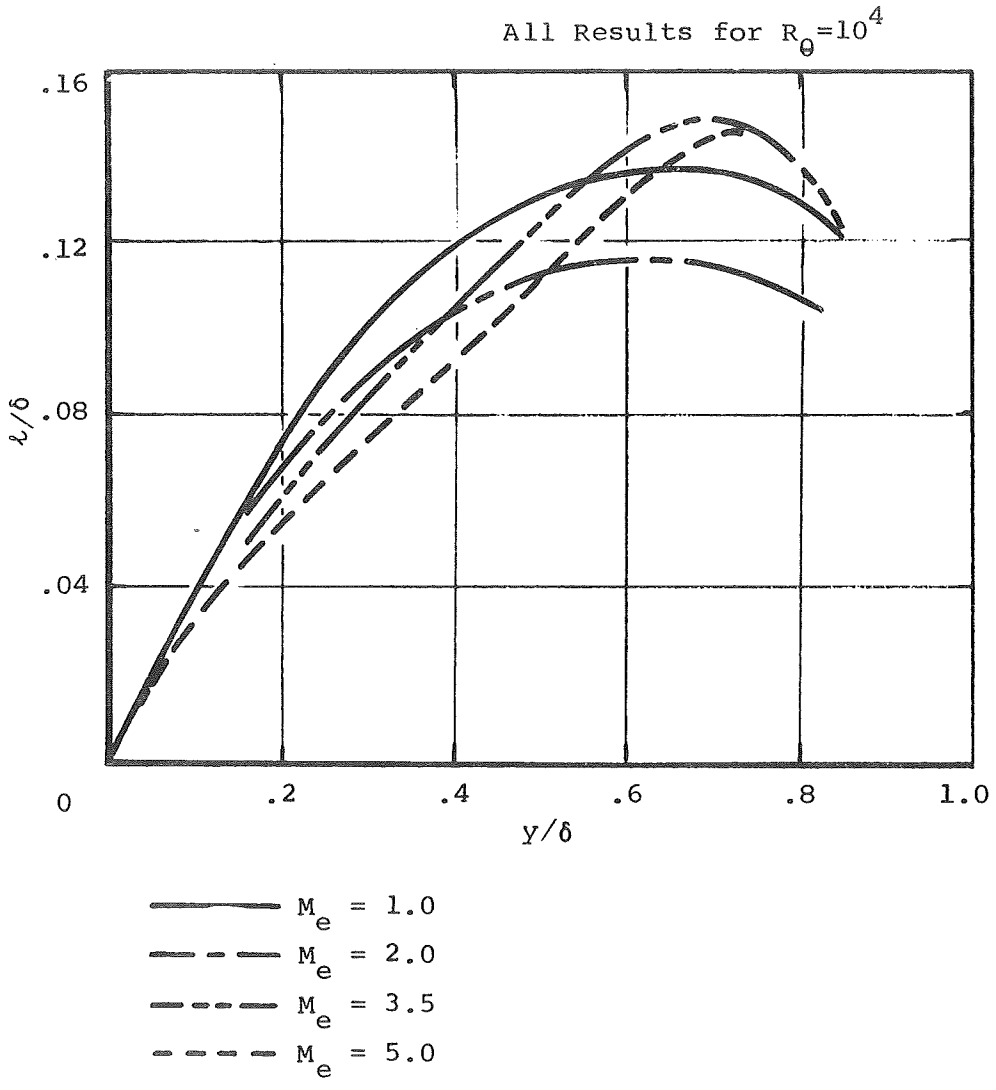

FIGURE 23- EFFECT OF M_e ON MIXING LENGTH DISTRIBUTION FOR NON-ADIABATIC FLOW (W=0.5)

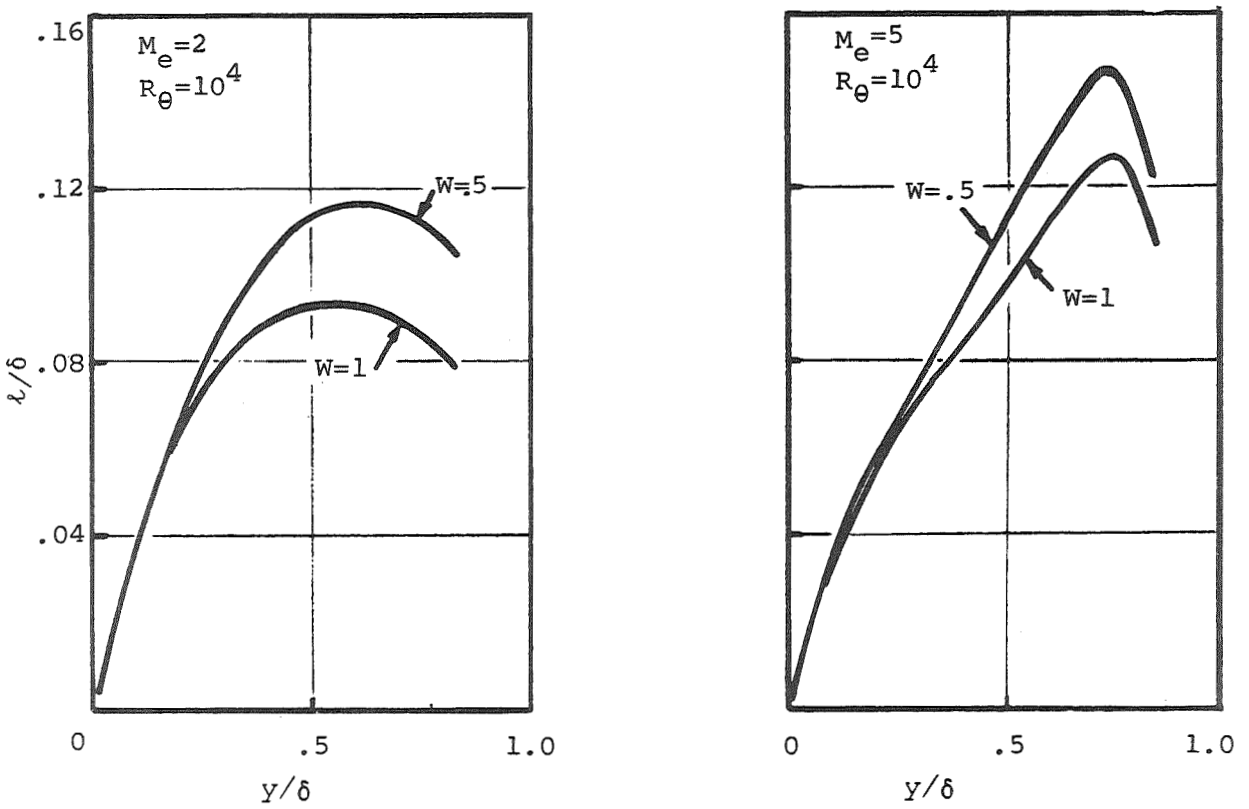

FIGURE 24 - EFFECT OF W ON MIXING LENGTH DISTRIBUTION

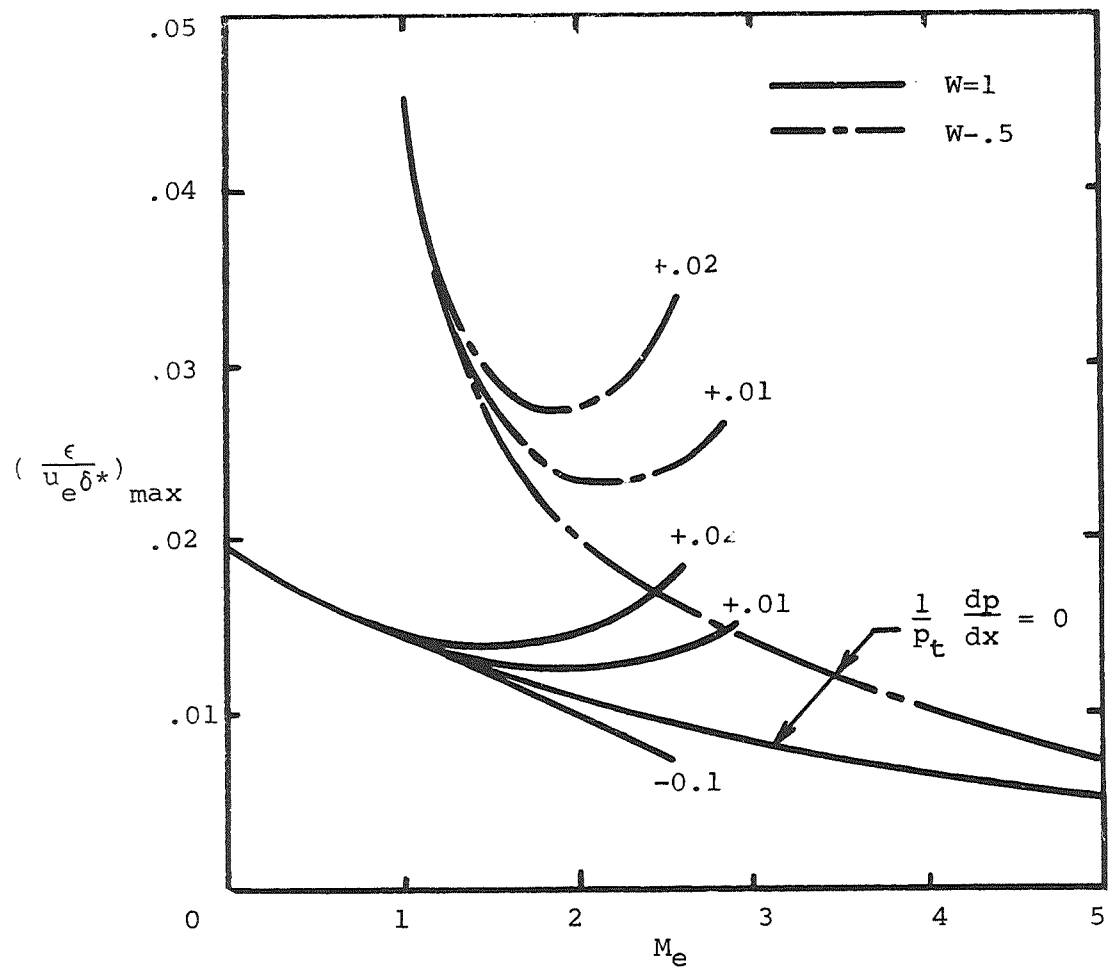

FIGURE 25- EFFECT OF PRESSURE GRADIENT AND MACH NUMBER ON EDDY VISCOSITY
$R_\theta = 10^4$

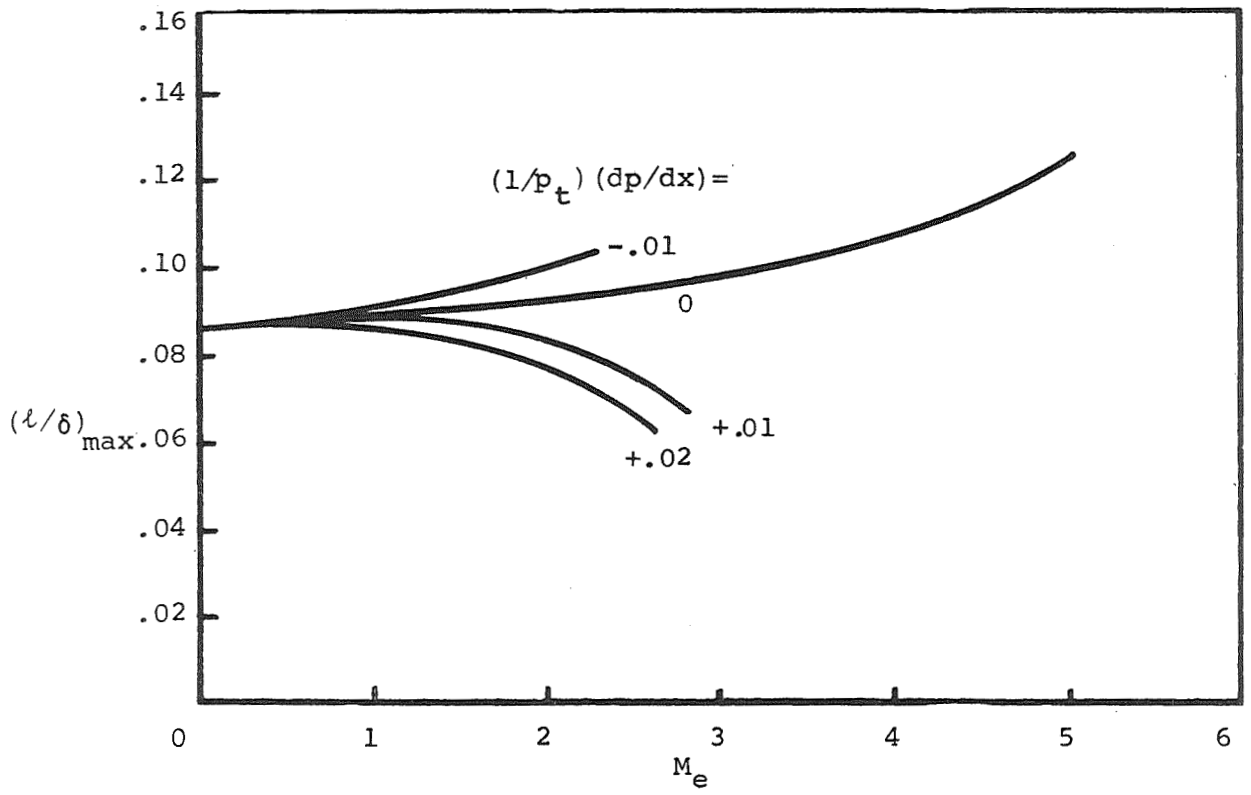

FIGURE 26 - EFFECT OF PRESSURE GRADIENT AND MACH NUMBER ON MIXING LENGTH FOR ADIABATIC FLOWS - $R_\theta = 10^4$

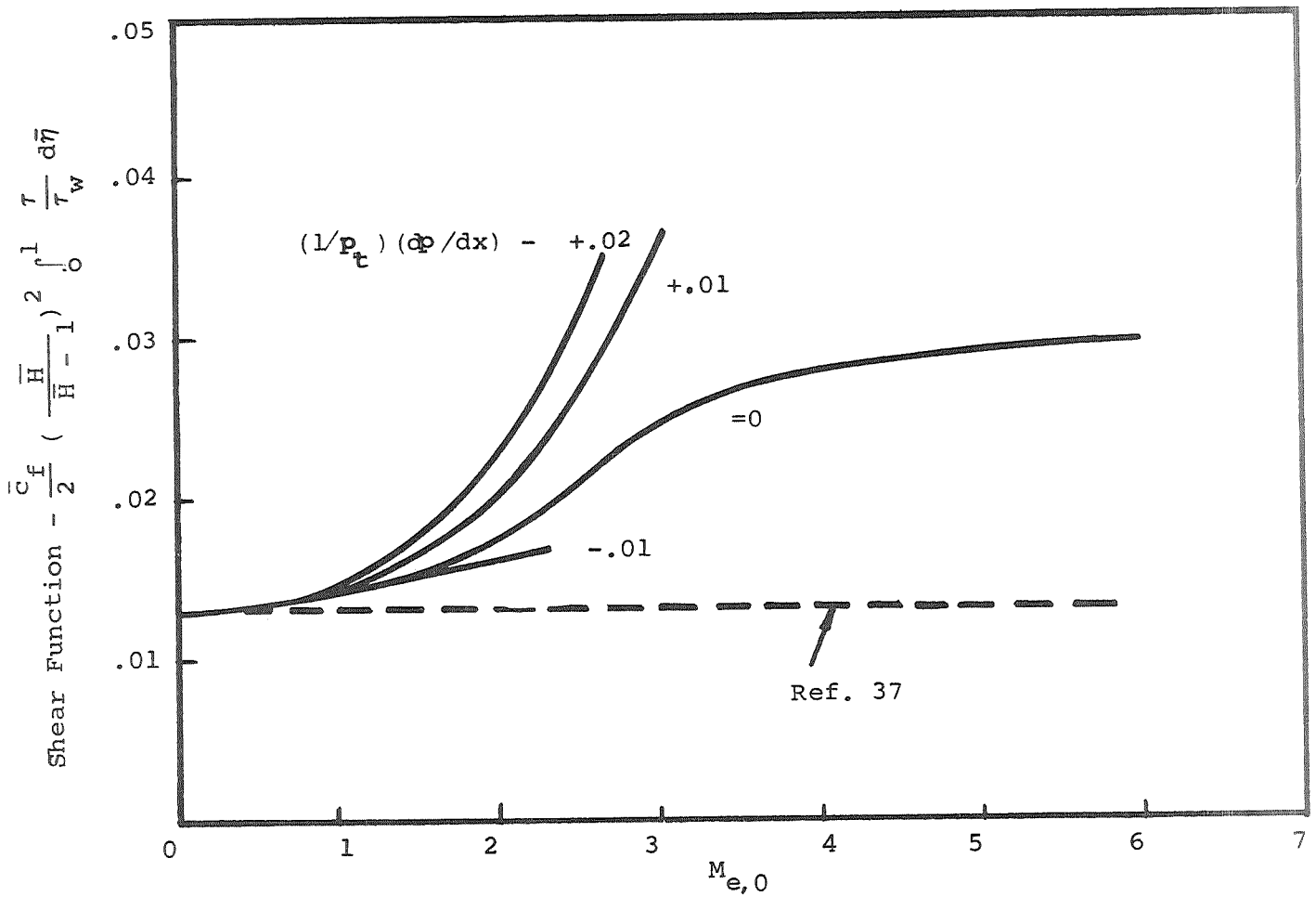

FIGURE 27- COMPARISON OF PRESENT CALCULATION FOR SHEAR FUNCTION WITH VALUES OF REF. 37- $R_\theta = 10^4$, W = 1

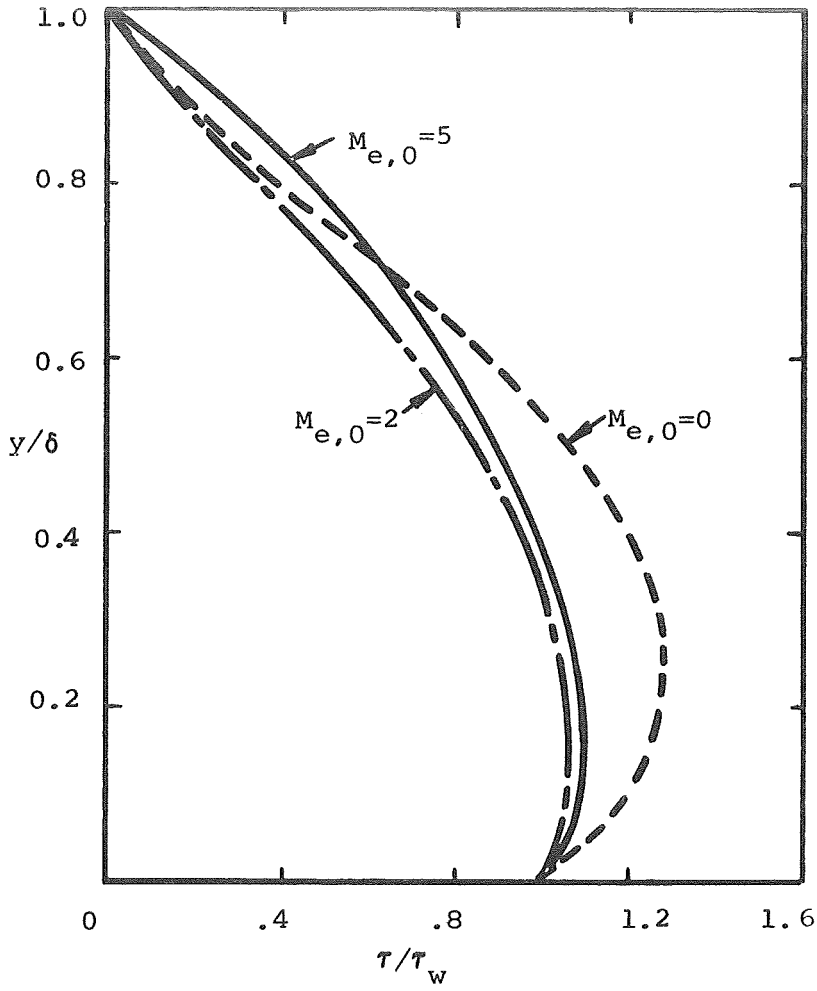

FIGURE 28- EFFECT OF MACH NUMBER LEVEL ON SHEAR DISTRIBUTION FOR ADIABATIC FLOW WITH PRESSURE GRADIENT

$R_\theta = 10^4 - (1/p_t)(dp/dx) = .01$

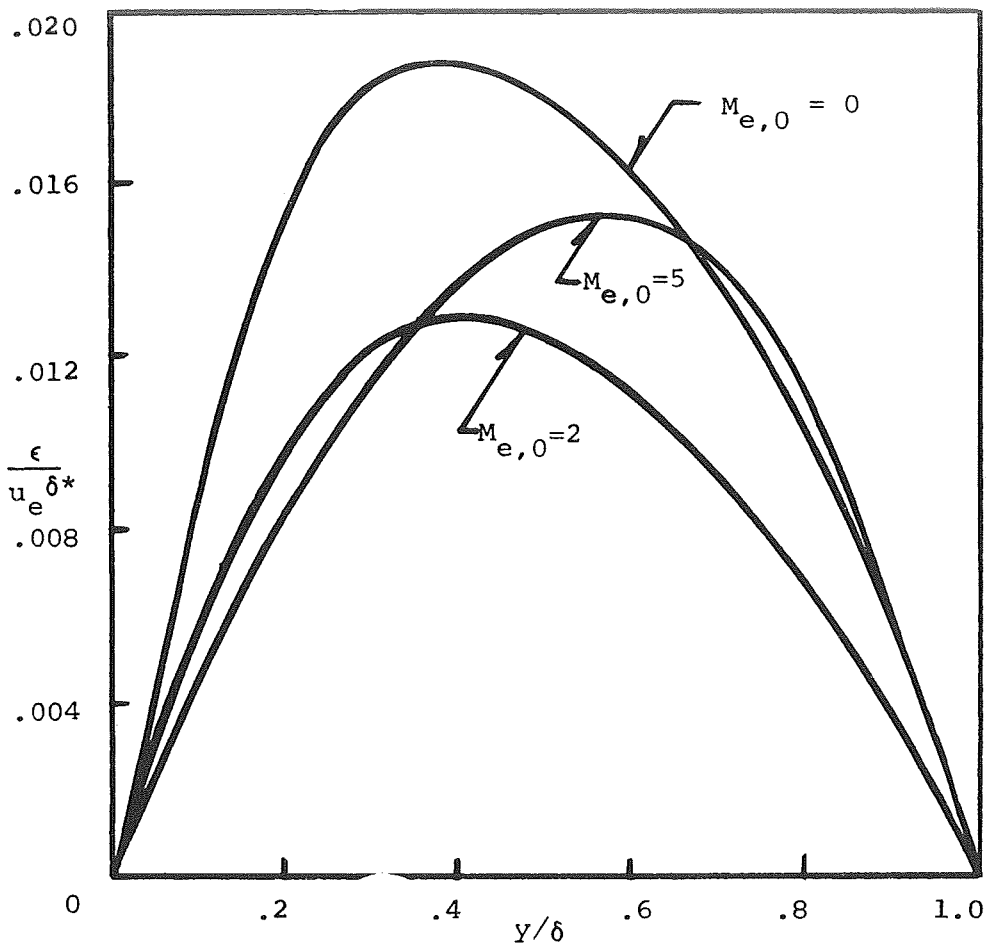

FIGURE 29- EFFECT OF MACH NUMBER LEVEL ON EDDY VISCOSITY DISTRIBUTION FOR ADIABATIC FLOW WITH PRESSURE GRADIENT - $R_\theta = 10^4$ - $(1/p_t)(dp/dx) = .01$

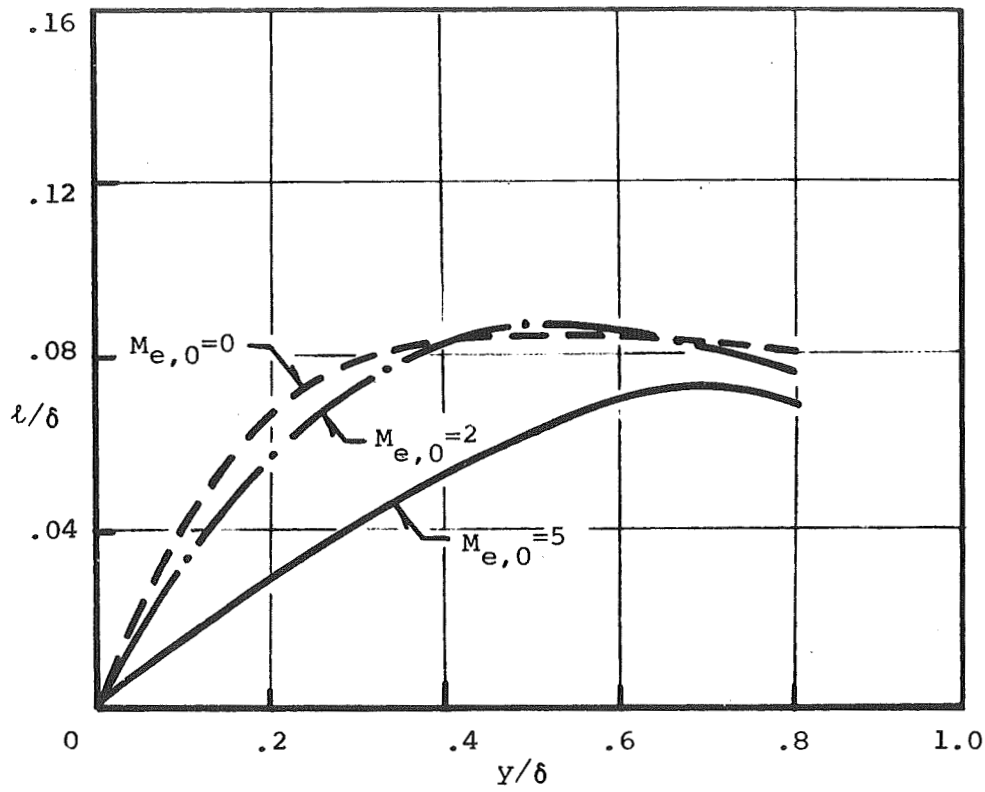

FIGURE 30 - EFFECT OF MACH NUMBER LEVEL ON MIXING LENGTH DISTRIBUTION FOR ADIABATIC FLOW WITH PRESSURE GRADIENT - $R_\theta = 10^4$; $(1/p_t)(dp/dx) = .01$

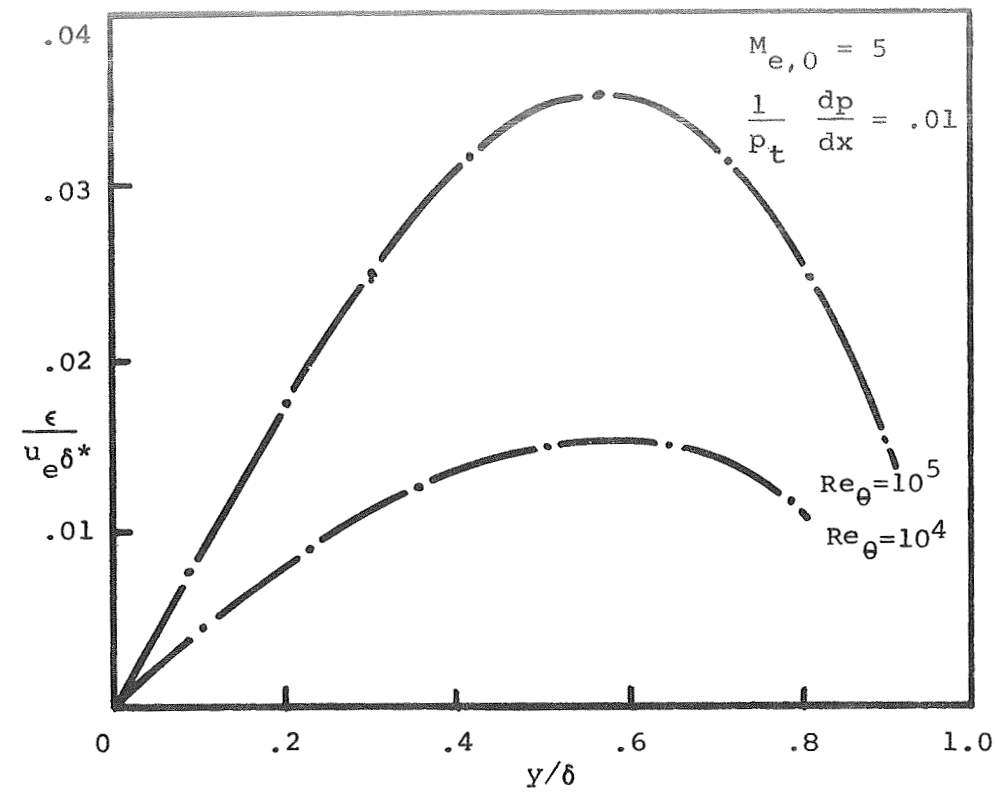

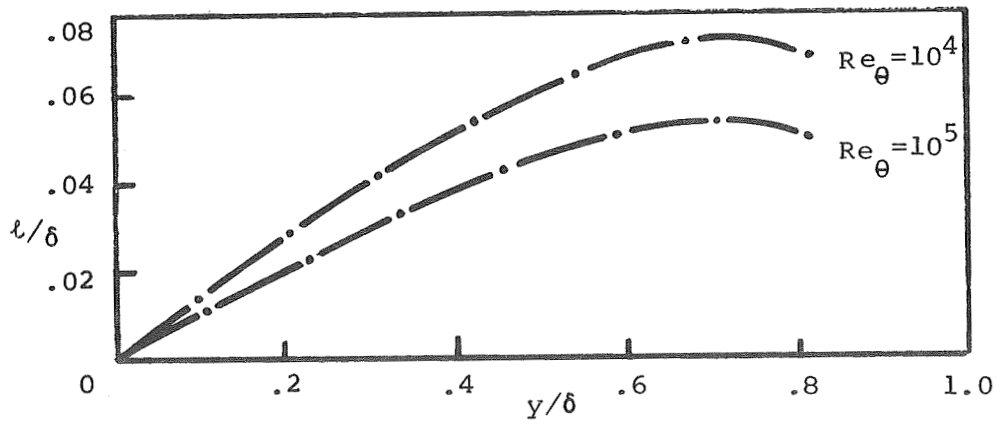

FIGURE 31 - EFFECT OF R_θ ON EDDY VISCOSITY AND MIXING LENGTH FOR ADIABATIC FLOW WITH PRESSURE GRADIENT $M_{e,0}=5$, $(1/p_t)(dp/dx) = .01$

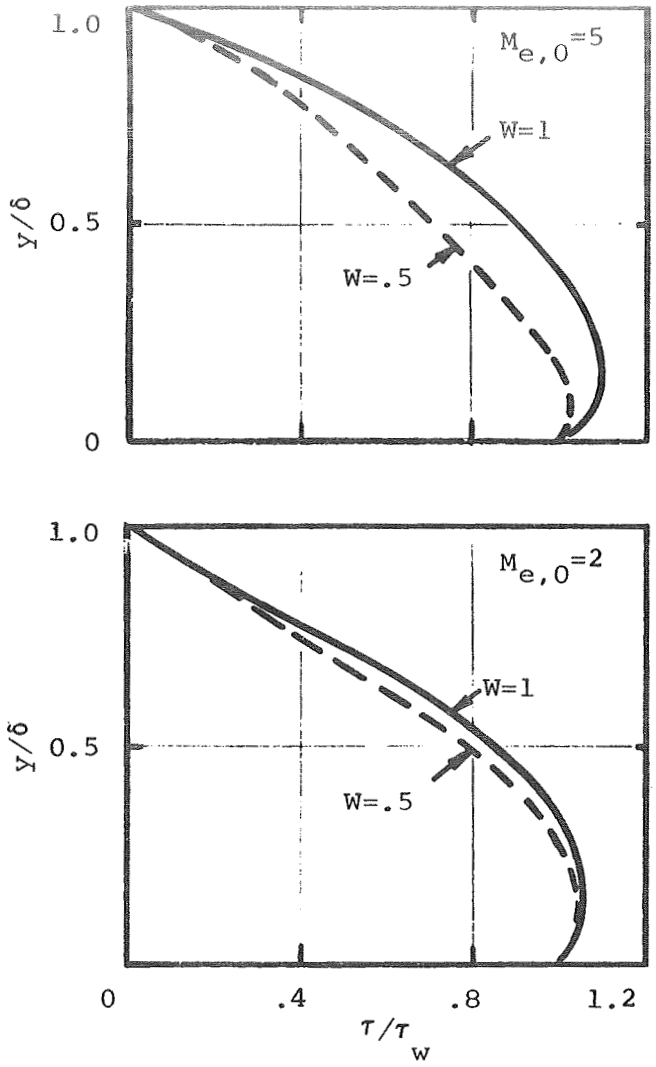

FIGURE 32- EFFECT OF HEAT TRANSFER ON SHEAR DISTRIBUTION FOR FLOW WITH PRESSURE GRADIENT $R_\theta = 10^4$

$(1/p_t)(dp/dx) = .01$, $W \equiv T_w/T_{t_e}$

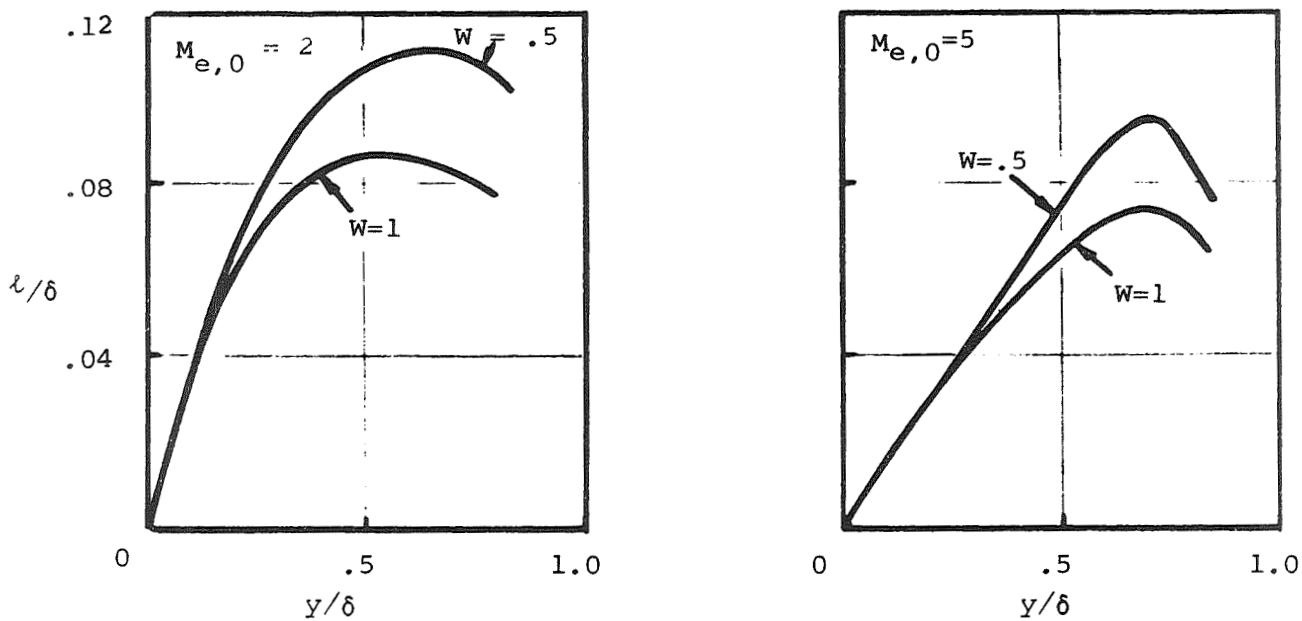

FIGURE 33 - EFFECT OF HEAT TRANSFER ON MIXING LENGTH DISTRIBUTION FOR FLOW WITH PRESSURE GRADIENT

$R_\theta = 10^4$ $\quad (1/p_t)(dp/dx) = .01$ $\quad W \equiv T_w/T_{t_e}$

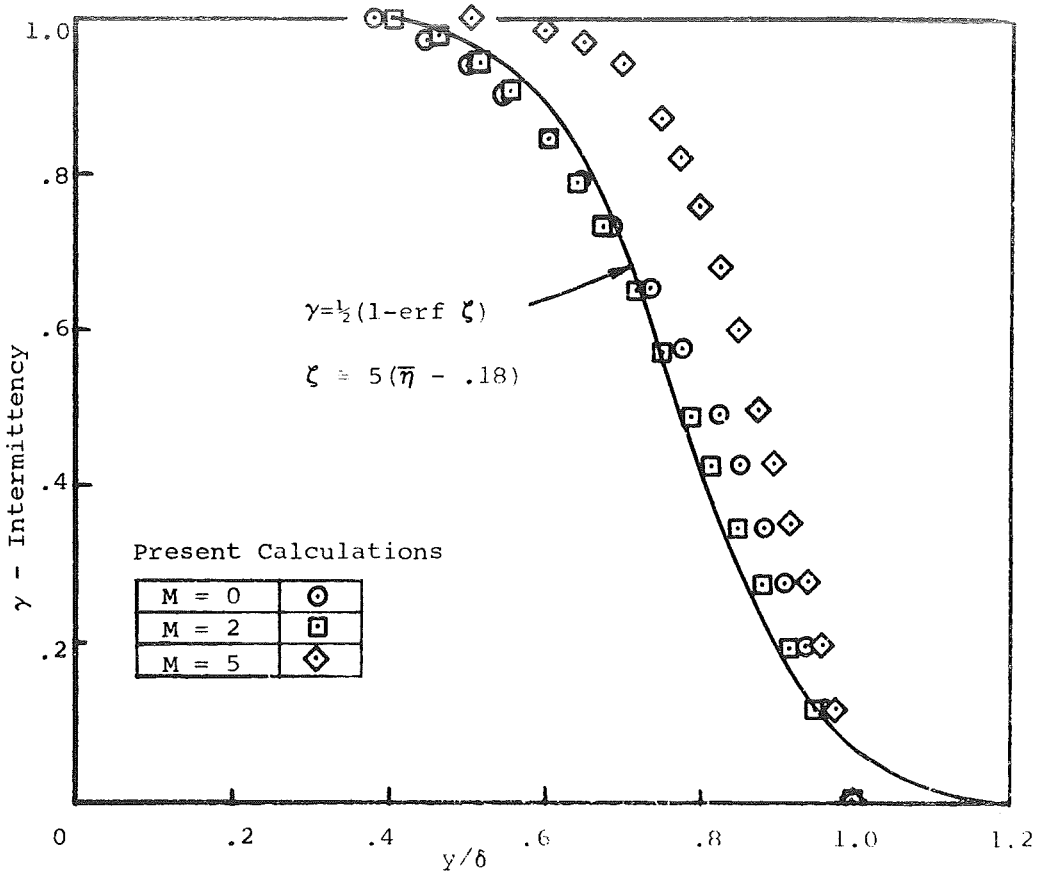

FIGURE 34 - COMPARISON OF CALCULATED INTERMITTENCY FACTOR WITH CURVE FIT OF LOW SPEED DATA

$R_\theta = 10^4$, $dp/dx = 0$, $T_w/T_{t_e} = 1.0$

NATIONAL AERONAUTICS AND SPACE ADMINISTRATION
WASHINGTON, D.C. 20546
OFFICIAL BUSINESS

FIRST CLASS MAIL

POSTAGE AND FEES PAID
NATIONAL AERONAUTICS AN
SPACE ADMINISTRATION

POSTMASTER: If Undeliverable (Section 158 Postal Manual) Do Not Retu

"The aeronautical and space activities of the United States shall be conducted so as to contribute . . . to the expansion of human knowledge of phenomena in the atmosphere and space. The Administration shall provide for the widest practicable and appropriate dissemination of information concerning its activities and the results thereof."

—NATIONAL AERONAUTICS AND SPACE ACT OF 1958

NASA SCIENTIFIC AND TECHNICAL PUBLICATIONS

TECHNICAL REPORTS: Scientific and technical information considered important, complete, and a lasting contribution to existing knowledge.

TECHNICAL NOTES: Information less broad in scope but nevertheless of importance as a contribution to existing knowledge.

TECHNICAL MEMORANDUMS: Information receiving limited distribution because of preliminary data, security classification, or other reasons.

CONTRACTOR REPORTS: Scientific and technical information generated under a NASA contract or grant and considered an important contribution to existing knowledge.

TECHNICAL TRANSLATIONS: Information published in a foreign language considered to merit NASA distribution in English.

SPECIAL PUBLICATIONS: Information derived from or of value to NASA activities. Publications include conference proceedings, monographs, data compilations, handbooks, sourcebooks, and special bibliographies.

TECHNOLOGY UTILIZATION PUBLICATIONS: Information on technology used by NASA that may be of particular interest in commercial and other non-aerospace applications. Publications include Tech Briefs, Technology Utilization Reports and Technology Surveys.

Details on the availability of these publications may be obtained from:

SCIENTIFIC AND TECHNICAL INFORMATION DIVISION
NATIONAL AERONAUTICS AND SPACE ADMINISTRATION
Washington, D.C. 20546